

HIGH-ENERGY NUCLEON COMPTON SCATTERING

Thesis by

Jonas Stasys Zmuidzinas

In Partial Fulfillment of the Requirements

For the Degree of

Doctor of Philosophy

California Institute of Technology

Pasadena, California

1963

ACKNOWLEDGMENTS

I wish to express my sincere thanks to Professor F. Zachariasen for his guidance, criticism, and encouragement. I am indebted to Professor M. Gell-Mann for suggesting the problem investigated here and for several illuminating conversations. My indebtedness extends to many members of the Physics Department of the Institute, especially to Professors S. C. Frautschi and R. L. Walker who have been most helpful.

Dr. P. Burt and Mr. R. Gerbracht have read the manuscript and have suggested a number of improvements; their assistance is gratefully acknowledged.

The financial support provided by the California Institute of Technology and by the Jet Propulsion Laboratory is most appreciated. In this connection, I wish to thank Dr. R. J. Mackin, Jr., for making available the facilities of the Jet Propulsion Laboratory for the preparation of this thesis.

Above all, I am truly grateful to my wife, Huguette, for her patience and understanding during the years of my studies.

ABSTRACT

The high-energy nucleon Compton scattering process is studied to second order in the electromagnetic coupling constant from the viewpoint of complex angular momenta. Assuming the validity of the Regge hypothesis about the asymptotic behavior of scattering amplitudes, formulae for total and differential cross sections in the forward and backward directions are derived. Residues of Regge poles in their physical regions are estimated on the basis of existing experimental data. The implications of possible Regge cuts are discussed.

TABLE OF CONTENTS

<u>PART</u>	<u>TITLE</u>	<u>PAGE</u>
I.	Introduction	1
II.	Kinematics	7
III.	Born Amplitudes	20
IV.	High-Energy Backward Compton Scattering	29
V.	High-Energy Forward Compton Scattering	69
VI.	Conclusions	86
	Appendix A	90
	Appendix B	97
	Appendix C	101
	References	115

I. INTRODUCTION

The concept of Regge poles has provided a connection between the low- and the high-energy regimes of elementary particle physics. Let us briefly review the basic ideas involved. Regge (1, 2) has shown that by considering solutions of the Schrödinger equation for a certain class of potentials for all (even complex) values of the angular momentum ℓ , the partial wave amplitude $f_\ell(E)$ is an analytic function of ℓ (and of energy E , of course) with a finite number of energy-dependent simple poles in the right-half ℓ -plane, $\ell > -\frac{1}{2}$. Physically, these (Regge) poles correspond to bound states or resonances of the physical system described by the Schrödinger equation. Near one such pole, the scattering amplitude takes the form

$$f_\ell(E) \approx \beta(E) / [\ell - \alpha(E)].$$

The equation $\ell = \alpha(E)$ defines a singular surface of $f_\ell(E)$ in the complex product space $\{\ell\} \times \{E\}$. The intersection of this Regge surface with the plane $\{\ell\} \times \{E: E \text{ real}\}$ defines what is called a Regge trajectory. If, for some real E , $\alpha(E)$ happens to be equal to a positive integer ℓ , then we have a bound state of that angular momentum and of energy E . If, however, $\alpha(E)$ has in addition an imaginary part, then we have a resonance whose width is proportional to $\Im \alpha(E)$.

As E varies continuously from $-\infty$ to $+\infty$, $\alpha(E)$ moves along the real axis and gives a sequence of bound states whenever it passes a positive integer for $E < 0$. As soon as E becomes positive, α acquires an imaginary part; increasing E further yields a set of resonances. Eventually, the trajectory turns around in the complex α -plane and heads toward negative values of $\text{Re } \alpha$. A typical Regge trajectory is shown in Fig. 1. One should note that no resonances are generated when $\text{Re } \alpha$ passes positive integers on the return journey. This is because the phase shift is now decreasing instead of increasing, as required for resonances. We see then that a set of bound states and resonances are correlated by the fact that they lie on the same Regge trajectory. There is, in general, more than one Regge trajectory in a given problem.

Another aspect of Regge's analysis was the demonstration that the behavior of the total scattering amplitude $f(E, \cos \theta)$ for large values of $\cos \theta$ is governed by Regge poles in the right-half ℓ -plane. Roughly speaking, for fixed E ,

$$f(E, \cos \theta) \xrightarrow{\cos \theta \rightarrow \infty} \frac{\beta(E)}{\sin \pi \alpha(E)} P_{\alpha(E)}(-\cos \theta).$$

This result is only of marginal interest in non-relativistic potential scattering but extremely significant, if applicable, in the relativistic case because here large $\cos \theta$ in one channel corresponds to large center-of-mass energies in crossed channels. In other words, the high-energy behavior of ampli-

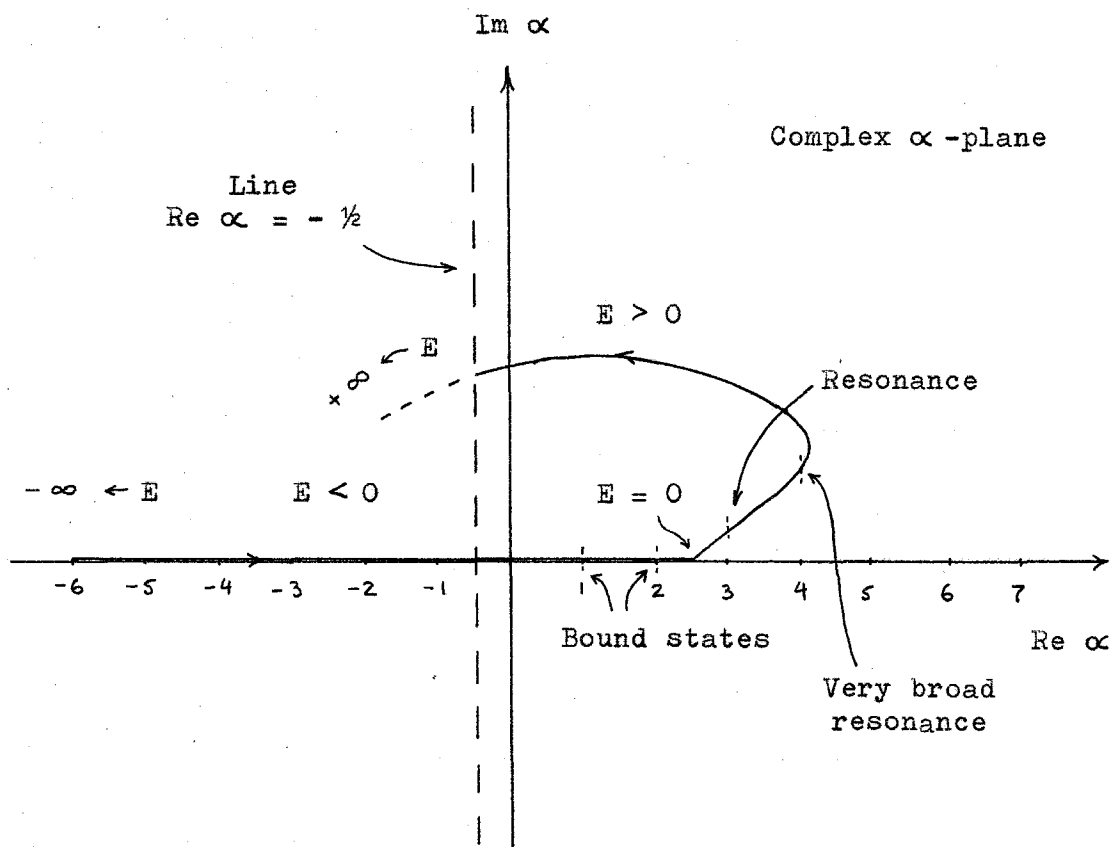


Figure 1. A typical Regge trajectory in the case of potential scattering.

tudes in one channel is determined by their low-energy behavior in crossed channels.

The Regge hypothesis, advanced by Chew, Frautschi, Gell-Mann, Mandelstam, Zachariasen, and others (3, 4), is the assumption that results of Regge's work apply, in an appropriately modified form, to relativistic scattering problems. It is very plausible and has led to several experimentally verified predictions. The major difficulty in applications of this hypothesis is the fact that very little is known about the behavior of Regge trajectories and their residues as functions of energy. No dynamical calculations have yet been performed for their determination in the relativistic case although a tentative scheme for dispersion-theoretic calculations has been given by Cheng and Sharp (5). The experience gained from the examination of the Schrödinger equation has been the main guide in the relativistic case.

In this thesis we investigate nucleon Compton scattering at high energies by applying the Regge hypothesis. Our work is based on the formalism developed by Hearn and Leader (6) for low-energy nucleon Compton scattering. By employing a set of gauge-invariant amplitudes throughout our work, we automatically insure gauge-invariant results. Infrared divergence difficulties, inherent in processes involving photons, are avoided by working to second order in the electromagnetic coupling constant. Our approach is purely phenomenological.

We attempt to calculate neither Regge trajectories nor their residues. Rather, we construct the Regge formalism for Compton scattering and relate, where possible, Regge pole residues to experimentally known quantities. The formulae we obtain for various cross sections should prove useful if and when high-energy nucleon Compton scattering experiments are performed. At present, the experimental data is very scarce for photon energies much above 400 MeV (7). Experimental difficulties in making proton Compton scattering experiments are mainly small cross sections ($d\sigma/d\Omega \sim 0.1 \mu\text{b/sr}$ for c.m. angles from 60° to 120° and energies ~ 300 MeV) and background from π^0 decays. Neutron Compton scattering experiments have to be made using deuterium with additional complications due to spectator protons.

In Part II, we discuss kinematics and introduce Mandelstam and helicity amplitudes for processes in the three channels associated with Compton scattering.

Part III contains a brief discussion of Regge trajectory contributions to different channels and also computations of Born amplitudes for N , π^0 , and η intermediate states.

The asymptotic forms of amplitudes and cross sections in the backward scattering direction of channel I are derived in Part IV; those for the forward direction are deduced in Part V.

Conclusions and applications of our work to electron

Compton scattering are contained in Part VI.

The three appendices present calculations of certain d-functions and of their asymptotic behavior, derivations of cross section formulae, and a discussion of analyticity properties of various amplitudes.

II. KINEMATICS

In this part we shall discuss kinematics and introduce amplitudes for the nucleon Compton scattering process. We shall follow the notation of Hearn and Leader (6) with minor modifications.

The processes of nucleon Compton scattering and nucleon-antinucleon annihilation into two photons are represented by the diagram of Fig. 2. Nucleon and photon four-momenta are denoted by p and k and their respective helicities by λ and μ . The three channels corresponding to Fig. 2 are

$$\text{I: } N_1 + \gamma_1 \rightarrow N_2 + \gamma_2, \quad s = (p_1 + k_1)^2 > 0;$$

$$\text{II: } N_1 + \gamma_2 \rightarrow N_2 + \gamma_1, \quad \bar{s} = (p_1 + k_2)^2 > 0;$$

$$\text{III: } N_1 + \bar{N}_2 \rightarrow \gamma_1 + \gamma_2, \quad t = (p_1 + p_2)^2 > 0.$$

The invariants s , \bar{s} , and t represent the total center-of-mass (c.m.) energy squared in their respective channels. We use the convention $a \cdot b = a_\mu b_\mu = a_0 b_0 - \underline{a} \cdot \underline{b}$. For future reference, we record kinematic variables for channels I and III in their c.m. systems:

$$\begin{aligned} \text{I: } p_1 &= (E, \underline{p}), \\ k_1 &= (p, -\underline{p}), \\ p_2 &= (-E, -\underline{p}'), \\ k_2 &= (-p, \underline{p}'), \end{aligned} \tag{2-1}$$

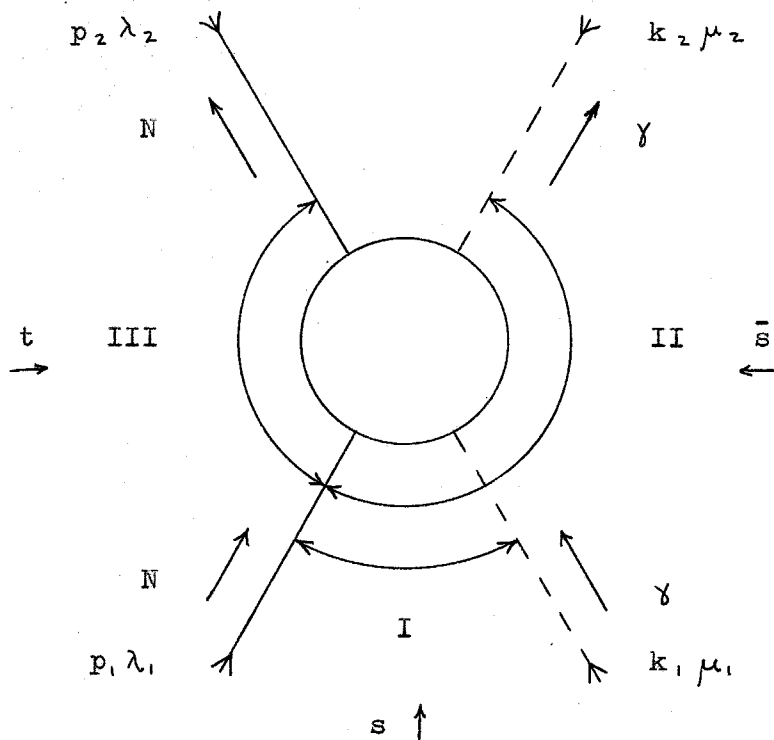


Figure 2. The three channels associated with the nucleon Compton scattering process. The nucleon and photon momenta are p and k , respectively. Nucleon helicities are λ ; those of the photons are μ .

$$s = W^2 = (E + p)^2,$$

$$E = (p^2 + m^2)^{1/2} = (s + m^2)/2W,$$

$$m = \text{nucleon mass},$$

$$p = |\underline{p}| = |\underline{p}'| = (s - m^2)/2W, \quad (2-1)$$

$$t = -2p^2(1 - x),$$

$$x = \underline{p} \cdot \underline{p}' / p^2 = [(s - m^2)^2 + 2st] / (s - m^2)^2,$$

$$\bar{s} = -2p^2(1 + x) + m^4/s;$$

$$\text{III: } p_1 = (\omega, \underline{q}),$$

$$p_2 = (\omega, -\underline{q}),$$

$$k_1 = (-\omega, -\underline{k}),$$

$$k_2 = (-\omega, \underline{k}),$$

$$t = W_t^2 = (2\omega)^2,$$

$$\omega = (q^2 + m^2)^{1/2}, \quad (2-2)$$

$$q = |\underline{q}| = (t/4 - m^2)^{1/2},$$

$$s = -\omega^2 - q^2 + 2\omega q x_t,$$

$$\bar{s} = -\omega^2 - q^2 - 2\omega q x_t,$$

$$x_t = \underline{q} \cdot \underline{k} / q\omega = (s - \bar{s})[t(t - 4m^2)]^{-1/2}.$$

The variables of channel II are defined by analogy with those of channel I. We denote the c.m. momentum in channel II by \bar{p} , the scattering angle by \bar{x} , etc. A set of relations similar to Eqs. 2-1 is obtained for this channel by simply barring appro-

priate variables. Thus $t = -2\bar{p}^2(1 - \bar{x})$, $\bar{E} = (\bar{p}^2 + m^2)^{1/2}$
 $= (\bar{s} + m^2)/2\bar{W}$, etc.

The S- and T-matrix elements for channel I are related by the formula

$$\begin{aligned} & \langle -p_2 \lambda_2 - k_2 \mu_2 | S | p_1 \lambda_1 k_1 \mu_1 \rangle \\ &= (2\pi)^6 \delta(\underline{p}_2 + \underline{p}_1) \delta(\underline{k}_2 + \underline{k}_1) \delta_{\lambda_2 \lambda_1} \delta_{\mu_2 \mu_1} \\ & - i(2\pi)^4 \delta(p_1 + p_2 + k_1 + k_2) (16 p_{10} p_{20} k_{10} k_{20})^{-1/2} \\ & \cdot \langle \lambda_2 \mu_2 | T | \lambda_1 \mu_1 \rangle. \end{aligned} \quad (2-3)$$

The T-matrix element can be written in the form

$$\begin{aligned} \langle \lambda_2 \mu_2 | T | \lambda_1 \mu_1 \rangle &= \bar{u}(-p_2 \lambda_2) \epsilon_{\mu}^+(-k_2 \mu_2) T_{\mu\nu} \epsilon_{\nu}(k_1 \mu_1) u(p_1 \lambda_1), \\ T_{\mu\nu} &= \sum_{i=1}^6 A_i(s, \bar{s}, t) C_{\mu\nu}^{(i)}. \end{aligned}$$

The A_i are invariant (Mandelstam) amplitudes and the $C_{\mu\nu}^{(i)}$ are Lorentz covariants constructed from Dirac gamma matrices and available four-vectors. The requirements of gauge, parity, and charge conjugation invariances are satisfied by the following set of covariants (6, 8):

$$\begin{aligned} C_{\mu\nu}^{(1)} &= P_{\mu}^{\prime} P_{\nu}^{\prime} / P^{\prime 2}, \\ C_{\mu\nu}^{(2)} &= N_{\mu} N_{\nu} / N^2, \\ C_{\mu\nu}^{(3)} &= \gamma_5 (N_{\mu} P_{\nu}^{\prime} - N_{\nu} P_{\mu}^{\prime}) / 2(P^{\prime 2} N^2)^{1/2}, \\ C_{\mu\nu}^{(4)} &= K P_{\mu}^{\prime} P_{\nu}^{\prime} / m P^{\prime 2}, \\ C_{\mu\nu}^{(5)} &= K N_{\mu} N_{\nu} / m N^2, \\ C_{\mu\nu}^{(6)} &= \gamma_5 K (N_{\mu} P_{\nu}^{\prime} + N_{\nu} P_{\mu}^{\prime}) / 2m(P^{\prime 2} N^2)^{1/2}, \end{aligned} \quad (2-4)$$

where

$$\begin{aligned}
 P'_\mu &= P_\mu - K_\mu (P \cdot K / K^2), \\
 P_\mu &= \frac{1}{2} (p_1 - p_2)_\mu, \\
 K_\mu &= \frac{1}{2} (k_1 - k_2)_\mu, \\
 N_\mu &= \epsilon_{\mu\nu\rho\sigma} P'_\nu K_\rho Q_\sigma, \\
 Q_\mu &= (k_1 + k_2)_\mu,
 \end{aligned} \tag{2-5}$$

and $\not{A} = \gamma \cdot a$. The fact that there exist only six independent amplitudes follows most easily by counting helicity amplitudes and observing restrictions imposed on them by parity conservation and time reversal invariance (9). Each invariant amplitude A_i may be decomposed into isoscalar and isovector parts:

$$A_i = A_i^S + A_i^V \tau_3. \tag{2-6}$$

The proton and the neutron scattering amplitudes are then expressed in terms of the invariant amplitudes A_i^P and A_i^N , where

$$\begin{aligned}
 A_i^P &= A_i^S + A_i^V, \\
 A_i^N &= A_i^S - A_i^V.
 \end{aligned} \tag{2-7}$$

Amplitudes for processes in channels II and III are obtained by sandwiching $T_{\mu\nu}$ between appropriate Dirac spinors and polarization vectors:

$$\begin{aligned}
 \text{II: } &< \lambda_2 \mu_2 | T | \lambda_1 \mu_1 > \\
 &= \bar{u}(-p_2, \lambda_2) \epsilon_\mu^\dagger(-k_1, \mu_1) T_{\mu\nu} \epsilon_\nu(k_2, \mu_2) u(p_1, \lambda_1),
 \end{aligned} \tag{2-8}$$

$$\text{III: } \langle \mu_1 \mu_2 | T | \lambda_1 \lambda_2 \rangle$$

$$= \bar{v}(p_2 \lambda_2) \epsilon_{\mu_2}^+(-k_2 \mu_2) \epsilon_{\nu}^+(-k_1 \mu_1) T_{\mu\nu} u(p_1 \lambda_1). \quad (2-9)$$

The two photons are indistinguishable in the annihilation of the $N\bar{N}$ -pair in channel III; this means that the amplitude $\epsilon_{\mu}^+ \epsilon_{\nu}^+ T_{\mu\nu}$ is invariant under the interchange of the two photons:

$$\begin{aligned} & \epsilon_{\mu}^+(-k_2 \mu_2) \epsilon_{\nu}^+(-k_1 \mu_1) T_{\mu\nu}(p_1, p_2, k_1, k_2) \\ &= \epsilon_{\mu}^+(-k_1 \mu_1) \epsilon_{\nu}^+(-k_2 \mu_2) T_{\mu\nu}(p_1, p_2, k_2, k_1). \end{aligned}$$

Thus

$$T_{\mu\nu}(p_1, p_2, k_1, k_2) = T_{\nu\mu}(p_1, p_2, k_2, k_1).$$

Since under $k_1 \leftrightarrow k_2$, $s \leftrightarrow \bar{s}$ and

$$\begin{aligned} C_{\nu\mu}^{(i)}(k_2, k_1) &= \epsilon_i C_{\mu\nu}^{(i)}(k_1, k_2), \\ \epsilon_i &= \begin{cases} +1, & i = 1, 2, 3, 6, \\ -1, & i = 4, 5, \end{cases} \end{aligned} \quad (2-10)$$

it follows that the A_i satisfy the crossing relation

$$A_i(\bar{s}, s, t) = \epsilon_i A_i(s, \bar{s}, t). \quad (2-11)$$

In order to discuss high-energy behavior of Compton scattering amplitudes, we shall be interested in examining the consequences of the Regge hypothesis for this process. To do this, we must introduce partial wave expansions of various amplitudes. Rather than working with the quite cumbersome multipole expansions, we shall use a decomposition into partial wave helicity amplitudes.

The helicity amplitudes are defined in terms of the T-matrix elements for channel I by the formula

$$\langle \lambda_2 \mu_2 | \phi(W, x) | \lambda_1 \mu_1 \rangle = - (8\pi W)^{-1} \langle \lambda_2 \mu_2 | T | \lambda_1 \mu_1 \rangle \quad (2-12)$$

and correspondingly for channels II and III. Differential cross sections are given by

$$(d\sigma/d\Omega)_X = |\langle \phi_X \rangle|^2, \quad (2-13)$$

where X denotes the channel number. Following Jacob and Wick (9), we write the following partial wave expansions in the three channels:

$$\begin{aligned} \text{I: } & \langle \lambda_2 \mu_2 | \phi(W, x) | \lambda_1 \mu_1 \rangle \\ & = p^{-1} \sum_J (2J+1) \bar{\Phi}_{\nu_2 \nu_1}^J(W) d_{\nu_1 \nu_2}^J(\theta), \end{aligned} \quad (2-14)$$

$$\begin{aligned} \text{II: } & \langle \lambda_2 \mu_2 | \bar{\phi}(\bar{W}, \bar{x}) | \lambda_1 \mu_1 \rangle \\ & = \bar{p}^{-1} \sum_J (2J+1) \bar{\Phi}_{\bar{\nu}_2 \bar{\nu}_1}^J(\bar{W}) d_{\bar{\nu}_1 \bar{\nu}_2}^J(\bar{\theta}), \end{aligned} \quad (2-15)$$

$$\begin{aligned} \text{III: } & \langle \mu_1 \mu_2 | \psi(W_t, x_t) | \lambda_1 \lambda_2 \rangle \\ & = (q\omega)^{-1/2} \sum_J (2J+1) \Psi_{\sigma_2 \sigma_1}^J(W_t) d_{\sigma_1 \sigma_2}^J(\theta_t), \end{aligned} \quad (2-16)$$

where $\theta = \cos^{-1} x$, etc., the $d_{\alpha\beta}^J$ are the usual reduced matrix elements of finite rotations defined by

$$d_{\alpha\beta}^J(\theta) = \langle J \alpha | \exp(-iJ_y \theta) | J \beta \rangle,$$

and

$$\nu_{1,2} = \lambda_{1,2} - \mu_{1,2},$$

$$\bar{\nu}_{1,2} = \lambda_{1,2} - \mu_{2,1},$$

$$\sigma_1 = \lambda_1 - \lambda_2,$$

$$\sigma_2 = \mu_1 - \mu_2.$$

We have used the abbreviations

$$\begin{aligned}\Phi_{\nu_2 \nu_1}^J &= \langle \lambda_2 \mu_2 | \phi^J | \lambda_1 \mu_1 \rangle, \\ \bar{\Phi}_{\bar{\nu}_2 \bar{\nu}_1}^J &= \langle \lambda_2 \mu_1 | \bar{\phi}^J | \lambda_1 \mu_2 \rangle, \\ \Psi_{\sigma_2 \sigma_1}^J &= \langle \mu_1 \mu_2 | \psi^J | \lambda_1 \lambda_2 \rangle.\end{aligned}\tag{2-17}$$

The conservation of parity and the time reversal invariance of the theory yield the following relations between partial wave helicity amplitudes (9):

$$\langle \lambda_2 \mu_2 | \phi^J | \lambda_1 \mu_1 \rangle = \eta \langle -\lambda_2 -\mu_2 | \phi^J | -\lambda_1 -\mu_1 \rangle,$$

$$\langle \lambda_2 \mu_2 | \phi^J | \lambda_1 \mu_1 \rangle = \langle \lambda_1 \mu_1 | \phi^J | \lambda_2 \mu_2 \rangle,$$

where η contains the product of intrinsic parities of the particles involved. The first relation reduces the number of independent amplitudes from sixteen to eight, and the second one eliminates two more amplitudes, leaving six, as asserted previously. We choose, in agreement with Hearn and Leader (6), the following set of independent helicity amplitudes:

$$\begin{aligned}\phi_1 &= \langle \tfrac{1}{2} 1 | \phi | \tfrac{1}{2} 1 \rangle, \\ \phi_2 &= \langle -\tfrac{1}{2} -1 | \phi | \tfrac{1}{2} 1 \rangle, \\ \phi_3 &= \langle \tfrac{1}{2} -1 | \phi | \tfrac{1}{2} 1 \rangle, \\ \phi_4 &= \langle -\tfrac{1}{2} 1 | \phi | \tfrac{1}{2} 1 \rangle,\end{aligned}\tag{2-18}$$

$$\begin{aligned}\phi_5 &= \langle -\frac{1}{2} \ 1 \mid \phi \mid -\frac{1}{2} \ 1 \rangle, \\ \phi_6 &= \langle \frac{1}{2} \ -1 \mid \phi \mid -\frac{1}{2} \ 1 \rangle.\end{aligned}\tag{2-18}$$

The choice of amplitudes for channel II is the same. For channel III, we take

$$\begin{aligned}\psi_1 &= \langle 1 \ -1 \mid \psi \mid \frac{1}{2} \ \frac{1}{2} \rangle, \\ \psi_2 &= \langle 1 \ 1 \mid \psi \mid \frac{1}{2} \ \frac{1}{2} \rangle, \\ \psi_3 &= \langle -1 \ -1 \mid \psi \mid \frac{1}{2} \ \frac{1}{2} \rangle, \\ \psi_4 &= \langle 1 \ -1 \mid \psi \mid \frac{1}{2} \ -\frac{1}{2} \rangle, \\ \psi_5 &= \langle -1 \ 1 \mid \psi \mid \frac{1}{2} \ -\frac{1}{2} \rangle, \\ \psi_6 &= \langle 1 \ 1 \mid \psi \mid \frac{1}{2} \ -\frac{1}{2} \rangle.\end{aligned}\tag{2-19}$$

In order to relate the helicity amplitudes to the invariant amplitudes A_i , we must compute matrix elements of covariants $C_{\mu\nu}^{(i)}$. We choose a representation in which

$$\begin{aligned}\not{u} &= mu, \\ \gamma_0 &= \begin{pmatrix} 1 & 0 \\ 0 & -1 \end{pmatrix}, \\ \underline{\gamma} &= \begin{pmatrix} 0 & \underline{\sigma} \\ -\underline{\sigma} & 0 \end{pmatrix}, \\ \gamma_5 &= \begin{pmatrix} 0 & i \\ i & 0 \end{pmatrix}.\end{aligned}$$

For the Dirac spinors, we have

$$u(p_1, \lambda_1) = \begin{pmatrix} N_+ \\ 2\lambda_1 N_- \end{pmatrix} \chi(\lambda_1),$$

$$u(-p_2, \lambda_2) = \begin{pmatrix} N_+ \\ 2\lambda_2 N_- \end{pmatrix} \cdot \exp(-i\sigma_y \theta/2) \chi(\lambda_2),$$

$$N_{\pm} = (E \pm m)^{1/2},$$

$$\chi(\lambda) = \begin{pmatrix} 1/2 + \lambda \\ 1/2 - \lambda \end{pmatrix},$$

$$\bar{u}u = 2m.$$

The polarization vectors are chosen purely spacelike:

$$\epsilon_0 \equiv 0,$$

$$\underline{\epsilon}(-\underline{p}, \mu_1) = 2^{-1/2}(\mu_1 \underline{e}_x - i \underline{e}_y),$$

$$\underline{\epsilon}(-\underline{p}', \mu_2) = 2^{-1/2}(\mu_2 \cos \theta \underline{e}_x - i \underline{e}_y - \mu_2 \sin \theta \underline{e}_z).$$

The notation $\underline{\epsilon}(-\underline{p}, \mu_1)$ means that the photon is traveling in the $-\underline{p}$ -direction along which the helicity μ_1 is defined. The form of polarization vectors is obtained as follows. We start with the basic polarization vectors

$$\underline{\epsilon}(\underline{p}, \mu) = -2^{-1/2}(\mu \underline{e}_x + i \underline{e}_y)$$

for a photon traveling in the $+z$ -direction. The polarization vector for a photon in the $-z$ -direction is then (9)

$$\underline{\epsilon}(-\underline{p}, \mu) = (-1)^{1-\mu} \exp(-i\pi J_y) \underline{\epsilon}(\underline{p}, \mu) = \underline{\epsilon}(\underline{p}, -\mu)$$

by either using rotation matrix for $\theta = \pi$ or by simply observing that $\underline{e}_x \rightarrow -\underline{e}_x$, $\underline{e}_y \rightarrow \underline{e}_y$, and $\underline{e}_z \rightarrow -\underline{e}_z$ under reflection about

the y-axis. The polarization vector in the $- \underline{p}'$ - direction is now obtained from $\underline{\epsilon}(- \underline{p}, \mu)$ by application of $\exp(- iJ_y \theta)$.

Writing

$$\begin{aligned} \langle \lambda_2 \mu_2 | C^{(1)} | \lambda_1 \mu_1 \rangle \\ = \bar{u}(- p_2 \lambda_2) \epsilon_{\mu}^+(- k_2 \mu_2) C_{\mu\nu}^{(1)} \epsilon_{\nu}(k_1 \mu_1) u(p_1 \lambda_1) \end{aligned}$$

and using above representations, we find

$$\begin{aligned} \langle \lambda_2 \mu_2 | C^{(1)} | \lambda_1 \mu_1 \rangle &= - \mu_1 \mu_2 \langle \lambda_2 \mu_2 | C^{(2)} | \lambda_1 \mu_1 \rangle, \\ \langle \lambda_2 \mu_2 | C^{(2)} | \lambda_1 \mu_1 \rangle &= - |\lambda_1 + \lambda_2| m \cos \frac{\theta}{2} + (\lambda_1 - \lambda_2) E \sin \frac{\theta}{2}, \\ \langle \lambda_2 \mu_2 | C^{(3)} | \lambda_1 \mu_1 \rangle &= - \frac{1}{2} (\mu_1 - \mu_2) |\lambda_1 - \lambda_2| p \sin \frac{\theta}{2}, \\ \langle \lambda_2 \mu_2 | C^{(4)} | \lambda_1 \mu_1 \rangle &= - \mu_1 \mu_2 \langle \lambda_2 \mu_2 | C^{(5)} | \lambda_1 \mu_1 \rangle, \\ \langle \lambda_2 \mu_2 | C^{(5)} | \lambda_1 \mu_1 \rangle &= - [|\lambda_1 + \lambda_2| W \cos \frac{\theta}{2} - (\lambda_1 - \lambda_2) m \sin \frac{\theta}{2}] \frac{p}{m}, \\ \langle \lambda_2 \mu_2 | C^{(6)} | \lambda_1 \mu_1 \rangle &= \frac{1}{2} (\mu_1 + \mu_2) (\lambda_1 + \lambda_2) (pW/m) \cos \frac{\theta}{2}. \end{aligned} \tag{2-20}$$

With the help of these expressions, we obtain

$$\begin{aligned} 8\pi W \phi_1 &= - [m(A_1 - A_2) + (pW/m)(A_4 - A_5 + A_6)] \cos \frac{\theta}{2}, \\ 8\pi W \phi_2 &= - [E(A_1 + A_2) + p(- A_3 + A_4 + A_5)] \sin \frac{\theta}{2}, \\ 8\pi W \phi_3 &= [m(A_1 + A_2) + (pW/m)(A_4 + A_5)] \cos \frac{\theta}{2}, \\ 8\pi W \phi_4 &= [E(A_1 - A_2) + p(A_4 - A_5)] \sin \frac{\theta}{2}, \\ 8\pi W \phi_5 &= - [m(A_1 - A_2) + (pW/m)(A_4 - A_5 - A_6)] \cos \frac{\theta}{2}, \\ 8\pi W \phi_6 &= [E(A_1 + A_2) + p(A_3 + A_4 + A_5)] \sin \frac{\theta}{2}. \end{aligned} \tag{2-21}$$

Inverting these equations, we obtain the desired expressions

for the A_i in terms of the helicity amplitudes:

$$\begin{aligned}
 A_1 &= \frac{2\pi}{p} \left[\frac{m}{\cos\theta/2} (\phi_1 - 2\phi_3 + \phi_5) - \frac{W}{\sin\theta/2} (\phi_2 - 2\phi_4 - \phi_6) \right], \\
 A_2 &= -\frac{2\pi}{p} \left[\frac{m}{\cos\theta/2} (\phi_1 + 2\phi_3 + \phi_5) + \frac{W}{\sin\theta/2} (\phi_2 + 2\phi_4 - \phi_6) \right], \\
 A_3 &= \frac{4\pi}{p} \frac{W}{\sin\theta/2} (\phi_2 + \phi_6), \\
 A_4 &= -\frac{2\pi m}{p^2} \left[\frac{E}{\cos\theta/2} (\phi_1 - 2\phi_3 + \phi_5) - \frac{m}{\sin\theta/2} (\phi_2 - 2\phi_4 - \phi_6) \right], \\
 A_5 &= \frac{2\pi m}{p^2} \left[\frac{E}{\cos\theta/2} (\phi_1 + 2\phi_3 + \phi_5) + \frac{m}{\sin\theta/2} (\phi_2 + 2\phi_4 - \phi_6) \right], \\
 A_6 &= -\frac{4\pi}{p} \frac{m}{\cos\theta/2} (\phi_1 - \phi_5).
 \end{aligned} \tag{2-22}$$

Similar formulae hold between the helicity and the invariant amplitudes in channel II provided we bar all relevant variables.

The antiparticle spinors are given by

$$v(\underline{p}, \lambda) = -i\gamma_5 u(\underline{p}, -\lambda);$$

using them, we find

$$\begin{aligned}
 \langle \mu_1, \mu_2 | C^{(1)} | \lambda_1, \lambda_2 \rangle &= \mu_1 \mu_2 \langle \mu_1, \mu_2 | C^{(2)} | \lambda_1, \lambda_2 \rangle, \\
 \langle \mu_1, \mu_2 | C^{(2)} | \lambda_1, \lambda_2 \rangle &= -(\lambda_1 + \lambda_2) q, \\
 \langle \mu_1, \mu_2 | C^{(3)} | \lambda_1, \lambda_2 \rangle &= |\lambda_1 + \lambda_2| (\mu_1 + \mu_2) \omega/2, \\
 \langle \mu_1, \mu_2 | C^{(4)} | \lambda_1, \lambda_2 \rangle &= \mu_1 \mu_2 \langle \mu_1, \mu_2 | C^{(5)} | \lambda_1, \lambda_2 \rangle, \\
 \langle \mu_1, \mu_2 | C^{(5)} | \lambda_1, \lambda_2 \rangle &= (\lambda_1 + \lambda_2) \omega \cos \theta_t + |\lambda_1 - \lambda_2| \frac{\omega^2}{m} \sin \theta_t, \\
 \langle \mu_1, \mu_2 | C^{(6)} | \lambda_1, \lambda_2 \rangle &= (\lambda_1 - \lambda_2) (\mu_1 - \mu_2) \frac{q\omega}{2m} \sin \theta_t,
 \end{aligned} \tag{2-23}$$

and

$$8\pi W_t \psi_1 = -q(A_1 - A_2) + \omega \cos \theta_t (A_4 - A_5), \tag{2-24}$$

$$\begin{aligned}
 8\pi W_t \psi_2 &= q(A_1 + A_2) - \omega A_3 - \omega \cos \theta_t (A_4 + A_5), \\
 8\pi W_t \psi_3 &= q(A_1 + A_2) + \omega A_3 - \omega \cos \theta_t (A_4 + A_5), \\
 8\pi W_t \psi_4 &= (\omega^2/m) \sin \theta_t (A_4 - A_5 - qA_6/\omega), \\
 8\pi W_t \psi_5 &= (\omega^2/m) \sin \theta_t (A_4 - A_5 + qA_6/\omega), \\
 8\pi W_t \psi_6 &= - (\omega^2/m) \sin \theta_t (A_4 + A_5).
 \end{aligned} \tag{2-24}$$

The solution of these equations for the A_i reads

$$\begin{aligned}
 A_1 &= (4\pi/q \sin \theta_t) [m \cos \theta_t (\psi_4 + \psi_5 - 2\psi_6) - \omega \sin \theta_t \\
 &\quad \cdot (2\psi_1 - \psi_2 - \psi_3)], \\
 A_2 &= (4\pi/q \sin \theta_t) [-m \cos \theta_t (\psi_4 + \psi_5 + 2\psi_6) + \omega \sin \theta_t \\
 &\quad \cdot (2\psi_1 + \psi_2 + \psi_3)], \\
 A_3 &= -8\pi(\psi_2 - \psi_3), \\
 A_4 &= (4\pi m/\omega \sin \theta_t)(\psi_4 + \psi_5 - 2\psi_6), \\
 A_5 &= - (4\pi m/\omega \sin \theta_t)(\psi_4 + \psi_5 + 2\psi_6), \\
 A_6 &= (8\pi m/q \sin \theta_t)(\psi_5 - \psi_4).
 \end{aligned} \tag{2-25}$$

III. BORN AMPLITUDES

In this part we calculate single-particle contributions to amplitudes in the three channels associated with Compton scattering. The results will be needed in Parts IV and V.

Let us first consider channel I (the following considerations are equally valid for channel II). The incoming nucleon (isospin $I = \frac{1}{2}$) and the incoming photon ($I =$ mixture of 0 and 1) can go into an intermediate state of baryon number 1 and isospin $1/2$ or $3/2$. The possible intermediate one-particle states are then those of the nucleon and its isobars; they are summarized in Table 1 (10).

Table 1

Regge trajectory (mass in MeV)	Width in MeV	J	I	P	σ	Average slope $\Delta\alpha/\Delta s$ in GeV^{-2}
$N_\alpha(940) \equiv N$	0	1/2	1/2	+	+	1.015
$N_\alpha(1688)$	100	5/2	1/2	+	+	1.005
$N_\alpha(2200)$?	9/2	1/2	+	+	
$\Delta_8(1238) \equiv N_3^*$	100	3/2	3/2	+	-	0.93
$\Delta_8(1920)$	200	7/2	3/2	+	-	1.09
$\Delta_8(2350)$?	11/2	3/2	+	-	
$N_\gamma(1512) \equiv N_1^*$	150	3/2	1/2	-	-	

Here J denotes the total angular momentum, P the parity, and

σ the signature (4) of the state. The average slope is computed using the formula

$$\Delta\alpha/\Delta s = (J_2 - J_1)/(m_2^2 - m_1^2),$$

where $m_{1,2}$ are the masses of physical states indicated in parentheses. The nucleon and its isobar Regge trajectories are plotted in Fig. 3.

The Born terms corresponding to an intermediate nucleon state are given by the amplitudes for the diagrams of Fig. 4:

$$\begin{aligned} T^B &\equiv - 8\pi W \not{\phi}^B \\ &= \bar{u}(-p_2, \lambda_2) \epsilon_\mu^*(-k_2, \mu) \{ [F_1 \gamma_\mu - F_2 i \sigma_{\mu\nu} k_{2\nu}] (s - m^2)^{-1} \\ &\quad \cdot (\not{p}_1 + \not{K}_1 + m) [F_1 \gamma_\rho + F_2 i \sigma_{\rho\sigma} k_{1\sigma}] \\ &\quad + [F_1 \gamma_\rho + F_2 i \sigma_{\rho\sigma} k_{1\sigma}] (\bar{s} - m^2)^{-1} (\not{p}_1 + \not{K}_2 + m) \\ &\quad \cdot [F_1 \gamma_\mu - F_2 i \sigma_{\mu\nu} k_{2\nu}] \} \epsilon_\rho(k_1, \mu_1), \end{aligned} \quad (3-1)$$

where

$$\begin{aligned} F_1 &= \frac{1}{2} e (1 + \tau_3), \\ F_2 &= \frac{1}{2} \frac{e}{2m} [\kappa_p + \kappa_n + (\kappa_p - \kappa_n) \tau_3], \\ \kappa_p &= 1.79, \\ \kappa_n &= -1.91. \end{aligned} \quad (3-2)$$

We use the convention

$$\sigma_{\mu\nu} = \frac{i}{2} (\gamma_\mu \gamma_\nu - \gamma_\nu \gamma_\mu). \quad (3-3)$$

Performing indicated operations in Eq. 3-1, specializing $\not{\phi}^B$

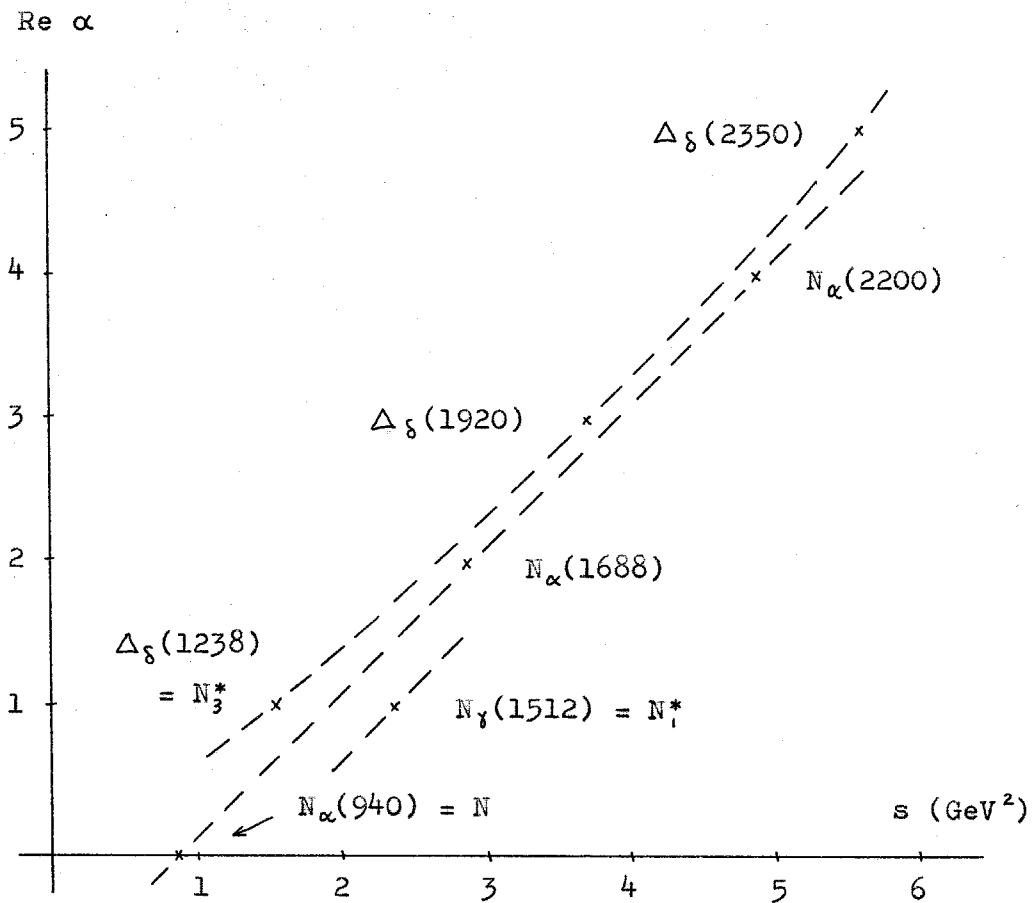


Figure 3. Regge trajectories of the nucleon and its isobars. Note that $\alpha = J - \frac{1}{2}$.

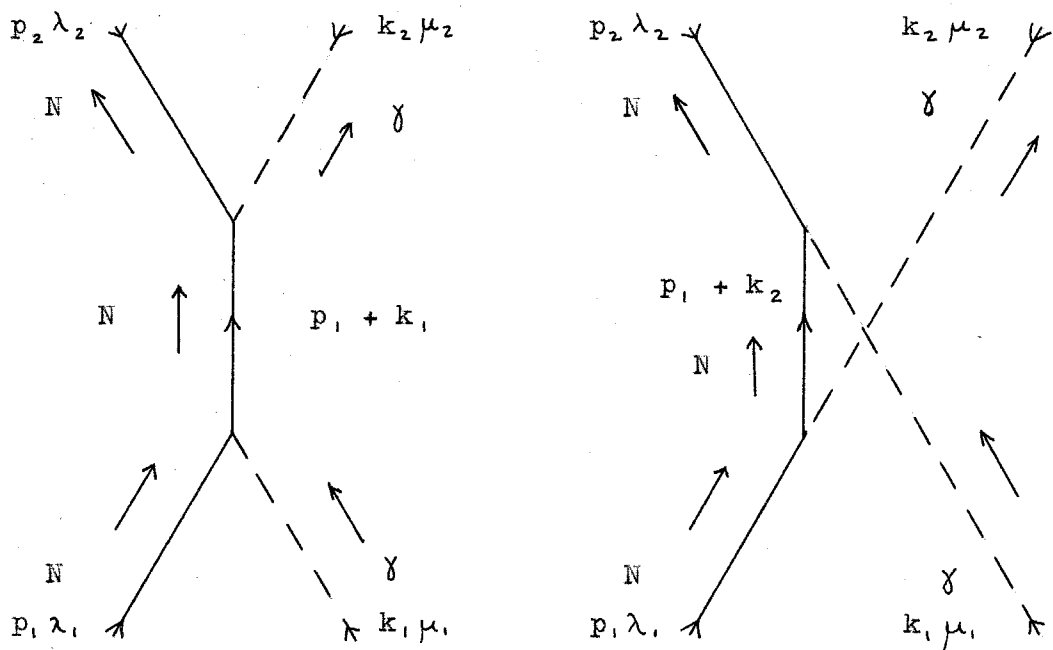


Figure 4. Born diagrams with a nucleon intermediate state in channels I and II.

to $\phi_1^B, \dots, \phi_6^B$, and substituting ϕ_k^B 's into Eqs. 2-22, we obtain

$$\begin{aligned}
 A_1^B &= 2mF_1^2 \left(\frac{1}{s - m^2} + \frac{1}{\bar{s} - m^2} \right), \\
 A_2^B &= 4F_2 (F_1 + mF_2), \\
 A_3^B &= 2mF_1 (F_1 + 2mF_2) \left(\frac{1}{s - m^2} + \frac{1}{\bar{s} - m^2} \right) - 4mF_2^2, \\
 A_4^B &= mF_1^2 \left(\frac{1}{s - m^2} - \frac{1}{\bar{s} - m^2} \right), \\
 A_5^B &= -m(F_1 + 2mF_2)^2 \left(\frac{1}{s - m^2} - \frac{1}{\bar{s} - m^2} \right), \\
 A_6^B &= -2mF_1 (F_1 + 2mF_2) \left(\frac{1}{s - m^2} + \frac{1}{\bar{s} - m^2} \right) + 4mF_2^2.
 \end{aligned} \tag{3-4}$$

Our Born amplitudes agree with those given by Hearn and Leader (6) except for the constant terms which they apparently have discarded.

We shall not need Born amplitudes involving intermediate N_1^* and N_3^* states since we shall compare isobar Regge amplitudes with Breit-Wigner formulae whose parameters will be obtained directly from experimental data.

Turning next to channel III, we note that it has baryon number zero and charge conjugation eigenvalue plus one. As will be shown in Part V, the possible Regge trajectories with these quantum numbers are P , σ , π^0 , η , and D , the hypothetical pseudovector meson trajectory. The properties of these states are summarized in Table 2 (10). The existence of σ as a physical particle is very much in doubt (11, 12).

Table 2

Name of state	Mass (MeV) of physical state	P	σ	Spin of physical state
P (Pomeranchon)	1000 ?	+	+	2 ?
σ (ABC)	280 ?	+	+	0 ?
π^0	135	-	+	0
η	548	-	+	0
D	?	+	-	1

It may be that its Regge trajectory turns down without quite reaching $J = 0$. We may mention that Hamilton et al. (13) find a strong enhancement of the $I = 0$, $J = 0$ wave at low c.m. energies in $\pi - \pi$ scattering although it fails to be a resonance. No evidence at all for the Dennery D-particle (14, 15) has been found so far. We may also note that there is a possibility for the existence of a second vacuum (Pomeranchuk) trajectory (16). If it should exist, our equations in Part V would have to be trivially modified by the inclusion of an extra term whenever the first Pomeranchuk Regge term appears.

In view of these uncertainties, we shall restrict ourselves to the computation of Born amplitudes for π^0 and η only. The relevant diagrams are shown in Fig. 5. Using the unitarity condition with a π^0 -intermediate state, we have

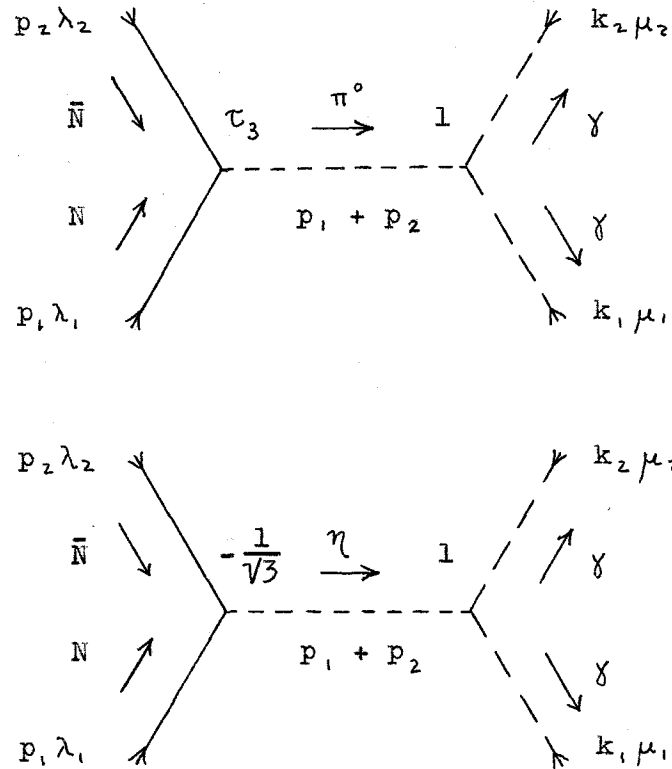


Figure 5. Born diagrams with π^0 and η intermediate states in channel III.

$$\langle \gamma \gamma | T_{\pi^0}^B | \bar{N} N \rangle = (t - m_\pi^2)^{-1} \langle \pi^0 | T | \gamma \gamma \rangle^* \langle \pi^0 | T | \bar{N} N \rangle. \quad (3-5)$$

The vertex functions are evaluated with π^0 on its mass shell; they are constants. We find

$$\begin{aligned} \langle \pi^0 | T | \bar{N} N \rangle &= f_{NN\pi} \tau_3 \bar{v}(p_2, \lambda_2) \gamma_5 u(p_1, \lambda_1) \\ &= f_{NN\pi} \tau_3 [-i m_\pi (\lambda_1 + \lambda_2)], \end{aligned} \quad (3-6)$$

$$\begin{aligned} \langle \pi^0 | T | \gamma \gamma \rangle^* &= f_{\gamma\gamma\pi} \epsilon_{\mu\nu\rho\sigma} \epsilon_\mu^*(-k_1, \mu_1) k_{1\nu} \epsilon_\rho^*(-k_2, \mu_2) k_{2\sigma} \\ &= f_{\gamma\gamma\pi} [-i m_\pi^2 (\mu_1 + \mu_2)/4]. \end{aligned} \quad (3-7)$$

The η diagram gives a similar result with $f_{NN\pi} \tau_3$ replaced by $-(1/\sqrt{3}) f_{NN\eta}$. The factor $-(1/\sqrt{3})$ is chosen in accordance with the D-coupling scheme of Gell-Mann's "eightfold way" (17) so that in the limit of exact unitary symmetry $f_{NN\pi} = f_{NN\eta}$. We obtain

$$\begin{aligned} 8\pi W_t \psi_2 &= -8\pi W_t \psi_3 \\ &= f_{\gamma\gamma\pi} f_{NN\pi} (t - m_\pi^2)^{-1} \frac{1}{2} m_\pi^2 \tau_3 - f_{\gamma\gamma\eta} f_{NN\eta} (t - m_\eta^2)^{-1} \frac{1}{2\sqrt{3}} m_\eta^2. \end{aligned}$$

The width for the decay $\pi^0 \rightarrow 2\gamma$ is given by

$$\begin{aligned} \Gamma_\pi &= 1/\tau_\pi = (32\pi^2 m_\pi)^{-1} \sum_{\mu_1, \mu_2} |\langle \gamma \gamma | T | \pi^0 \rangle|^2 \\ &= |f_{\gamma\gamma\pi}|^2 m_\pi^3 / 64\pi, \end{aligned} \quad (3-8)$$

where τ_π is the π^0 -lifetime. Hence

$$f_{\gamma\gamma\pi} = \frac{8}{m_\pi^2} \sqrt{\frac{\Gamma_\pi m_\pi}{\tau_\pi}}$$

with a positive sign choice. A similar expression holds for $f_{\gamma\gamma\eta}$. According to our normalization conventions of the

amplitudes, $f_{NN\pi} = g$, the usual pion-nucleon coupling constant with

$$g^2/4\pi \approx 14.5.$$

It follows from Eqs. 2-25 that

$$A_L = \delta_{13} \left(- \frac{8}{t - m_\pi^2} \sqrt{\frac{\pi m_\pi}{\tau_\pi}} g \tau_3 + \frac{8/\sqrt{3}}{t - m_\eta^2} \sqrt{\frac{\pi m_\eta}{\tau_\eta}} f_{NN\eta} \right). \quad (3-9)$$

In the limit of unitary symmetry, we should have $g = f_{NN\eta}$. If the symmetry is not too badly broken by interactions, then we might expect that g and $f_{NN\eta}$ should at least have the same sign.

IV. HIGH-ENERGY BACKWARD

COMPTON SCATTERING

In this part we shall make use of the Regge hypothesis to determine the high-energy behavior of nucleon Compton scattering in the backward direction; we shall also discuss experimental implications of our results. To be more specific, our program is the following. Starting with partial wave helicity amplitudes in channel II, we shall construct parity eigenamplitudes and continue them to complex values of the angular momentum J , obtaining a set of amplitudes exhibiting Regge pole singularities. Using the complex- J unitarity condition, we shall relate nucleon isobar Regge residues for Compton scattering to those for the pion photoproduction process; the latter residues will be taken from experiment. We shall use perturbation theory results of Part III to evaluate the nucleon Regge residues. Making certain assumptions, we shall estimate differential cross sections and discuss the possibility of their oscillatory behavior.

According to the Regge hypothesis, the high-energy behavior of a scattering process in a given channel is controlled by Regge poles in crossed channels. In our case, the high-energy behavior of the Compton scattering amplitude in the backward direction in channel I is controlled by Regge poles in channel II. This can easily be seen as follows.

For fixed total c.m. energy squared \bar{s} in channel II, the cosine of the scattering angle in that channel, $x = \cos \theta$, is proportional to the total c.m. energy squared s in channel I by the barred counterpart of the last of equations 2-1 (with the substitution $\bar{p} = (\bar{s} - m^2)/2\bar{s}^{1/2}$):

$$s = -\frac{1}{2\bar{s}} (\bar{s} - m^2)^2 (1 + \bar{x}) + m^4/\bar{s}, \quad (4-1)$$

or, in the limit of large s ,

$$\bar{x} \simeq -2s\bar{s}/(\bar{s} - m^2)^2. \quad (4-2)$$

(Note that \bar{s} cannot equal m^2 for finite \bar{x} since then we would have $s = m^2$ from Eq. 4-1 which is certainly not "large.")

Amplitudes in channel II will have the Regge form

$$A \sim \beta(\bar{s}) P_{\alpha(\bar{s})}(\bar{x}) \sim \beta(\bar{s}) s^{\alpha(\bar{s})}, \quad s \rightarrow \infty,$$

and, by crossing, so will the amplitudes in channel I. From

$$\begin{aligned} \bar{s} &= -\frac{1}{2s} (s - m^2)^2 (1 + x) + m^4/s \\ &\xrightarrow{s \rightarrow \infty} -\frac{1}{2} s(1 + x) < 0, \end{aligned}$$

we see that in order that \bar{s} remain fixed, we must let $x \rightarrow -1$ as $s \rightarrow \infty$, i.e., we must restrict our attention to backward scattering angles in channel I.

We proceed then to "reggeize" amplitudes in channel II. The ways of doing this have been discussed by several authors. Frautschi, Gell-Mann, and Zachariasen (4) have conjectured a set of rules for reactions involving four particles of arbi-

trary spins. A more explicit formulation of the "reggeizing" procedure has been given by Gell-Mann (18). Rather than following the rules, we shall present a somewhat detailed exposition of our reggeizing procedure. This, we believe, will be more illuminating because of the considerable algebraic complexity of the nucleon Compton scattering problem. Since channels I and II are in all respects identical, we shall reggeize channel I and thereby save ourselves writing a multitude of barred letters. The results will then immediately be applicable to channel II by simply barring all relevant variables. We start with a partial wave expansion of the helicity amplitudes for channel I, Eq. 2-14:

$$\varphi_k(W, x) = p^{-1} \sum_J (2J + 1) \bar{\Phi}_k^J(W) \Delta_k^J(x), \quad (4-3)$$

where

$$\varphi_k(W, x) = \begin{cases} \phi_k(W, x)/\cos \frac{\theta}{2}, & k = 1, 3, 5, \\ \phi_k(W, x)/\sin \frac{\theta}{2}, & k = 2, 4, 6, \end{cases} \quad (4-4)$$

and

$$\begin{aligned} \Delta_1^J(x) &= d_{-1/2, -1/2}^J(\theta)/\cos \frac{\theta}{2}, \\ \Delta_2^J(x) &= d_{-1/2, 1/2}^J(\theta)/\sin \frac{\theta}{2}, \\ \Delta_3^J(x) &= d_{-1/2, 3/2}^J(\theta)/\cos \frac{\theta}{2}, \\ \Delta_4^J(x) &= d_{-1/2, -3/2}^J(\theta)/\sin \frac{\theta}{2}, \\ \Delta_5^J(x) &= d_{-3/2, -3/2}^J(\theta)/\cos \frac{\theta}{2}, \\ \Delta_6^J(x) &= d_{-3/2, 3/2}^J(\theta)/\sin \frac{\theta}{2}. \end{aligned} \quad (4-5)$$

The Φ_k^J , $k = 1, \dots, 6$ are to be identified with the Φ_{ν_2, ν_1}^J according to the definitions of Eqs. 2-17 and 2-18. The d - and Δ -functions are tabulated in Appendix A together with their asymptotic behavior. At this point we note that the Δ 's defined above contain no half-angle trigonometric functions and are just linear combinations of Legendre polynomials $P_\ell(x)$ (and their derivatives) with ℓ integral for J half-integral. The connection between the Mandelstam amplitudes A_i and the helicity amplitudes φ_k is given by

$$A_i(s, \bar{s}, t) = \sum_{k=1}^6 \mathcal{A}_{ik}(W) \varphi_k(W, x), \quad (4-6)$$

where the coefficients $\mathcal{A}_{ik}(W)$ can be read off from Eqs. 2-22. Since the A_i are even and p , E , and W are odd under the substitution $W \rightarrow -W$, it follows by direct examination of the \mathcal{A}_{ik} that they and the φ_k have the following symmetries:

$$\mathcal{A}_{ik}(-W) = (-1)^k \mathcal{A}_{ik}(W), \quad (4-7)$$

$$\varphi_k(-W, x) = (-1)^k \varphi_k(W, x). \quad (4-8)$$

As a consequence of the last equation, we see that

$$\Phi_k^J(-W) = (-1)^{l+k} \Phi_k^J(W). \quad (4-9)$$

The identity (9)

$$d_{\lambda\mu}^J(\pi - \theta) = (-1)^{J+\lambda} d_{\lambda, -\mu}^J(\theta)$$

allows us to conclude that

$$\Delta_i^J(-x) = (-1)^{J-1/2} \Delta_i^J(x), \quad (4-10)$$

$$\begin{aligned}\Delta_3^J(-x) &= (-1)^{J-1/2} \Delta_4^J(x), \\ \Delta_5^J(-x) &= (-1)^{J+1/2} \Delta_6^J(x).\end{aligned}\tag{4-10}$$

We shall be interested in certain linear combinations of Δ 's which will be needed for an analytic continuation in the angular momentum J . These are the positive and negative signature Δ 's defined by

$$\begin{aligned}\Delta_{1,2}^{J(+)}(x) &= \frac{1}{2} [\Delta_{1,2}^J(x) \pm \Delta_{2,1}^J(-x)], \\ \Delta_{3,4}^{J(+)}(x) &= \frac{1}{2} [\Delta_{3,4}^J(x) \pm \Delta_{4,3}^J(-x)], \\ \Delta_{5,6}^{J(\pm)}(x) &= \frac{1}{2} [\Delta_{5,6}^J(x) \mp \Delta_{6,5}^J(-x)].\end{aligned}\tag{4-11}$$

The inverse relations are

$$\Delta_k^J(x) = \Delta_k^{J(+)}(x) + \Delta_k^{J(-)}(x), \quad k = 1, \dots, 6.\tag{4-12}$$

The functions $\Delta_k^{J(\pm)}$ obey the following relations:

$$\Delta_k^{J(+)}(x) = \begin{cases} \Delta_k^J(x), & J = 1/2, 5/2, \dots \\ 0, & J = 3/2, 7/2, \dots \end{cases}\tag{4-13}$$

$$\Delta_k^{J(-)}(x) = \begin{cases} 0, & J = 1/2, 5/2, \dots \\ \Delta_k^J(x), & J = 3/2, 7/2, \dots \end{cases}\tag{4-14}$$

$$\begin{aligned}\Delta_{1,3}^{J(\pm)}(-x) &= \pm \Delta_{2,4}^{J(\pm)}(x), \\ \Delta_5^{J(\pm)}(-x) &= \mp \Delta_6^{J(\pm)}(x).\end{aligned}\tag{4-15}$$

The last two equations state the line reversal transformation properties (18) of the Δ -functions. Let us briefly recall the significance of this transformation. Consider a nucleon,

e.g., Regge pole in channel II, Fig. 6. This Regge pole will control the high-energy backward Compton scattering in channel I, as already explained in the beginning of this part; it will also control the high-energy process in channel III which is the nucleon-antinucleon annihilation into two photons. By reversing the nucleon and photon lines N_2 and γ_1 in Fig. 6a, we effectively switch channels I and III. This is equivalent to the change $\bar{x} \rightarrow -\bar{x}$ as one can easily see from Eqs. 2-1:

$$s \simeq -2\bar{p}^2(1 + \bar{x}) \xrightarrow{\bar{x} \rightarrow -\bar{x}} -2\bar{p}^2(1 - \bar{x}) = t$$

for large s . The asymptotic amplitudes for the Compton scattering process will be proportional to $\Delta_k^{J(+)}(\bar{x})$ and those for the $N\bar{N}$ -annihilation to $\Delta_k^{J(+)}(-\bar{x})$, related by Eqs. 4-15 to $\Delta_k^{J(+)}(\bar{x})$. This establishes a connection between asymptotic amplitudes of two different processes.

Let us now write the Watson-Sommerfeld representation (1, 2) for the partial wave expansion given by Eq. 4-3:

$$\varphi_k(W, x) = \frac{1}{2\pi i} \int_C dJ \frac{\pi(2J+1)}{\sin \pi(J - \frac{1}{2})} \cdot \frac{1}{p} [\Phi_k^{J(+)}(W) \Delta_k^{J(+)}(x) - \bar{\Phi}_k^{J(-)}(W) \Delta_k^{J(-)}(x)]. \quad (4-16)$$

The contour C encloses the positive real J -axis in a counter-clockwise direction. The continued partial wave amplitudes $\bar{\Phi}_k^{J(\pm)}$ are equal to the physical partial wave amplitudes for every other half-integer J , depending on the signature:

$$\bar{\Phi}_k^{J(+)} = \Phi_k^J, \quad J = 1/2, 5/2, \dots,$$

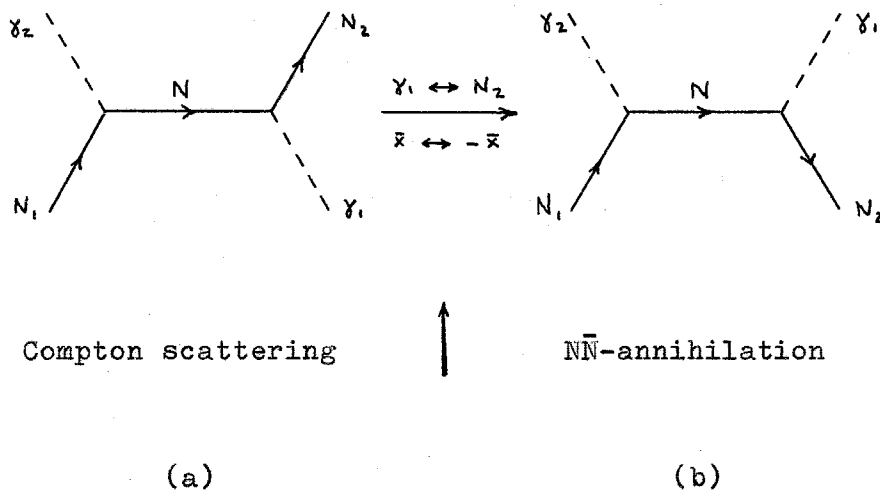


Figure 6. Diagrams for line-reversed processes ($\gamma_1 \leftrightarrow N_2$).

$$\Phi_k^{J(-)} = \Phi_k^J, \quad J = 3/2, 7/2, \dots$$

The necessity of introducing positive and negative signature analytic continuations of physical partial wave amplitudes is well known (4) and is associated with the fact that exchange potentials are always present in relativistic scattering problems due to the existence of crossed channels.

Before proceeding with the deformation of the contour C , we wish to construct amplitudes of definite parity. If $|J M ; \lambda, \lambda_1\rangle$ denotes the state of two particles of spins s_1, s_2 and helicities λ_1, λ_2 in their c.m. system with total angular momentum J and its projection M along the direction of the momentum of particle 1, then Jacob and Wick (9) have shown that

$$P |J M ; \lambda, \lambda_1\rangle = (-1)^{J-s_1-s_2} \eta_1 \eta_2 |J M ; -\lambda, -\lambda_1\rangle, \quad (4-17)$$

where P is the parity operator and η_1 and η_2 are the intrinsic parities of the particles. We can construct states of definite parity for the nucleon-photon system by taking

$$|J M ; 3/2 \pm\rangle = 2^{-1/2} (|J M ; 1/2 -1\rangle \pm |J M ; -1/2 1\rangle),$$

$$|J M ; 1/2 \pm\rangle = 2^{-1/2} (|J M ; 1/2 1\rangle \pm |J M ; -1/2 -1\rangle).$$

Indices $3/2$ and $1/2$ denote the value of the total helicity $|\lambda - \mu|$ and \pm distinguish states of opposite parity. These states are not eigenstates of total spin but can be expressed in terms of the latter by means of Clebsch-Gordan coefficients. We can now define eigenamplitudes of total angular momentum

and parity:

$$\begin{aligned}
 f_{11}^{J\pm} &\equiv \langle 1/2 \pm | \phi^J | 1/2 \pm \rangle = \Phi_{11}^J \pm \Phi_{12}^J, \\
 f_{31}^{J\pm} &= \langle 3/2 \pm | \phi^J | 1/2 \pm \rangle = \Phi_{33}^J \pm \Phi_{34}^J, \\
 f_{33}^{J\pm} &= \langle 3/2 \pm | \phi^J | 3/2 \pm \rangle = \Phi_{55}^J \pm \Phi_{66}^J.
 \end{aligned} \tag{4-18}$$

Note that amplitudes of the type $\langle \pm | \bar{+} \rangle$ vanish because of assumed conservation of parity. The inverse relations of Eqs. 4-18 are

$$\begin{aligned}
 \Phi_{1,2}^J &= \frac{1}{2} (f_{11}^{J\pm} \pm f_{11}^{J\pm}), \\
 \Phi_{3,4}^J &= \frac{1}{2} (f_{31}^{J\pm} \pm f_{31}^{J\pm}), \\
 \Phi_{5,6}^J &= \frac{1}{2} (f_{33}^{J\pm} \pm f_{33}^{J\pm}).
 \end{aligned} \tag{4-19}$$

As shown in Appendix B, the elastic unitarity condition for the helicity amplitudes $\Phi_{v_2 v_1}^J$ reads

$$\begin{aligned}
 \text{Abs } \Phi_{v_2 v_1}^J &\equiv \frac{1}{2i} [\Phi_{v_2 v_1}^J (W + i\epsilon) - \Phi_{v_2 v_1}^J (W - i\epsilon)] \\
 &= \sum_v \Phi_{v v_2}^{J*} \Phi_{v v_1}^J, \quad W \geq m.
 \end{aligned} \tag{4-20}$$

Substitution of Eqs. 4-19 into Eq. 4-20 reveals that

$$\text{Abs } f^{J\pm} = f^{J\pm} * f^{J\pm} \tag{4-21}$$

with

$$\begin{aligned}
 f^{J\pm} &= \begin{pmatrix} f_{11}^{J\pm} & f_{13}^{J\pm} \\ f_{31}^{J\pm} & f_{33}^{J\pm} \end{pmatrix}, \\
 f_{13}^{J\pm} &= f_{31}^{J\pm}.
 \end{aligned} \tag{4-22}$$

Thus we can make the following identification:

$$S_{ij}^{J\pm} = \delta_{ij} + 2i f_{ij}^{J\pm}, \quad i, j = 1, 3, \quad (4-23)$$

where

$$\sum_k S_{ik}^J S_{kj}^J = \delta_{ij}.$$

Let us consider the contributions of various single-particle intermediate states to the reaction $N + \gamma \rightarrow N + \gamma$. Since $\eta_\gamma = -1$ and since we can arbitrarily choose $\eta_N = +1$, we find that

$$P |J M; |\lambda - \mu| \pm \rangle = \pm (-1)^{J-1/2} |J M; |\lambda - \mu| \pm \rangle.$$

Using the fact that the intermediate nucleon in the process $N + \gamma \rightarrow N \rightarrow N + \gamma$ has positive parity and $J = 1/2$, we conclude that it can contribute only to amplitudes f_{ij}^{J+} ; this will remain true after the intermediate nucleon has been reggeized, in which case it will contribute to amplitudes f_{ij}^{J+} of positive signature. Similarly, the N_3^* Regge trajectory will contribute to negative signature f_{ij}^{J+} amplitudes, while negative signature f_{ij}^{J-} will receive contributions from the N_1^* trajectory.

From Eqs. 4-18 and from the reflection properties of the Φ_k^J , Eq. 4-9, we find that

$$f_{ij}^{J+}(W) = f_{ij}^{J-}(-W). \quad (4-24)$$

This relation, as pointed out by Gribov (19), implies that associated with each fermion Regge trajectory there is a dual trajectory with the same quantum numbers except for opposite parity, both trajectories coinciding at $W = 0$.

Bearing the foregoing in mind, we deform the contour C in Eq. 4-16 by expanding it to infinity in the right-half J -plane, thereby picking up $-2\pi i$ times the residues of the singularities of the partial wave amplitudes in the complex J -plane (Regge singularities), with the result

$$\begin{aligned} \varphi_k(W, x) = & - \frac{1}{2\pi i} \int_{C'} dJ \frac{\pi(2J+1)}{\cos \pi J} \frac{1}{p} [\Phi_k^{J(+)}(W) \Delta_k^{J(+)}(x) \\ & - \Phi_k^{J(-)}(W) \Delta_k^{J(-)}(x)] + \varphi_k^R(W, x). \end{aligned} \quad (4-25)$$

Here C' denotes the contour shown in Fig. 7 and $\varphi_k^R(W, x)$ contains contributions of Regge poles and cuts, if any. For our case, the Regge term reads, assuming that there are no cuts,

$$\begin{aligned} \varphi_k^R(W, x) = & - \frac{\pi}{p} \left\{ \frac{\alpha_N(W) + 1}{\sin \pi \alpha_N(W)} R_k^N(W) \Delta_k^{\alpha_N(W)+1/2(+)}(x) \right. \\ & - (-1)^{1+k} \frac{\alpha_{N_1^*}(W) + 1}{\sin \pi \alpha_{N_1^*}(W)} R_k^{N_1^*}(W) \Delta_k^{\alpha_{N_1^*}(W)+1/2(-)}(x) \\ & - \frac{\alpha_{N_3^*}(W) + 1}{\sin \pi \alpha_{N_3^*}(W)} R_k^{N_3^*}(W) \Delta_k^{\alpha_{N_3^*}(W)+1/2(-)}(x) \left. \right\} \\ & - \frac{\pi}{p} (-1)^{1+k} \{W \rightarrow -W\}. \end{aligned} \quad (4-26)$$

The terms $(-1)^{1+k} \{W \rightarrow -W\}$ are the contributions of dual Regge poles mentioned above, the factor $(-1)^{1+k}$ arising from the parity \pm signs in Eqs. 4-19; the origin of this factor in the N_1^* contribution is the same. The quantities R_k are the residues of the f -amplitudes defined by

$$\begin{aligned} R_{1,2}^A(W) & \equiv R_{11}^A(W) = \text{Res}_{J=\alpha_A(W)+1/2} f_{11}^{JP}(W), \\ R_{3,4}^A(W) & \equiv R_{31}^A(W) = \text{Res}_{J=\alpha_A(W)+1/2} f_{31}^{JP}(W), \\ R_{5,6}^A(W) & \equiv R_{33}^A(W) = \text{Res}_{J=\alpha_A(W)+1/2} f_{33}^{JP}(W). \end{aligned} \quad (4-27)$$

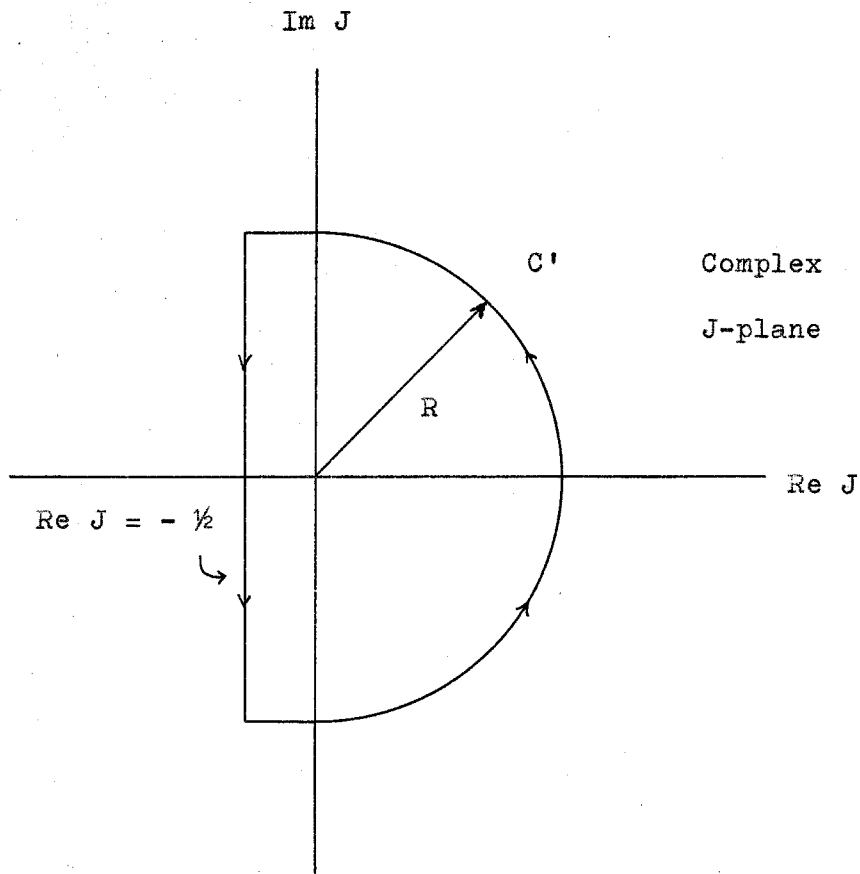


Figure 7. The contour C' of Eq. 4-25. The radius R of the semicircle tends to infinity.

The particle type index A is correlated with parity P (and with signature σ) according to Table 1, p. 20.

Before further discussing reggeized amplitudes, let us investigate the implications of unitarity on the residues R_i . The strictly elastic ($N\gamma$ -intermediate state) unitarity relation, Eq. 4-20, gives a contribution of order e^2 higher than would one involving an $N\pi$ -intermediate state. Since we are working to order e^2 throughout, we neglect the former state. To treat the latter, we introduce pion photoproduction helicity amplitudes:

$$\begin{aligned} \langle \lambda | \xi | \lambda, \mu_i \rangle &= - (8\pi W)^{-1} \langle N\pi | T | N\gamma \rangle \\ &= (pr)^{-1/2} \sum_J (2J+1) Z_{\lambda, \lambda_i, -\mu_i}^J(W) d_{\lambda, -\mu_i, \lambda}^J(\theta'), \end{aligned} \quad (4-28)$$

where θ' is the scattering angle between final and initial nucleon momenta, and r is the c.m. momentum of the $N\pi$ -system.

The four independent helicity amplitudes can be taken as

$$\begin{aligned} \xi_1 &= \langle \frac{1}{2} | \xi | \frac{1}{2} 1 \rangle, \\ \xi_2 &= \langle -\frac{1}{2} | \xi | \frac{1}{2} 1 \rangle, \\ \xi_3 &= \langle -\frac{1}{2} | \xi | -\frac{1}{2} 1 \rangle, \\ \xi_4 &= \langle \frac{1}{2} | \xi | -\frac{1}{2} 1 \rangle. \end{aligned} \quad (4-29)$$

Again, we can form parity and total angular momentum $N\pi$ eigenstates:

$$\begin{aligned} |J M ; \pm \rangle &= 2^{-1/2} (|J M ; \frac{1}{2} \rangle \mp |J M ; -\frac{1}{2} \rangle), \\ P |J M ; \pm \rangle &= \pm (-1)^{J-1/2} |J M ; \pm \rangle. \end{aligned}$$

The partial wave parity eigenamplitudes can be defined in the same way as before:

$$\begin{aligned} h_1^{J\pm} &\equiv \langle \pm | \xi^J | 1/2 \pm \rangle = Z_1^J \mp Z_2^J, \\ h_3^{J\pm} &\equiv \langle \pm | \xi^J | 3/2 \pm \rangle = - (Z_3^J \mp Z_4^J), \end{aligned} \quad (4-30)$$

where

$$\begin{aligned} Z_1^J &= Z_{1/2, -1/2}^J = - Z_{-1/2, 1/2}^J, \\ Z_2^J &= Z_{-1/2, -1/2}^J = - Z_{1/2, 1/2}^J, \\ Z_3^J &= Z_{-1/2, -3/2}^J = - Z_{1/2, 3/2}^J, \\ Z_4^J &= Z_{1/2, -3/2}^J = - Z_{-1/2, 3/2}^J. \end{aligned} \quad (4-31)$$

As shown in Appendix B, the unitarity condition in channel I takes the form

$$\text{Abs } \Phi_{J_2 \nu_2}^J = \sum_{\lambda} Z_{\lambda \nu_2}^{J*} Z_{\lambda \nu_1}^J,$$

with $\nu_i = \lambda_i - \mu_i$. Using Eqs. 4-18, 4-30, and 4-31 in the above unitarity relation, we find

$$\text{Abs } f_{ij}^{J\pm}(W) = h_i^{J\pm*}(W) h_j^{J\pm}(W), \quad i, j = 1, 3, \quad (4-32)$$

for $W \geq m + m_\pi$. For the time being we neglect complications caused by the isospin in our amplitudes. The unitarity relation, Eq. 4-32, is exact (to order e^2) in the region $m + 2m_\pi > W \geq m + m_\pi$. Our goal is to estimate the residues of the N_i^* and N_3^* Regge poles in Compton scattering amplitudes in terms of experimentally known residues at these poles in pion photo-production amplitudes. For this purpose we shall use the

unitarity relation derived above (or, rather, its reggeized version) which should not be too bad for the N_3^* resonance since it occurs near the two-pion production threshold. The approximation may be much worse for the N_1^* resonance occurring above the 4π -production threshold.

It is well known that the partial wave amplitudes for complex angular momentum satisfy a unitarity relation which, for our amplitudes, reads

$$\begin{aligned} f_{ij}^{(k)}(J, W) - f_{ij}^{(k)*}(J^*, W) \\ = 2i h_i^{(k)*}(J^*, W) h_j^{(k)}(J, W), \quad i, j = 1, 3, \end{aligned} \quad (4-33)$$

for $W \geq m + m_\pi$. The index k denotes collectively the fixed quantum numbers of the channel:

$$(k) = (P, \sigma, I)$$

or, equivalently, the type of Regge trajectory according to Table 1, p. 20, 1 standing for N_1^* , 2 for N , and 3 for N_3^* .

The amplitudes can be written as

$$\begin{aligned} f_{ij}^{(k)}(J, W) &= F_{ij}^{(k)}(J, W) + \frac{R_{ij}^{(k)}(W)}{J - \frac{1}{2} - \alpha_k(W)}, \\ h_i^{(k)}(J, W) &= H_i^{(k)}(J, W) + \frac{Q_i^{(k)}(W)}{J - \frac{1}{2} - \alpha_k(W)}, \end{aligned} \quad (4-34)$$

for all values of J and W by explicitly displaying the Regge pole terms. We assume that R and Q are the total residues of f and h , respectively, so that both F and H are nonsingular at $J = \frac{1}{2} + \alpha_k(W)$. Only one Regge pole contributes in a given amplitude of index k since the quantum numbers of the nucleon

and the $N\pi$ -resonances are all different and no other resonances, not lying on the N and $N_{1,3}^*$ trajectories, are known at present.

Substituting Eqs. 4-34 into Eq. 4-33, multiplying by $J - \frac{1}{2} - \alpha_k(W)$, and taking $J \approx \frac{1}{2} + \alpha_k(W)$, we obtain

$$\begin{aligned} R_{ij}^{(k)}(W) &= R_{ij}^{(k)*}(W) \left[1 + \frac{2i\mathfrak{I}m\alpha_k(W)}{J - \frac{1}{2} - \alpha_k(W)} \right]^{-1} \\ &= 2i \frac{Q_i^{(k)*}(W) Q_j^{(k)}(W)}{J - \frac{1}{2} - \alpha_k(W)} \left[1 + \frac{2i\mathfrak{I}m\alpha_k(W)}{J - \frac{1}{2} - \alpha_k(W)} \right]^{-1}. \end{aligned} \quad (4-35)$$

Since, according to the general ideas on the behavior of Regge trajectories, the imaginary part of α is positive above threshold, we see that in the limit $J \rightarrow \frac{1}{2} + \alpha_k(W)$ we have

$$R_{ij}^{(k)}(W) = Q_i^{(k)*}(W) Q_j^{(k)}(W) / \mathfrak{I}m\alpha_k(W), \quad W \geq m + m_\pi. \quad (4-36)$$

We can express the $R_{ij}^{(k)}(m_k)$ in terms of the residues $Q_i^{(k)}(m_k)$ and the quantity $\mathfrak{I}m\alpha_k(m_k)$ related to the width of the k th resonance. We cannot evaluate the $R_{ij}^{(k)}(m_k)$ directly because we have no information on Compton scattering amplitudes for polarized particles.

We now wish to express photoproduction helicity amplitudes in terms of multipole amplitudes used in analyses of experimental data. The connection is

$$\langle \lambda | \mathcal{F} | \lambda, \mu, \rangle = -i \chi^+(-\lambda) e^{i\sigma_3 \theta/2} \mathcal{F} \chi(-\lambda), \quad (4-37)$$

where, according to Chew, Goldberger, Low, and Nambu (20),

$$\begin{aligned} \mathcal{F} &= i \underline{\sigma} \cdot \underline{e} \mathcal{F}_1 + (\underline{p} \cdot \underline{r})^{-1} \underline{\sigma} \cdot \underline{r} \underline{\sigma} \cdot \underline{p} \times \underline{e} \mathcal{F}_2 \\ &+ i (\underline{p} \cdot \underline{r})^{-1} \underline{\sigma} \cdot \underline{p} \underline{r} \cdot \underline{e} \mathcal{F}_3 + i r^{-2} \underline{\sigma} \cdot \underline{r} \underline{r} \cdot \underline{e} \mathcal{F}_4, \end{aligned} \quad (4-38)$$

- \underline{r} = momentum of pion,

- \underline{p} = momentum of photon,

$\underline{\epsilon} = \underline{\epsilon}(\underline{p}, \mu)$ = polarization of photon.

The minus signs of λ 's in Pauli spinors arise because of our convention, contrary to that of CGLN, taking the initial nucleon to be traveling in the positive z-direction. Using the representations of Part II, we find

$$\begin{aligned}\zeta_1 &= \sqrt{2} [\mathcal{F}_1 + \mathcal{F}_2 + \frac{1}{2}(1 + \cos \theta) (\mathcal{F}_3 + \mathcal{F}_4)] \sin \frac{\theta}{2}, \\ \zeta_2 &= \sqrt{2} [-\mathcal{F}_1 + \mathcal{F}_2 + \frac{1}{2}(1 - \cos \theta) (\mathcal{F}_3 - \mathcal{F}_4)] \cos \frac{\theta}{2}, \\ \zeta_3 &= -2^{-1/2}(1 + \cos \theta) (\mathcal{F}_3 + \mathcal{F}_4) \sin \frac{\theta}{2}, \\ \zeta_4 &= 2^{-1/2}(1 - \cos \theta) (\mathcal{F}_3 - \mathcal{F}_4) \cos \frac{\theta}{2}.\end{aligned}\tag{4-39}$$

Multipole expansions of the \mathcal{F}_i , given by CGLN, read

$$\begin{aligned}\mathcal{F}_1 &= \sum_{\ell=0}^{\infty} \{(\ell M_{\ell}^{+} + E_{\ell}^{+})P'_{\ell+1} + [(\ell + 1)M_{\ell}^{-} + E_{\ell}^{-}]P'_{\ell-1}\}, \\ \mathcal{F}_2 &= \sum_{\ell=1}^{\infty} [(\ell + 1)M_{\ell}^{+} + \ell M_{\ell}^{-}]P'_{\ell}, \\ \mathcal{F}_3 &= \sum_{\ell=1}^{\infty} [(E_{\ell}^{+} - M_{\ell}^{+})P'_{\ell+1} + (E_{\ell}^{-} + M_{\ell}^{-})P'_{\ell-1}], \\ \mathcal{F}_4 &= \sum_{\ell=1}^{\infty} (M_{\ell}^{+} - E_{\ell}^{+} - M_{\ell}^{-} - E_{\ell}^{-})P'_{\ell},\end{aligned}\tag{4-40}$$

where $J = \ell \pm \frac{1}{2}$, corresponding to the \pm superscripts on multipole amplitudes. Expanding the ζ 's of Eqs. 4-39 in partial waves, comparing with the multipole expansions of the \mathcal{F} 's, and using Eqs. 4-30, we find

$$\begin{aligned}
 h_1^{J+} &= \sqrt{pr/2} [\ell M_\ell^+ + (\ell + 2) E_\ell^+], \\
 h_1^{J-} &= \sqrt{pr/2} [(\ell + 2) M_{\ell+1}^- - \ell E_{\ell+1}^-], \\
 h_3^{J+} &= \sqrt{pr/2} \sqrt{\ell(\ell + 2)} (E_\ell^+ - M_\ell^+), \\
 h_3^{J-} &= -\sqrt{pr/2} \sqrt{\ell(\ell + 2)} (M_{\ell+1}^- + E_{\ell+1}^-),
 \end{aligned} \tag{4-41}$$

where now $J = \ell + \frac{1}{2}$. We shall be interested in $N_{1,3}^*$ resonances with $J = 3/2$ for which

$$\begin{aligned}
 h_1^{3/2+} &= \sqrt{pr/2} (M_1^+ + 3E_1^+), \\
 h_1^{3/2-} &= \sqrt{pr/2} (3M_2^- - E_2^-), \\
 h_3^{3/2+} &= \sqrt{3pr/2} (E_1^+ - M_1^+), \\
 h_3^{3/2-} &= -\sqrt{3pr/2} (M_2^- + E_2^-).
 \end{aligned} \tag{4-42}$$

To take into account the isospin or charge degrees of freedom, we define four amplitudes corresponding to four possible pion photoproduction processes (dropping irrelevant subscripts):

$$\begin{aligned}
 h^{(+)} &= \langle n \pi^+ | h | p \gamma \rangle, \\
 h^{(0)} &= \langle p \pi^0 | h | p \gamma \rangle, \\
 h^{(-)} &= \langle p \pi^- | h | n \gamma \rangle, \\
 h^{(n)} &= \langle n \pi^0 | h | n \gamma \rangle.
 \end{aligned} \tag{4-43}$$

It can be shown (21) that there are only three independent charge amplitudes; thus we may express the last one, e.g., in terms of the other three:

$$h^{(n)} = h^{(0)} + \frac{1}{\sqrt{2}} (h^{(+)} - h^{(-)}). \tag{4-44}$$

The unitarity relation, Eq. 4-32, now reads

$$\text{Abs } f = \text{Abs } (f^s + f^v \tau_3) \quad (4-45)$$

with

$$\begin{aligned} \text{Abs } f^s &= \frac{1}{2} [h^{(+)*} h^{(+)} + h^{(0)*} h^{(0)} + h^{(-)*} h^{(-)} + h^{(n)*} h^{(n)}], \\ \text{Abs } f^v &= \frac{1}{2} [h^{(+)*} h^{(+)} + h^{(0)*} h^{(0)} - h^{(-)*} h^{(-)} - h^{(n)*} h^{(n)}]. \end{aligned} \quad (4-46)$$

Experimental data can be fitted by assuming Breit-Wigner formulae for the multipole amplitudes:

$$\begin{aligned} E_1^{+(\alpha)}(W) &\approx \frac{e_1^{+(\alpha)}}{W - m_3 + i\Gamma_3/2}, \\ M_1^{+(\alpha)}(W) &\approx \frac{m_1^{+(\alpha)}}{W - m_3 + i\Gamma_3/2}, \\ E_2^{-(\alpha)}(W) &\approx \frac{e_2^{-(\alpha)}}{W - m_1 + i\Gamma_1/2}, \\ M_2^{-(\alpha)}(W) &\approx \frac{m_2^{-(\alpha)}}{W - m_1 + i\Gamma_1/2}, \\ m_{1,3} &= m_{N_{1,3}}, \end{aligned} \quad (4-47)$$

for energies W near resonances m_1 , or m_3 ; the index α runs over $+$, 0 , $-$, and n in accordance with Eqs. 4-43. By expanding α_k near $W = m$,

$$\begin{aligned} \alpha_k(W) \Big|_{W \approx m_k} &\approx 1 + (W - m_k) \epsilon_k + i I_k, \\ \epsilon_k &= \text{Re } \alpha'_k(m_k), \\ I_k &= \text{Im } \alpha'_k(m_k), \quad k = 1, 3, \end{aligned} \quad (4-48)$$

we can write

$$h_i^{(k,\alpha)}(J, W) \Big|_{\substack{W \approx m_k \\ J = 5/2}} \approx \frac{-Q_i^{(k,\alpha)}(m_k)/\epsilon_k}{W - m_k + i I_k/\epsilon_k}. \quad (4-49)$$

Comparing Eqs. 4-42, 4-47, and 4-49, we obtain

$$\begin{aligned}
 Q_1^{(3,\alpha)}(m_3) &= -\sqrt{p_3 r_3/2} \epsilon_3 (3e_1^{+(\alpha)} + m_1^{+(\alpha)}), \\
 Q_3^{(3,\alpha)}(m_3) &= -\sqrt{3p_3 r_3/2} \epsilon_3 (e_1^{+(\alpha)} - m_1^{+(\alpha)}), \\
 Q_1^{(1,\alpha)}(m_1) &= \sqrt{p_1 r_1/2} \epsilon_1 (e_2^{-(\alpha)} - 3m_2^{-(\alpha)}), \\
 Q_3^{(1,\alpha)}(m_1) &= \sqrt{3p_1 r_1/2} \epsilon_1 (e_2^{-(\alpha)} + m_2^{-(\alpha)}), \\
 I_k &= \epsilon_k \Gamma_k/2,
 \end{aligned} \tag{4-50}$$

where

$$\begin{aligned}
 p_k &= (m_k^2 - m^2)/2m_k, \\
 r_k &= \{[m_k^2 - (m + m_\pi)^2][m_k^2 - (m - m_\pi)^2]\}^{1/2}/2m_k.
 \end{aligned} \tag{4-51}$$

Salin and Gourdin (22, 23, 24) have recently analyzed positive and neutral pion photoproduction data; using their results, we find the following values for the residues of Eqs. 4-47:

$$\begin{aligned}
 e_1^{+(+)} &= -1.61 \times 10^{-4} \Gamma_3/m, \\
 e_1^{+(0)} &= 3.58 \times 10^{-4} \Gamma_3/m, \\
 m_1^{+(+)} &= 3.60 \times 10^{-2} \Gamma_3/m, \\
 m_1^{+(0)} &= -7.20 \times 10^{-2} \Gamma_3/m, \\
 e_2^{-(+)} &= e_2^{-(0)} = -2.57 \times 10^{-2} \Gamma_1/m, \\
 m_2^{-(+)} &= m_2^{-(0)} = 5.96 \times 10^{-4} \Gamma_1/m.
 \end{aligned} \tag{4-52}$$

From Eq. 4-50 we obtain

$$\begin{aligned}
 Q_1^{(1,+)}(m_1) &= Q_1^{(1,0)}(m_1) = -0.0163 I_1, \\
 Q_3^{(1,+)}(m_1) &= Q_3^{(1,0)}(m_1) = -0.0311 I_1,
 \end{aligned} \tag{4-53}$$

$$\begin{aligned}
 Q_1^{(3,+)}(m_3) &= -0.0150 I_3, \\
 Q_1^{(3,0)}(m_3) &= 0.0299 I_3, \\
 Q_3^{(3,+)}(m_3) &= 0.0264 I_3, \\
 Q_3^{(3,0)}(m_3) &= -0.0528 I_3.
 \end{aligned}
 \tag{4-53}$$

The unitarity relation, Eq. 4-36, for the case of proton Compton scattering gives

$$\begin{aligned}
 R_{11}^{(1,p)} &= 0.534 \times 10^{-3} I_1, \\
 R_{31}^{(1,p)} &= 1.01 \times 10^{-3} I_1, \\
 R_{33}^{(1,p)} &= 1.93 \times 10^{-3} I_1, \\
 R_{11}^{(3,p)} &= 1.12 \times 10^{-3} I_3, \\
 R_{31}^{(3,p)} &= -1.97 \times 10^{-3} I_3, \\
 R_{33}^{(3,p)} &= 3.48 \times 10^{-3} I_3.
 \end{aligned}
 \tag{4-54}$$

As a check, we compute the proton Compton scattering cross section at the position of the N_3^* resonance at $\theta = 90^\circ$ in the c.m. system. Keeping only the $J = 3/2$ partial wave, we find

$$\begin{aligned}
 \frac{d\sigma}{d\Omega} (W = m_3, \theta = \pi/2) &= \frac{1}{4} \sum_{\lambda, \mu_1} |\langle \lambda_2 \mu_2 | \phi(m_3, 0) | \lambda, \mu_1 \rangle|^2 \\
 &\approx \frac{4}{p_3^2} \sum_{\nu_1, \nu_2} |\Phi_{\nu_2 \nu_1}^{3/2}(m_3) d_{\nu_1 \nu_2}^{3/2}(\pi/2)|^2 \\
 &= 0.118 \mu\text{b/sr}.
 \end{aligned}
 \tag{4-55}$$

This compares with the experimental value of $0.143 \pm 0.009 \mu\text{b/sr}$ given by DeWire et al. (7). Presumably, the inclusion of neglected partial waves would increase the value of the com-

puted cross section. Note that the result in Eq. 4-55 is quite sensitive to the magnitude of the photoproduction amplitudes $h^{3/2}$. Since the cross section is proportional to the fourth power of production amplitude residues, a change of, e.g., 5% in $h^{3/2}$ would produce a change of more than 20% in the cross section.

We have not evaluated neutron residues because there is very little experimental data on π^- - and π^0 -photoproduction from neutrons. Note that, because of Eq. 4-44, we would need only one additional set of data on either $h^{(-)}$ or $h^{(n)}$ amplitudes. The results of Sands et al. (25) have shown that

$$\frac{\sigma(\gamma + n \rightarrow \pi^- + p)}{\sigma(\gamma + p \rightarrow \pi^+ + n)} \sim 1.5$$

for incident photon energies in the range $\sim 200 - 360$ MeV.

Thus a rough guess for the amplitudes would be

$$h^{(-)} \approx \sqrt{1.5} h^{(+)}.$$

Neutron residues could now be computed using this estimate. We shall not stop to do this.

Returning to reggeized amplitudes, Eqs. 4-26, let us consider the nucleon Regge terms in more detail. Using the factorability theorem of residues (5, 26), or which Eq. 4-36 is a particular case, and taking the asymptotic form of the Δ -functions given by Eqs. A-26, we find

$$\varphi_{1,2}^R \sim - \frac{1 + e^{-i\pi\alpha}}{2\sin\pi\alpha} \frac{m}{W^2} \tilde{\eta}^2 (\bar{s}/\bar{s}_0)^\alpha \pm (W \rightarrow -W), \quad (4-56)$$

$$\begin{aligned}\varphi_{3,4}^R &\sim - \frac{1 + e^{-i\pi\alpha}}{2\sin\pi\alpha} \frac{m}{W^2} \tilde{\gamma}_3 \tilde{\gamma}_1 (\bar{s}/\bar{s}_0)^\alpha \pm (W \rightarrow -W), \\ \varphi_{5,6}^R &\sim + \frac{1 + e^{-i\pi\alpha}}{2\sin\pi\alpha} \frac{m}{W^2} \tilde{\gamma}_3^2 (\bar{s}/\bar{s}_0)^\alpha + (W \rightarrow -W),\end{aligned}\quad (4-56)$$

where

$$\begin{aligned}\tilde{\gamma}_1^2 &= \frac{2W^2}{m} \sqrt{\pi} \bar{s}_0^\alpha \frac{1}{p} (-p^2)^{-\alpha} R_{11} \Gamma(\alpha + 3/2) / \Gamma(\alpha + 1), \\ \tilde{\gamma}_3 \tilde{\gamma}_1 &= -\sqrt{\alpha/(\alpha + 2)} (R_{31}/R_{11}) \tilde{\gamma}_1^2, \\ \tilde{\gamma}_3^2 &= [\alpha/(\alpha + 2)] (R_{33}/R_{11}) \tilde{\gamma}_1^2,\end{aligned}\quad (4-57)$$

and \bar{s}_0 is a fixed quantity of dimensions mass squared (18).

As shown in Appendix C, the residues $\tilde{\gamma}_{i,3}$ have no discontinuities below the threshold $W = m$; this is exactly the region of interest to us in deriving asymptotic properties of amplitudes. The square root factors in Eqs. 4-57 come from d-functions corresponding to different helicity states. In general, we shall have factors $\sqrt{\alpha/(\alpha + 2)}$ for $|\lambda - \mu| = 3/2$, $\sqrt{\alpha(\alpha - 1)/(\alpha + 2)(\alpha + 3)}$ for $|\lambda - \mu| = 5/2$, etc., as can easily be verified from Eq. A-23. The factor W^{-2} in Eqs. 4-56 has been written out explicitly because of the expected behavior $\varphi \sim 1/W^2$ or $\tilde{\gamma}_i \tilde{\gamma}_j \sim \text{const.}$ at $W = 0$. This is demonstrated in Appendix C.

Substituting Eqs. 4-56 into Eqs. 2-22, we obtain

$$\begin{aligned}A_{1,2}^R &\sim \frac{4\pi m/W}{W \pm m} \tilde{\gamma}_+^2 \frac{1 + e^{-i\pi\alpha}}{2\sin\pi\alpha} (\bar{s}/\bar{s}_0)^\alpha + (W \rightarrow -W), \\ A_3^R &\sim - \frac{8\pi m}{W^2 - m^2} \tilde{\gamma}_+ \tilde{\gamma}_- \frac{1 + e^{-i\pi\alpha}}{2\sin\pi\alpha} (\bar{s}/\bar{s}_0)^\alpha - (W \rightarrow -W), \\ A_{4,5}^R &\sim \pm \frac{4\pi m^2/W}{(W \pm m)^2} \tilde{\gamma}_+^2 \frac{1 + e^{-i\pi\alpha}}{2\sin\pi\alpha} (\bar{s}/\bar{s}_0)^\alpha \pm (W \rightarrow -W), \\ A_6^R &\sim \frac{8\pi m^2/W}{W^2 - m^2} \tilde{\gamma}_+ \tilde{\gamma}_- \frac{1 + e^{-i\pi\alpha}}{2\sin\pi\alpha} (\bar{s}/\bar{s}_0)^\alpha + (W \rightarrow -W),\end{aligned}\quad (4-58)$$

where

$$\tilde{\eta}_{\pm} = \tilde{\eta}_1 \pm \tilde{\eta}_3. \quad (4-59)$$

It appears that the Mandelstam amplitudes have a number of kinematical poles at $W = \pm m$ in addition to the poles coming from $(\sin \pi \alpha)^{-1}$. Thus A_5 would have a pole of order three at $W = m$. It would be quite embarrassing if this were really the case. Obviously, the cancellations must come from the factors $\tilde{\eta}_+$ and $\tilde{\eta}_-$. In fact, if we assume that $\tilde{\eta}_- \sim \text{constant}$ and $\tilde{\eta}_+ \sim W - m$ at $W = m$, then we see that all amplitudes except A_2 have simple poles at $W = m$; this is consistent with the zero residue of A_2 found in Part III. To get rid of these fictitious poles formally, let us redefine η 's:

$$\eta_{\pm}(W) = \frac{2m}{W \mp m} \tilde{\eta}_{\pm}(W). \quad (4-60)$$

Then we have

$$\begin{aligned} A_{1,2}^R &\sim \frac{\pi m}{W} (W \pm m) \eta_{\mp}^2 \frac{1 + e^{-i\pi\alpha}}{2\sin\pi\alpha} (\bar{s}/\bar{s}_0)^{\alpha} + (W \rightarrow -W) \\ A_3^R &\sim -\frac{2\pi}{m} \eta_+ \eta_- \frac{1 + e^{-i\pi\alpha}}{2\sin\pi\alpha} (\bar{s}/\bar{s}_0)^{\alpha} - (W \rightarrow -W), \\ A_{4,5}^R &\sim \pm \frac{\pi}{W} \eta_{\mp}^2 \frac{1 + e^{-i\pi\alpha}}{2\sin\pi\alpha} (\bar{s}/\bar{s}_0)^{\alpha} \pm (W \rightarrow -W), \\ A_6^R &\sim \frac{2\pi}{W} \eta_+ \eta_- \frac{1 + e^{-i\pi\alpha}}{2\sin\pi\alpha} (\bar{s}/\bar{s}_0)^{\alpha} + (W \rightarrow -W), \end{aligned} \quad (4-61)$$

where now $\eta_{\pm} \sim \text{constant}$ at $W = m$. It is readily seen that our assumptions about the behavior of $\tilde{\eta}_{\pm}$'s and the factoring property of the residues imply, for proton residues at least, that

$$R_{11} \sim c_1^2 p,$$

$$R_{31} \sim c_3 c_1 p^{1/2},$$

$$R_{33} \sim c_3^2,$$

at $W = m$ for some constants c_1 and c_3 . If we require that the reggeized Mandelstam amplitudes A_i^R should agree at the pole $s = m^2$ (to order e^2 in which we are working) with the nucleon Born amplitudes A_i^B calculated in Part III, then it follows by straightforward comparison that

$$\begin{aligned}\gamma_+^2(m) &= \frac{1}{2} m \alpha'(m) (F_1 + 2mF_2)^2, \\ \gamma_+(m) \gamma_-(m) &= -\frac{1}{2} m \alpha'(m) F_1 (F_1 + 2mF_2), \\ \gamma_-^2(m) &= \frac{1}{2} m \alpha'(m) F_1^2.\end{aligned}\tag{4-62}$$

We note that by comparing A_2^B and A_2^R at $W = m$ we would be tempted to conclude that

$$\gamma_+^2(m) = 2m \alpha'(m) F_2 (F_1 + mF_2),$$

in contradiction to the first of Eqs. 4-62. There is no difficulty, however, since A_2^B and A_2^R have no poles at $W = m$, and hence their comparison is not valid because of possible contributions from neglected parts of the amplitude $A_2 = A_2^B + \dots$.

From Eqs. 4-62 we find

$$\begin{aligned}\gamma_+(m) &= \sqrt{m \alpha'(m)/2} (F_1 + mF_2), \\ \gamma_-(m) &= -\sqrt{m \alpha'(m)/2} F_1,\end{aligned}\tag{4-63}$$

with a positive choice of phase for γ_+ . Substituting numbers from Eqs. 3-2, we obtain

$$\begin{aligned}\eta_+^2(m) &= (0.266 + 0.096\tau_3)m\alpha'(m), \\ \eta_+(m)\eta_-(m) &= -0.065(1 + \tau_3)m\alpha'(m), \\ \eta_-^2(m) &= 0.0232(1 + \tau_3)m\alpha'(m).\end{aligned}\tag{4-64}$$

If we use the estimated value

$$\alpha'(m) \approx [2W d\alpha/dW^2]_{W \approx m} \approx 1.88 \times 10^{-3} \text{ MeV}^{-1}$$

from Table 1, p. 20, then we get

$$\begin{aligned}\eta_+^2(m) &= 0.47 + 0.17\tau_3, \\ \eta_+(m)\eta_-(m) &= -0.115(1 + \tau_3), \\ \eta_-^2(m) &= 0.041(1 + \tau_3).\end{aligned}\tag{4-65}$$

The N_1^* and N_3^* Regge trajectory contributions to the Mandelstam amplitudes can be computed in the same manner as those of the nucleon. Omitting details, we find the following asymptotic form of the Mandelstam amplitudes containing the three Regge poles:

$$\begin{aligned}A_{1,2}^R &\sim \frac{\pi}{mW} [(W \mp m)\rho^{(1)}\eta_{\mp}^{(1)2} + (W \pm m)\rho^{(2)}\eta_{\mp}^{(2)2} \\ &\quad - (W \pm m)\rho^{(3)}\eta_{\mp}^{(3)2}] + (W \rightarrow -W), \\ A_3^R &\sim \frac{2\pi}{m} (-\rho^{(1)}\eta_+^{(1)}\eta_-^{(1)} - \rho^{(2)}\eta_+^{(2)}\eta_-^{(2)} + \rho^{(3)}\eta_+^{(3)}\eta_-^{(3)}) + (W \rightarrow -W) \\ A_{4,5}^R &\sim \frac{\pi}{W} (\mp \rho^{(1)}\eta_{\mp}^{(1)2} \pm \rho^{(2)}\eta_{\mp}^{(2)2} \mp \rho^{(3)}\eta_{\mp}^{(3)2}) + (W \rightarrow -W), \\ A_6^R &\sim \frac{2\pi}{m} (-\rho^{(1)}\eta_+^{(1)}\eta_-^{(1)} + \rho^{(2)}\eta_+^{(2)}\eta_-^{(2)} - \rho^{(3)}\eta_+^{(3)}\eta_-^{(3)}) + (W \rightarrow -W),\end{aligned}\tag{4-66}$$

where in our condensed notation

$$\rho^{(k)} = \frac{1 + \sigma_k e^{-i\pi\alpha_k}}{2\sin\pi\alpha_k} \left(\frac{s}{s_0}\right)^{\alpha_k},\tag{4-67}$$

$$\eta_{\pm}^{(k)} = \frac{2m}{W \mp \pi_k m} \tilde{\eta}_{\pm}^{(k)}, \quad (4-67)$$

$$\tilde{\eta}_{\pm}^{(k)} = \tilde{\eta}_1^{(k)} \pm \tilde{\eta}_3^{(k)}, \quad k = 1, 2, 3,$$

and σ_k and π_k are respectively the signature and the parity of the k th Regge trajectory. The $\tilde{\eta}_{1,3}^{(k)}$ are defined by Eqs. 4-57 for all three values of k .

From Eq. B-7, we get the following expression for the asymptotic differential scattering cross section in the backward direction of channel I:

$$\left. \frac{d\sigma}{d\Omega} \right|_{\theta \approx \pi} \xrightarrow{s \rightarrow \infty} \frac{1}{128\pi^2} \left\{ |A_1^R + A_4^R|^2 + |A_2^R + A_5^R|^2 + \frac{1}{2} \left[|A_3^R|^2 + \frac{s(1 + \cos \theta)}{2m^2} |A_6^R|^2 \right] \right\}. \quad (4-68)$$

It is important to note that the A_i^R in this formula represent $A_i^R(s, \bar{s}, t) = \epsilon_i A_i(\bar{s}, s, t)$, where $A_i^R(\bar{s}, s, t)$ are given by Eq. 4-66 with $W \rightarrow \bar{W}$ and $\bar{s}, \bar{s}_0 \rightarrow s, s_0$, and ϵ_i by Eq. 2-10. This is the point where we use crossing relations to express scattering amplitudes in channel I in terms of those in channel II. Substituting Eqs. 4-66 into Eq. 4-68, we could obtain a formula for the differential cross section involving all three Regge poles and their duals. The formula is quite long and not very enlightening. Let us consider possible simplifications. From Fig. 3, p. 22, we see that N_3^* is the highest-lying trajectory for $\bar{s} \simeq m^2$. If this continues to be true in the region $\bar{s} < 0$, as it is possible to expect, then the N_3^* trajectory will be the dominant one, and we may discard the

contributions of the N and N^* trajectories in Eq. 4-68, provided that we consider only very high energies. Since the nucleon and its isobar Regge trajectories lie relatively closely together, one should not expect this approximation to be very good at lower energies. Keeping only the N_3^* terms, we find

$$\frac{d\sigma}{d\Omega} \sim \frac{1}{128m^2} \left\{ (|\rho|^2 + |\rho'|^2) (|\eta_+|^4 + 4|\eta_+\eta_-|^2 + |\eta_-|^4) + 2\text{Re}[\rho\rho'(\eta_+^4 + \eta_-^4)] \right\}, \quad (4-69)$$

where

$$\begin{aligned} \rho &= \rho^{(3)}(\bar{W}, s) = \frac{1 - e^{-i\pi\alpha_3(\bar{W})}}{2\sin\pi\alpha_3(\bar{W})} \left(\frac{s}{s_0}\right)^{\alpha_3(\bar{W})}, \\ \rho' &= \rho^{(3)}(\bar{W}, s^*) = \frac{1 - e^{+i\pi\alpha_3(\bar{W})}}{2\sin\pi\alpha_3(\bar{W})} \left(\frac{s}{s_0}\right)^{\alpha_3(\bar{W})}, \\ \eta_{\pm} &= \eta_{\pm}^{(3)}(\bar{W}). \end{aligned} \quad (4-70)$$

As discussed in Appendix C, α and η_{\pm} are in general complex for \bar{W} purely imaginary corresponding to $\bar{s} < 0$; hence we need the absolute value and the real part signs in Eq. 4-69. In order to investigate the validity of this equation, we must first discuss certain kinematical features of Compton scattering.

As remarked in the beginning of this part, the c.m. energy squared s and the scattering angle θ in channel I are related to the c.m. energy squared \bar{s} in channel II by the formula

$$\bar{s} \equiv \bar{W}^2 = - (s - m^2)^2(1 + \cos\theta)/2s + m^4/s. \quad (4-71)$$

Since θ is physical, we must have $|\cos\theta| \leq 1$ and hence

$$2 - s \leq \bar{s} \leq 1/s, \quad (4-72)$$

with s and \bar{s} henceforth in units of the nucleon mass squared.

From Eq. 4-1, we have

$$\bar{x} = -1 - 2(s\bar{s} - 1)/(\bar{s} - 1)^2. \quad (4-73)$$

Substituting Eq. 4-71 into Eq. 4-73, we find

$$\bar{x} = -1 + 2s^2 \cos^2 \theta/2 [1 + (s - 1) \cos^2 \theta/2]^{-2}. \quad (4-74)$$

The Regge formalism is valid provided \bar{x} is reasonably large.

An inspection of Eq. 4-74 shows that this is the case whenever s is large and $\cos \theta/2$ is small or $\theta \lesssim \pi$. It is not sufficient to have only large s since

$$\lim_{s \rightarrow \infty} \bar{x} = -1 + 2/\cos^2 \theta/2$$

can range from 1 to $+\infty$, depending on θ . The lab system angle is given by

$$\cos \theta_L = \frac{(s + 1) \cos^2 \theta/2 - 1}{(s - 1) \cos^2 \theta/2 + 1}. \quad (4-75)$$

We note the formula

$$\bar{x} = -1 + \frac{1}{2} [(1 + \cos \theta_L)^2 + \sin^2 \theta_L s] \quad (4-76)$$

obtained from Eqs. 4-74 and 4-75. Maximizing \bar{x} in this formula with respect to $\cos \theta_L$ for fixed s , we find that

$$\cos \theta_L = (s - 1)^{-1}, \quad s \geq 2, \quad (4-77)$$

yields the maximum

$$\max \bar{x} = \frac{1}{2} [s - 1 + (s - 1)^{-1}] \xrightarrow{s \rightarrow \infty} \frac{s}{2}. \quad (4-78)$$

Thus for a given c.m. energy $W \geq \sqrt{2}$, the Regge formalism "works best" at lab angles given by

$$\theta_L = \cos^{-1}(s-1)^{-1} \xrightarrow{s \rightarrow \infty} \frac{\pi}{2}; \quad (4-79)$$

this is very fortunate from an experimental point of view. The c.m. angle θ and \bar{s} corresponding to this "optimum" lab angle are respectively

$$\theta = 2 \cos^{-1}(s-1)^{-1/2} \xrightarrow{s \rightarrow \infty} \pi$$

and

(4-80)

$$\bar{s} = -1 + 2/s \xrightarrow{s \rightarrow \infty} -1.$$

The results of this discussion are summarized graphically in Fig. 8.

The cross section formula takes a very simple form if $\bar{W} \approx 0$. Since α and γ_{\pm} are real for \bar{W} real below $\bar{W}_0 = 1 + m_{\pi}$, we expect that their imaginary parts will be small for $\bar{W} \approx 0$. If we set $\gamma_{\pm}(\bar{W}) = \gamma_{\pm}(0)$ and neglect the imaginary part of $\alpha(\bar{W})$, then Eq. 4-69 simplifies to

$$\frac{d\sigma}{d\Omega} \sim \frac{1}{128} \sec^2 \frac{\pi \alpha(\bar{W})}{2} [\gamma_+^2(0) + \gamma_-^2(0)]^2 \left(\frac{s}{s_0}\right)^{2\alpha(\bar{W})}. \quad (4-81)$$

We cannot have \bar{W} equal to zero exactly since then $\bar{x} = 1$ and the Regge formulae do not apply. To investigate under which circumstances Eq. 4-81 might be valid, let us assume that \bar{W} is nonzero but small, say $|\bar{W}| = 0.1$. If we take $\bar{x} \approx 10$, then Eq. 4-73 gives $W \approx 21.4$. In the lab system, the photon energy is

$$E_{\gamma} = (W^2 - 1)/2 \approx 230$$

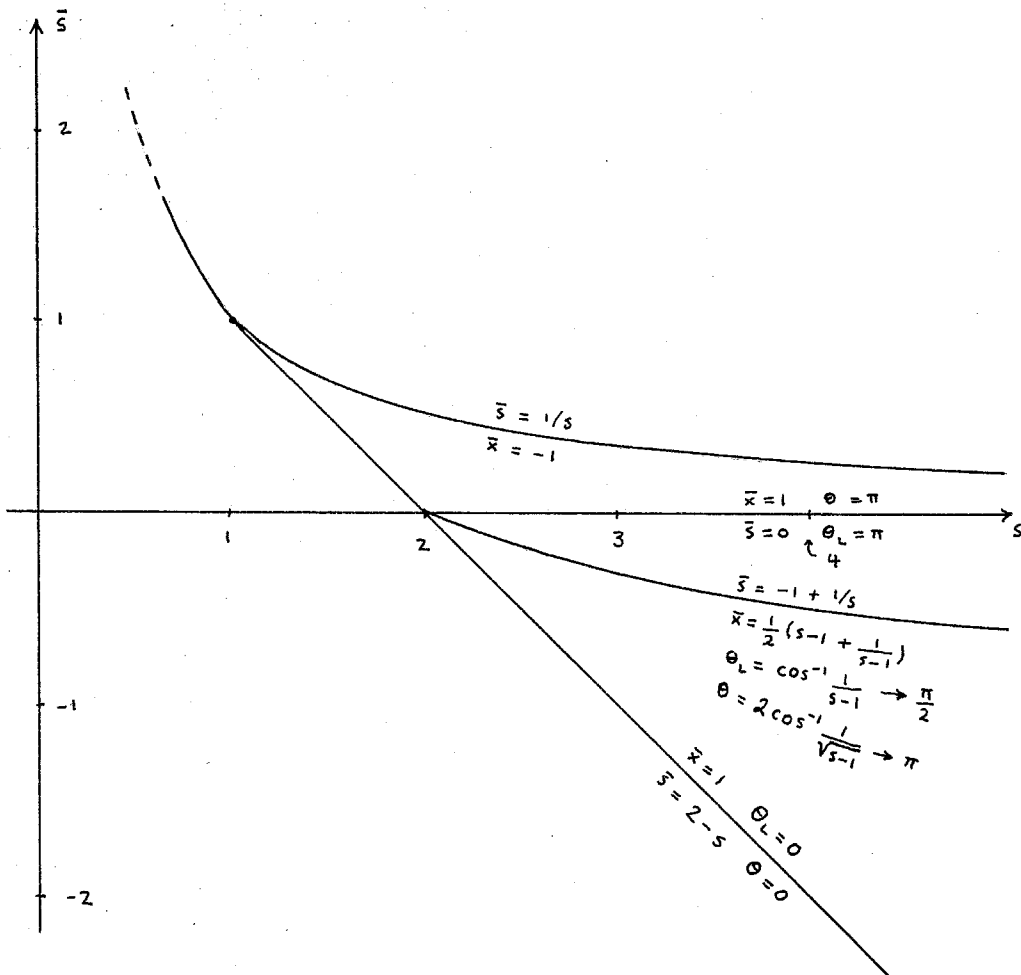


Figure 8. Graphical summary of kinematics for Compton scattering. The physical region for channel I lies between the curves $\bar{s} = 2 - s$ and $\bar{s} = 1/s$. The line of "maximum validity" of Regge formalism (\bar{x} greatest for fixed s) is $\bar{s} = -1 + 1/s$.

or approximately 216 GeV. This energy is much too high to be practical at present. If we take a larger value of $|\bar{W}|$, then we can reduce W considerably. For example, $|\bar{W}| = 0.8$ and $\bar{x} = 10$ yield $E_\gamma \approx 9.7$ GeV which is a quite reasonable energy for present-day machines; however, the approximations leading to Eq. 4-81 are of very doubtful validity for as large a value of $|\bar{W}|$ as 0.8.

Let us investigate the conditions under which it is legitimate to neglect the N and N^* Regge terms in Eqs. 4-69 and 4-81. For these formulae to be valid to 10%, say, we must have

$$(s/s_0)^{2[\alpha_3(\bar{W}) - \alpha_2(\bar{W})]} \gtrsim 10,$$

neglecting factors depending on \bar{W} only. If we assume, for a rough estimate, that

$$\alpha_3(\bar{W}) - \alpha_2(\bar{W}) \approx \alpha_3(m) - \alpha_2(m) \approx 0.47,$$

then

$$W \gtrsim 3.4 \sqrt{s_0}.$$

A typical value for s_0 might be m^2 ; in this case

$$W \gtrsim 3.2 \text{ GeV},$$

corresponding to photon lab energies $E_\gamma \gtrsim 4.9$ GeV.

The foregoing estimates should give one an idea of the applicability of Eqs. 4-69 and 4-81 under present-day experimental conditions. Let us now try to estimate the cross sections

given by Eq. 4-81. For the lack of dynamical calculations of Regge pole trajectories and their residues, we must resort to reasonable guesses about their behavior as functions of \bar{W} .

Our assumptions are the following:

(1) $\Re \alpha(\bar{W})$ for $-1 \lesssim \bar{s} \lesssim 0$ is approximated by a parabolic fit in \bar{s} based on the three experimental points $\alpha = 1, 3$, and 5 :

$$\Re \alpha(\bar{W}) \simeq -0.196 + 0.635 \bar{s} + 0.0314 \bar{s}^2. \quad (4-82)$$

(2) $\Im \alpha(\bar{W})$ for $-1 \lesssim \bar{s} \lesssim 0$ is approximated by a term linear in \bar{W} :

$$\Im \alpha(\bar{W}) \simeq |\bar{W}| \alpha'(0). \quad (4-83)$$

(3) The values of $\tilde{\eta}_+$ and $\tilde{\eta}_-$ for $-1 \lesssim \bar{s} \lesssim 0$ are roughly the same as those at $\bar{W} = m_3$.

Three comments should be made regarding these approximations. First, no terms involving odd powers in \bar{W} can be present in Eq. 4-82. This can be seen as follows. Assuming that α is regular at $\bar{W} = 0$, we have the expansion

$$\alpha(\bar{W}) = \alpha(0) + \bar{W} \alpha'(0) + \frac{1}{2} \bar{W}^2 \alpha''(0) + \dots \quad (4-84)$$

Since α is a real analytic function of \bar{W} , $\alpha(\bar{W}) = \alpha^*(\bar{W}^*)$, as shown in Appendix C, and since $\bar{W}^* = -\bar{W}$ for \bar{W} pure imaginary, we find

$$\Re \alpha(\bar{W}) = \frac{1}{2} [\alpha(\bar{W}) + \alpha^*(\bar{W})]$$

$$\begin{aligned}
 &= \frac{1}{2} [\alpha(\bar{W}) + \alpha(-\bar{W})] \\
 &= \alpha(0) + \frac{1}{2} \bar{W}^2 \alpha''(0) + O(\bar{W}^4).
 \end{aligned}$$

Note that all the derivatives $\alpha^{(n)}(0)$, $n = 0, 1, 2, \dots$, are real (the reality of odd derivatives follows by examining the series for $\Im \alpha$). Secondly, Eq. 4-83 follows from Eq. 4-84 by neglecting terms of order $|\bar{W}|^3$ and higher. We remark that $\alpha'(0)$ is a parameter of the theory to be determined by experiment. Thirdly, we assume that $\tilde{\eta}_+$ and $\tilde{\eta}_-$, rather than η_+ and η_- , are approximately constant. This is because $\tilde{\eta}_\pm$ behave like constants both at $\bar{W} = 1$ and $\bar{W} = 0$ whereas η_\pm have kinematical singularities at $\bar{W} = \pm 1$ as one notices from Eq. 4-67.

Considering the proton Compton scattering process and making the approximation (3), we find

$$\begin{aligned}
 \eta_\pm(\bar{W}) &\simeq 2(\bar{W} + 1)^{-1} \tilde{\eta}_\pm(m_3), \\
 \tilde{\eta}_+^2(m_3) &\simeq 0.2 s_0, \\
 \tilde{\eta}_-^2(m_3) &\simeq 9.8 \times 10^{-5} \tilde{\eta}_+^2(0);
 \end{aligned} \tag{4-85}$$

we can safely neglect η_-^2 in comparison to η_+^2 within this approximation. From Eq. 4-69, we obtain

$$\begin{aligned}
 \frac{d\sigma}{d\Omega} &\sim \frac{1}{256} \left(\frac{s}{s_0} \right)^{2\Re\alpha} \left[\cos^2 \frac{\pi \Re\alpha}{2} + \sinh^2 \frac{\pi \Im\alpha}{2} \right]^{-1} \\
 &\cdot |\eta_+|^4 \left\{ \cosh(\pi \Im\alpha) + \cos \left[2(\Im\alpha \cdot \log \frac{s}{s_0} \right. \right. \\
 &\left. \left. + \arg \sec \frac{\pi\alpha}{2} + \arg \eta_+^2) \right] \right\}.
 \end{aligned} \tag{4-86}$$

The cosine term represents oscillations in the differential cross section. These oscillations will be discussed below; for the time being, let us set the cosine term equal to one in order to get an approximate upper bound on the cross section. Using Eqs. 4-82 and 4-85, we find

$$\frac{d\sigma}{d\Omega} \lesssim 1.1 |\bar{W} - 1|^{-4} s_0^2 \left(\frac{s}{s_0}\right)^{2\Re\alpha} [1 + \cosh(\pi \Im\alpha) \cdot \left[\cos^2 \frac{\pi \Re\alpha}{2} + \sinh^2 \frac{\pi \Im\alpha}{2}\right]^{-1}] \mu\text{b/sr.} \quad (4-87)$$

A point to bear in mind is that all our formulae for the differential cross sections are valid provided that $\Re\alpha(\bar{W}) > -\frac{1}{2}$ for the values of \bar{W} considered. If we accept Eq. 4-82, then these formulae become invalid for $|\bar{W}| \gtrsim 0.7$ corresponding to $\Re\alpha(0.7i) = -\frac{1}{2}$. If, however, the N_3^* Regge trajectory should be flatter than as indicated by Eq. 4-82, then the region of validity of our cross section formulae would be extended. A possible way to investigate the shape of this trajectory (if it dominates!) would be to do experiments keeping \bar{W} fixed and varying s . One would then try to see whether the formula

$$\left(\frac{d\sigma}{d\Omega}\right)_{s_1} / \left(\frac{d\sigma}{d\Omega}\right)_{s_2} = \left(\frac{s}{s_0}\right)^{2\Re\alpha(\bar{W})} \quad (4-88)$$

holds. Should this be the case, one would obtain a point on the trajectory for this fixed value of \bar{W} . The trajectory could then be mapped out by repeating the procedure at several different values of \bar{W} .

To avoid the above-mentioned difficulty of having $\Re\alpha < -\frac{1}{2}$, let us consider the case with $\bar{W} = 0.5i$. If we take $\bar{x} = 10$, then

the photon lab energy and angle are 13.8 GeV and 122° , respectively. We have $\Re\alpha(0.5i) \simeq -0.35$. If we again take $s_0 = 1$ and neglect $\Im\alpha$, then from Eq. 4-87 we obtain

$$\frac{d\sigma}{d\Omega} \lesssim 0.18 \text{ } \mu\text{b/sr.}$$

Corresponding to $E_\gamma \sim 25$ GeV, we find $d\sigma/d\Omega \sim 0.12 \text{ } \mu\text{b/sr}$; this represents a rather modest decrease from the previous value. The insensitivity of the cross section to changes in energy is just the reflection of the smallness of $\Re\alpha$. The rather high values of differential cross sections obtained (to be compared with $d\sigma/d\Omega \sim 0.15 \text{ } \mu\text{b/sr}$ for the cross section at the N_3^* resonance given on p. 49) suggest that the approximation (3) may be rather poor or that the replacement of the cosine term by unity is not appropriate.

It has been pointed out by Gribov (19) that the presence of complex-conjugate (dual) Regge poles should lead to an oscillatory behavior of cross sections in the backward direction as functions of the c.m. scattering angle θ . However, according to Kinoshita (27), there are no such oscillations in spin-averaged $N\pi$ -scattering cross sections although they appear in polarization formulae. It is interesting to examine this question in our case. As we have seen, Eq. 4-86 does exhibit oscillations in the differential cross section. However, they are small since the oscillating cosine terms are dominated by the hyperbolic cosines as soon as $\Im\alpha$ becomes appreciable (where the Regge formalism is "most valid"). Sizable oscillations

occur only for small $\mathcal{J}_m \alpha$ corresponding to small $|\bar{W}|$, hence to c.m. angles very close to 180° if W is large. In order to determine whether it is experimentally possible to detect the oscillations, let us estimate their amplitude and angular spread. For fixed s , let us define the ratio

$$R = (d\sigma/d\Omega)_{\min} / (d\sigma/d\Omega)_{\max} \quad (4-89)$$

between adjacent cross section extrema; note that $0 < R \leq 1$ and that this definition is useful only if the extrema are relatively closely spaced. From Eq. 4-86 we find

$$R = \frac{\cosh(\pi \mathcal{J}_m \alpha) - 1}{\cosh(\pi \mathcal{J}_m \alpha) + 1}. \quad (4-90)$$

This equation is valid provided $\mathcal{J}_m \alpha \neq 0$. If $\mathcal{J}_m \alpha = 0$, then we have to retain terms in η_{\pm}^2 ; from Eq. 4-69 we get

$$R = 2 |\eta_- / \eta_+|^2 \quad (\mathcal{J}_m \alpha = 0). \quad (4-91)$$

Assuming that $\mathcal{J}_m \alpha$ is small but nonzero and using the approximation $\mathcal{J}_m \alpha \approx |\bar{W}| \alpha'(0)$, we find

$$R \equiv R(s, \theta) \approx \left[\frac{\pi}{2} |\bar{W}| \alpha'(0) \right]^2$$

$$\xrightarrow{s \rightarrow \infty} \frac{\pi^2}{4} [\alpha'(0)]^2 \frac{1 + \cos \theta_L}{1 - \cos \theta_L}. \quad (4-92)$$

From the experimental point of view, it is desirable to have R as small as possible in order to obtain large maximum to minimum differential cross section ratios. However, small R presupposes small values of $|\bar{W}|$ which, as we have seen, invalidate the Regge formalism unless one goes to excessively high energies. Hopefully, $\alpha'(0)$ is sufficiently small to allow one to use reason-

able values of $|\bar{W}|$. We see that one can use Eq. 4-92 to determine $\alpha'(0)$ from experimental measurements of R. Of course, the oscillations will be difficult to detect experimentally unless there are reasonably large (but not too large!) angular separations between adjacent cross section extrema. Let us derive a formula for the magnitude of these separations. From Eq. 4-86, we have the expression

$$2\pi = |\Delta(2\mathcal{J}_m\alpha \log \frac{s}{s_0})| \quad (4-93)$$

for the angle between two adjacent maxima. Now

$$\begin{aligned} |\Delta \mathcal{J}_m\alpha| &\simeq |\Delta \bar{W}| \cdot |\alpha'(0)| \\ &= |\alpha'(0)| (4s|\bar{W}|)^{-1} (s-1)^2 \sin\theta \Delta\theta \end{aligned}$$

from Eq. 4-71. Converting the result to lab angles, we find that Eq. 4-93 yields

$$\begin{aligned} \Delta\theta_L &= \pi \left\{ |\alpha'(0)| \log \frac{s}{s_0} (s-1)^2 [s+1 - (s-1)\cos\theta_L]^{-3/2} \right. \\ &\quad \left. \cdot [s-3 + (s-1)\cos\theta_L]^{-1/2} \sin\theta_L \right\}^{-1} \\ &\xrightarrow{s \rightarrow \infty} \frac{2\pi \sin^2\theta_L/2}{|\alpha'(0)| \log(s/s_0)} \cdot \end{aligned} \quad (4-94)$$

We see that the angular separation depends inversely on the energy but only mildly so. One would expect that by a proper choice of θ_L and s it should be possible to obtain experimentally acceptable values of $\Delta\theta_L$. Of course, this possibility depends on the value of $|\alpha'(0)|$ about which we have no information whatsoever. To obtain an idea of the numbers involved, let us arbitrarily demand that $\bar{x} \gtrsim 10$ for the Regge formalism to be

applicable. Because of the errors in measuring cross sections, one may want $1/R \sim 4$ (or larger). Given these values of \bar{x} and R (with $s_0 = 1$) and using Eqs. 4-76, 4-92, and 4-94, we have calculated the photon lab energy E_γ , angle θ_L , and the angular separation $\Delta\theta_L$ for several values of $|\alpha'(0)|$. The results are presented in Table 3.

Table 3

$ \alpha'(0) $	E_γ (GeV)	θ_L (degrees)	$\Delta\theta_L$ (degrees)
0.01	26.4	35	800
0.1	9.4	90	588
1	30.3	145	78
1.5	62.0	156	47
2	106	162	32
10	5160	176	3.9

We see from this table that with the presently available energies (~ 25 GeV) it might be just barely possible to detect the oscillations provided that $\alpha'(0)$ is of the order of unity. To see this in more detail, let us take $E_\gamma = 25$ GeV and a smaller value of \bar{x} , say $\bar{x} = 5$. Then we find $1/R = 6.52$ and $\Delta\theta_L = 85^\circ$ for $|\alpha'(0)| = 1$, and $1/R = 1.63$ and $\Delta\theta_L = 42^\circ$ for $|\alpha'(0)| = 2$. Of course, the experimental situation would be greatly improved if one had higher energies available. Thus with $E_\gamma = 100$ GeV and $\bar{x} = 5$, e.g., one finds

$$R = 0.0405 |\alpha'(0)|^2,$$

$$\Delta \theta_L = 67.5^\circ / |\alpha'(0)|.$$

Clearly, a much larger range of values of $|\alpha'(0)|$ exists for which both R and $\Delta \theta_L$ are reasonably small.

V. HIGH-ENERGY FORWARD

COMPTON SCATTERING

In this part we shall obtain the high-energy limits of nucleon Compton scattering amplitudes in the forward direction.

Regge poles in channel III control the asymptotic behavior of scattering amplitudes in channel I. Demonstration of this fact is analogous to the one given in Part IV for the backward scattering direction. One notes from $t = -2p^2(1-x)$ that for fixed t and $p \propto s \rightarrow \infty$, the cosine of the scattering angle, x , must approach unity.

The reggeizing of channel III is somewhat simpler than that of channel II since boson trajectories are involved having no dual poles.

We start again with a partial wave expansion, Eq. 2-16:

$$\tilde{\Psi}_k(W_t, x_t) = (q\omega)^{-1/2} \sum_J (2J+1) \Psi_k^J(W_t) \mathcal{J}_k^J(x_t) \quad (5-1)$$

with

$$\tilde{\Psi}_k = \begin{cases} \Psi_k, & k = 1, 2, 3, \\ \Psi_k / \sin \theta_t, & k = 4, 5, 6, \end{cases} \quad (5-2)$$

$$\mathcal{J}_1^J(x_t) = d_{02}^J(\theta_t),$$

$$\mathcal{J}_{2,3}^J(x_t) = d_{00}^J(\theta_t),$$

$$\mathcal{J}_{4,5}^J(x_t) = d_{1, \pm 2}^J(\theta_t) / \sin \theta_t, \quad (5-3)$$

$$\mathcal{J}_6^J(x_t) = d_{10}^J(\theta_t) / \sin \theta_t.$$

The correlation between the notations ψ_k and $\psi_{\sigma_1\sigma_2}$ is given by Eqs. 2-17 and 2-19; e.g.,

$$\psi_3 = \langle -1 -1 | \psi | \frac{1}{2} \frac{1}{2} \rangle = \psi_{0-,0}.$$

Again, we introduce the positive and negative signature \mathcal{J} -functions:

$$\begin{aligned} \mathcal{J}_k^{J(\pm)}(x_t) &= \frac{1}{2} [\mathcal{J}_k^J(x_t) \pm \mathcal{J}_k^J(-x_t)], \quad k = 1, 2, 3, \\ \mathcal{J}_{4,5}^{J(\pm)}(x_t) &= \frac{1}{2} [\mathcal{J}_{4,5}^J(x_t) \mp \mathcal{J}_{5,4}^J(-x_t)], \\ \mathcal{J}_6^{J(\pm)}(x_t) &= \frac{1}{2} [\mathcal{J}_6^J(x_t) \mp \mathcal{J}_6^J(-x_t)]. \end{aligned} \quad (5-4)$$

They satisfy

$$\begin{aligned} \mathcal{J}_k^{J(+)}(x_t) &= \begin{cases} \mathcal{J}_k^J(x_t), & J = 0, 2, \dots, \\ 0, & J = 1, 3, \dots, \end{cases} \\ \mathcal{J}_k^{J(-)}(x_t) &= \begin{cases} 0, & J = 0, 2, \dots, \\ \mathcal{J}_k^J(x_t), & J = 1, 3, \dots \end{cases} \end{aligned} \quad (5-5)$$

The line reversal properties of these functions are

$$\begin{aligned} \mathcal{J}_{1,2,3}^{J(\pm)}(-x_t) &= \pm \mathcal{J}_{1,2,3}^{J(\pm)}(x_t), \\ \mathcal{J}_{4,5,6}^{J(\pm)}(-x_t) &= \mp \mathcal{J}_{4,5,6}^{J(\pm)}(x_t). \end{aligned} \quad (5-6)$$

Note that the photon exchange $k_1 \leftrightarrow k_2$, $\mu_1 \leftrightarrow \mu_2$ implies that $\sin \theta_t \leftrightarrow -\sin \theta_t$ as well as $\cos \theta_t \leftrightarrow -\cos \theta_t$.

Now we turn to the construction of partial wave parity eigenamplitudes. Let us first define NN -states of definite parity:

$$|J M; 1 \pm \rangle = 2^{-1/2} (|J M; -\frac{1}{2} \frac{1}{2} \rangle \pm |J M; \frac{1}{2} -\frac{1}{2} \rangle), \quad (5-7)$$

$$|J M ; 0 \pm \rangle = 2^{-1/2} (|J M ; \frac{1}{2} \frac{1}{2} \rangle \pm |J M ; -\frac{1}{2} -\frac{1}{2} \rangle). \quad (5-7)$$

The first three states we call the relativistic triplet states and the last one the relativistic singlet state; following the notation of Chilton (28), we write

$$\begin{aligned} t_{\pm}^{JM} &= |J M ; 1 \pm \rangle, & P &= \pm (-1)^J, \\ t_0^{JM} &= |J M ; 0 + \rangle, & P &= (-1)^J, \\ s^{JM} &= |J M ; 0 - \rangle, & P &= -(-1)^J. \end{aligned} \quad (5-8)$$

(Our t_{\pm}^{JM} differs from that of Chilton by a minus sign.) The parities of the states are determined by Eq. 4-17 remembering that the intrinsic parity of an $N\bar{N}$ -system is -1 . It should be noted that the relativistic singlet-triplet states are not the usual nonrelativistic singlet-triplet states of definite angular momentum L . In fact, using the relation (9)

$$\begin{aligned} |J M ; L S \rangle &= \left(\frac{2L+1}{2J+1} \right)^{1/2} \sum_{\lambda_1, \lambda_2} C(L S J ; 0, \lambda_1, -\lambda_2) \\ &\cdot C(\frac{1}{2} \frac{1}{2} S ; \lambda_1, -\lambda_2) |J M ; \lambda_1 \lambda_2 \rangle, \end{aligned} \quad (5-9)$$

we find

$$\begin{aligned} |J M ; J+1, 1 \rangle &= \sqrt{\frac{J}{2J+1}} t_{+}^{JM} - \sqrt{\frac{J+1}{2J+1}} t_0^{JM}, \\ |J M ; J, 1 \rangle &= t_{-}^{JM}, \end{aligned} \quad (5-10)$$

$$|J M ; J-1, 1 \rangle = \sqrt{\frac{J+1}{2J+1}} t_{+}^{JM} + \sqrt{\frac{J}{2J+1}} t_0^{JM},$$

for the nonrelativistic triplet states ($S = 1$) and

$$|J M ; J, 0 \rangle = s^{JM} \quad (5-10)$$

for the singlet ($S = 0$) state.

Using the result (29) that the charge conjugation eigenvalues are $C = (-1)^{L+S}$ for a $p\bar{p}$ - or $n\bar{n}$ -system, we find that our states have the following C-eigenvalues:

$$\begin{aligned} C t_{\pm}^{JM} &= \pm (-1)^J t_{\pm}^{JM}, \\ C t_0^{JM} &= (-1)^J t_0^{JM}, \\ C s^{JM} &= (-1)^J s^{JM}. \end{aligned} \quad (5-11)$$

Next, we define two-photon states of definite parity:

$$\begin{aligned} |JM; 2 \pm\rangle &= 2^{-1/2}(|JM; -1 1\rangle \pm |JM; 1 -1\rangle), \\ |JM; 0 \pm\rangle &= 2^{-1/2}(|JM; 1 1\rangle \pm |JM; -1 -1\rangle). \end{aligned} \quad (5-12)$$

Their parity is given by

$$P |JM; \rho \pm\rangle = \pm (-1)^J |JM; \rho \pm\rangle, \quad \rho = 0, 2,$$

and $C = 1$ as for any even-number photon state.

Transition amplitudes of definite parity for the reaction $N\bar{N} \rightarrow 2\gamma$ can now be defined:

$$\begin{aligned} g_{00}^{J\pm} &= \langle 0 \pm | \psi^J | 0 \pm \rangle = \Psi_2^J \pm \Psi_3^J, \\ g_{20}^{J\pm} &= \langle 2 \pm | \psi^J | 0 \pm \rangle = \langle -1 1 | \psi^J | \frac{1}{2} \frac{1}{2} \rangle \pm \Psi_1^J, \\ g_{01}^{J\pm} &= \langle 0 \pm | \psi^J | 1 \pm \rangle = \langle -1 -1 | \psi^J | \frac{1}{2} -\frac{1}{2} \rangle \pm \Psi_6^J, \\ g_{21}^{J\pm} &= \langle 2 \pm | \psi^J | 1 \pm \rangle = \Psi_4^J \pm \Psi_5^J. \end{aligned} \quad (5-13)$$

The boson nature of photons and the assumed charge conjugation invariance impose certain restrictions on amplitudes. Since

$$\psi_2 = \langle 1 1 | \psi | \frac{1}{2} \frac{1}{2} \rangle = \langle 1 1 | \psi | \frac{1}{2} \frac{1}{2} \rangle |_{\theta_t \rightarrow \pi + \theta_t}$$

and

$$d_{00}^J(\pi + \theta_t) = (-1)^J d_{00}^J(\theta_t),$$

we find that

$$\Psi_2^J = (-1)^J \Psi_1^J$$

or

$$\Psi_2^J = 0 \text{ for odd } J. \quad (5-14)$$

The same conclusion holds for Ψ_3^J and Ψ_6^J . Under the exchange of the two photons, we have

$$\langle 1 -1 | \psi | \frac{1}{2} \frac{1}{2} \rangle = \langle -1 1 | \psi | \frac{1}{2} \frac{1}{2} \rangle |_{\theta_t \rightarrow \pi + \theta_t}.$$

In terms of partial waves, we find

$$\langle 1 -1 | \psi^J | \frac{1}{2} \frac{1}{2} \rangle d_{02}^J(\theta_t) = \langle -1 1 | \psi^J | \frac{1}{2} \frac{1}{2} \rangle d_{0,-2}^J(\pi + \theta_t)$$

or

$$\langle -1 1 | \psi^J | \frac{1}{2} \frac{1}{2} \rangle = (-1)^J \Psi_1^J. \quad (5-15)$$

The amplitudes $\psi_{4,5}$ go into each other under the photon exchange.

Thus

$$\Psi_4^J d_{12}^J(\theta_t) = \Psi_5^J d_{1,-2}^J(\pi + \theta_t)$$

or

$$\Psi_4^J = (-1)^J \Psi_5^J. \quad (5-16)$$

From Eqs. 5-7 and 5-8 we find

$$|J M ; + \frac{1}{2} \pm \frac{1}{2} \rangle = 2^{-1/2} (t_+^{JM} \pm t_-^{JM}). \quad (5-17)$$

Using the first of Eqs. 5-11, we get

$$C | J M ; + \frac{1}{2} \pm \frac{1}{2} > = (-1)^J | J M ; \pm \frac{1}{2} \mp \frac{1}{2} > . \quad (5-18)$$

Hence

$$< -1 -1 | \psi^J | \frac{1}{2} - \frac{1}{2} > = < 1 1 | \psi^J | - \frac{1}{2} \frac{1}{2} > \quad (P)$$

$$= (-1)^J < 1 1 | \psi^J | \frac{1}{2} - \frac{1}{2} > \quad (C)$$

$$= (-1)^J \Psi_6^J. \quad (5-19)$$

Using Eqs. 5-11, 5-14, 5-15, 5-16, and 5-19, we find the following nonvanishing amplitudes from Eqs. 5-13:

$$g_{00}^{J\pm} = \Psi_2^J \pm \Psi_3^J, \quad J \text{ even},$$

$$g_{20}^{J+} = 2 \Psi_1^J, \quad J \text{ even},$$

$$g_{01}^{J+} = 2 \Psi_6^J, \quad J \text{ even},$$

$$g_{21}^{J\pm} = \Psi_4^J \pm \Psi_5^J \equiv 2 \Psi_4^J = \pm 2 \Psi_5^J \quad \begin{cases} J \text{ even}, \\ J \text{ odd}. \end{cases} \quad (5-20)$$

The inverse relations read

$$\Psi_1^J = \frac{1}{2} g_{20}^{J+}, \quad J \text{ even},$$

$$\Psi_{2,3}^J = \frac{1}{2} (g_{00}^{J+} \pm g_{00}^{J-}), \quad J \text{ even},$$

$$\Psi_4^J = \frac{1}{2} g_{21}^{J\pm} \quad \begin{cases} J \text{ even}, \\ J \text{ odd}, \end{cases}$$

$$\Psi_5^J = \pm \frac{1}{2} g_{21}^{J\pm} \quad \begin{cases} J \text{ even}, \\ J \text{ odd}, \end{cases} \quad (5-21)$$

$$\Psi_6^J = \frac{1}{2} g_{01}^{J+}, \quad J \text{ even}.$$

We can rewrite Eq. 5-1 in the form

$$\begin{aligned}
 \tilde{\Psi}_k(W_t, x_t) &= (q\omega)^{-1/2} \sum_J (2J+1) \Psi_k^J(W_t) [\mathcal{Y}_k^{J(+)}(x_t) + \mathcal{Y}_k^{J(-)}(x_t)] \\
 &= (q\omega)^{-1/2} \sum_{J \text{ even}} (2J+1) \Psi_k^J(W_t) \mathcal{Y}_k^{J(+)}(x_t) \\
 &\quad + (q\omega)^{-1/2} \sum_{J \text{ odd}} (2J+1) \Psi_k^J(W_t) \mathcal{Y}_k^{J(-)}(x_t). \tag{5-22}
 \end{aligned}$$

Substituting the g-amplitudes from Eqs. 5-21, we find

$$\begin{aligned}
 \tilde{\Psi}_1(W_t, x_t) &= \frac{1}{2}(q\omega)^{-1/2} \sum_{J \text{ even}} (2J+1) g_{20}^{J+}(W_t) \mathcal{Y}_1^{J(+)}(x_t), \\
 \tilde{\Psi}_{2,3}(W_t, x_t) &= \frac{1}{2}(q\omega)^{-1/2} \sum_{J \text{ even}} (2J+1) [g_{00}^{J+}(W_t) \pm g_{00}^{J-}(W_t)] \mathcal{Y}_{2,3}^{J(+)}(x_t), \\
 \tilde{\Psi}_{4,5}(W_t, x_t) &= \frac{1}{2}(q\omega)^{-1/2} \sum_{J \text{ even}} (2J+1) g_{21}^{J+}(W_t) \mathcal{Y}_{4,5}^{J(+)}(x_t) \tag{5-23} \\
 &\quad \pm \frac{1}{2}(q\omega)^{-1/2} \sum_{J \text{ odd}} (2J+1) g_{21}^{J-}(W_t) \mathcal{Y}_{4,5}^{J(-)}(x_t), \\
 \tilde{\Psi}_6(W_t, x_t) &= \frac{1}{2}(q\omega)^{-1/2} \sum_{J \text{ even}} (2J+1) g_{01}^{J+}(W_t) \mathcal{Y}_6^{J(+)}(x_t).
 \end{aligned}$$

We see that $\tilde{\Psi}_4$ and $\tilde{\Psi}_5$ are the only amplitudes containing the negative signature \mathcal{Y} -functions. Since ρ^0 and ω trajectories both have negative signature, they may be expected to contribute to amplitudes g_{21}^{J-} . However, this amplitude is nonzero only for odd values of J and represents a transition from an $N\bar{N}$ -state of positive parity to a two-photon final state. Since the parities of ρ^0 and ω are negative, they cannot contribute to this amplitude. We are left with P , σ , π^0 , and η . They contribute to the following amplitudes:

$$\begin{aligned}
 P, \sigma &\rightarrow g_{00}^{J+}, g_{01}^{J+}, g_{20}^{J+}, g_{21}^{J+}, \\
 \pi^0, \eta &\rightarrow g_{00}^{J-}.
 \end{aligned}$$

The amplitude g_{21}^{J-} would receive contributions from a positive parity negative signature Regge trajectory, should one exist.

We shall keep this possibility in mind by retaining $g_{2,1}^{J-}$ in our work.

Writing the Watson-Sommerfeld representation for the amplitudes of Eqs. 5-23, we obtain

$$\tilde{\Psi}_k(W_t, x_t) = I_k(W_t, x_t) + \tilde{\Psi}_k^R(W_t, x_t). \quad (5-24)$$

The I_k are the integral contributions obtained from Eqs. 5-23 by the replacement

$$\sum_{\substack{J \text{ even} \\ \text{odd}}} \rightarrow \pm \frac{1}{2\pi i} \int_{C'} dJ \frac{\pi}{\sin \pi J},$$

where C' is shown in Fig. 7, p. 40, and

$$\begin{aligned} \tilde{\Psi}_1(W_t, x_t) &= -\pi(q\omega)^{-1/2} \left\{ \frac{\alpha_P(t) + 1/2}{\sin \pi \alpha_P(t)} R_{2,0}^P(W_t) \mathcal{G}_1^{\alpha_P(t)(+)}(x_t) \right. \\ &\quad \left. + (P \rightarrow \sigma) \right\}, \\ \tilde{\Psi}_{1,3}(W_t, x_t) &= -\pi(q\omega)^{-1/2} \left\{ \frac{\alpha_P(t) + 1/2}{\sin \pi \alpha_P(t)} R_{0,0}^P(W_t) \mathcal{G}_{2,3}^{\alpha_P(t)(+)}(x_t) \right. \\ &\quad \left. + (P \rightarrow \sigma) \pm (P \rightarrow \pi) \pm (P \rightarrow \eta) \right\}, \\ \tilde{\Psi}_{4,5}(W_t, x_t) &= -\pi(q\omega)^{-1/2} \left\{ \frac{\alpha_P(t) + 1/2}{\sin \pi \alpha_P(t)} R_{2,1}^P(W_t) \mathcal{G}_{4,5}^{\alpha_P(t)(+)}(x_t) \right. \\ &\quad \left. + (P \rightarrow \sigma) + \frac{\alpha_D(t) + 1/2}{\sin \pi \alpha_D(t)} R_{2,1}^D(W_t) \mathcal{G}_{4,5}^{\alpha_D(t)(-)}(x_t) \right\}, \\ \tilde{\Psi}_6(W_t, x_t) &= -\pi(q\omega)^{-1/2} \left\{ \frac{\alpha_P(t) + 1/2}{\sin \pi \alpha_P(t)} R_{0,1}^P(W_t) \mathcal{G}_6^{\alpha_P(t)(+)}(x_t) \right. \\ &\quad \left. + (P \rightarrow \sigma) \right\}. \end{aligned} \quad (5-25)$$

The residues of Regge poles are defined, just as in Part IV, by

$$R_{ij}^A(W_t) = \text{Res}_{J=\alpha_A(t)} g_{ij}^{J\pm}(W_t), \quad i = 0, 2, \quad j = 0, 1. \quad (5-26)$$

Using the factorability theorem of the residues (5, 27) and the asymptotic form of the \mathcal{V} -functions given by Eqs. A-27, we find

$$\begin{aligned}\tilde{\Psi}_1^R &\sim - \frac{1 + e^{-i\pi\alpha_P}}{2\sin\pi\alpha_P} W_t^{-1} \tilde{\eta}_2^{\gamma\gamma P} \tilde{\eta}_0^{N\bar{N}P} (s/s_0)^{\alpha_P} - (P \rightarrow \sigma), \\ \tilde{\Psi}_{2,3}^R &\sim - \frac{1 + e^{-i\pi\alpha_P}}{2\sin\pi\alpha_P} W_t^{-1} \tilde{\eta}_0^{\gamma\gamma P} \tilde{\eta}_0^{N\bar{N}P} (s/s_0)^{\alpha_P} - (P \rightarrow \sigma) \\ &\quad + (P \rightarrow \pi) + (P \rightarrow \eta),\end{aligned}\quad (5-27)$$

$$\begin{aligned}\tilde{\Psi}_{4,5}^R &\sim - \frac{1 + e^{-i\pi\alpha_P}}{2\sin\pi\alpha_P} W_t^{-1} \tilde{\eta}_2^{\gamma\gamma P} \tilde{\eta}_1^{N\bar{N}P} (s/s_0)^{\alpha_P} x_t^{-1} - (P \rightarrow \sigma) \\ &\quad + \frac{1 - e^{-i\pi\alpha_D}}{2\sin\pi\alpha_D} W_t^{-1} \tilde{\eta}_2^{\gamma\gamma D} \tilde{\eta}_1^{N\bar{N}D} (s/s_0)^{\alpha_D} x_t^{-1}, \\ \tilde{\Psi}_6^R &\sim - \frac{1 + e^{-i\pi\alpha_P}}{2\sin\pi\alpha_P} W_t^{-1} \tilde{\eta}_0^{\gamma\gamma P} \tilde{\eta}_1^{N\bar{N}P} (s/s_0)^{\alpha_P} x_t^{-1} - (P \rightarrow \sigma),\end{aligned}$$

where

$$\begin{aligned}\tilde{\eta}_0^{\gamma\gamma A} \tilde{\eta}_0^{N\bar{N}A} &= \sqrt{\pi} W_t(q\omega)^{-1/2} \frac{\Gamma(\alpha_A + 3/2)}{\Gamma(\alpha_A + 1)} R_{00}^A (-s_0/q\omega)^{\alpha_A}, \\ \tilde{\eta}_0^{\gamma\gamma A} \tilde{\eta}_1^{N\bar{N}A} &= -\sqrt{\frac{\alpha_A}{\alpha_A + 1}} (R_{01}^A/R_{00}^A) \tilde{\eta}_0^{\gamma\gamma A} \tilde{\eta}_0^{N\bar{N}A}, \\ \tilde{\eta}_2^{\gamma\gamma A} \tilde{\eta}_0^{N\bar{N}A} &= -\sqrt{\frac{\alpha_A}{\alpha_A + 1}} \sqrt{\frac{\alpha_A - 1}{\alpha_A + 2}} (R_{20}^A/R_{00}^A) \tilde{\eta}_0^{\gamma\gamma A} \tilde{\eta}_0^{N\bar{N}A}, \\ \tilde{\eta}_2^{\gamma\gamma A} \tilde{\eta}_1^{N\bar{N}A} &= \left(-\sqrt{\frac{\alpha_A}{\alpha_A + 1}}\right)^2 \sqrt{\frac{\alpha_A - 1}{\alpha_A + 2}} (R_{21}^A/R_{00}^A) \tilde{\eta}_0^{\gamma\gamma A} \tilde{\eta}_0^{N\bar{N}A}.\end{aligned}\quad (5-28)$$

The asymptotic form of Mandelstam amplitudes is

$$\begin{aligned}A_{1,2}^R &\sim \frac{4\pi}{q\omega} \frac{1 + e^{-i\pi\alpha_P}}{2\sin\pi\alpha_P} (\tilde{\eta}_0^{\gamma\gamma P} + \tilde{\eta}_2^{\gamma\gamma P})(m\tilde{\eta}_1^{N\bar{N}P} - \omega\tilde{\eta}_0^{N\bar{N}P})(s/s_0)^{\alpha_P} \\ &\quad + (P \rightarrow \sigma), \\ A_3^R &\sim \frac{8\pi}{\omega} \frac{1 + e^{-i\pi\alpha_\pi}}{2\sin\pi\alpha_\pi} \tilde{\eta}_0^{\gamma\gamma\pi} \tilde{\eta}_0^{N\bar{N}\pi} (s/s_0)^{\alpha_\pi} + (\pi \rightarrow \eta), \\ A_{4,5}^R &\sim \frac{8\pi m q}{\omega s} \frac{1 + e^{-i\pi\alpha_P}}{2\sin\pi\alpha_P} (\tilde{\eta}_0^{\gamma\gamma P} + \tilde{\eta}_2^{\gamma\gamma P}) \tilde{\eta}_1^{N\bar{N}P} (s/s_0)^{\alpha_P} \\ &\quad + (P \rightarrow \sigma), \\ A_6^R &\sim \frac{16\pi m}{s} \frac{1 - e^{-i\pi\alpha_D}}{2\sin\pi\alpha_D} \tilde{\eta}_2^{\gamma\gamma D} \tilde{\eta}_1^{N\bar{N}D} (s/s_0)^{\alpha_D}.\end{aligned}\quad (5-29)$$

We observe that each Mandelstam amplitude receives contributions from Regge trajectories of fixed parity and signature.

Let us consider the amplitude A_3^R which involves π^0 and η Regge trajectories only. Comparing A_3^R at $t = m_\pi^2$ and at $t = m_\eta^2$ with the corresponding pole terms calculated in Part III, we find

$$\begin{aligned}\tilde{\eta}^{\gamma\gamma\pi}(m_\pi^2) \tilde{\eta}^{N\bar{N}\pi}(m_\pi^2) &= -\frac{1}{2} g_{\pi\pi} m_\pi^{3/2} (\pi/\tau_\pi)^{1/2}, \\ \tilde{\eta}^{\gamma\gamma\eta}(m_\eta^2) \tilde{\eta}^{N\bar{N}\eta}(m_\eta^2) &= \frac{1}{2\sqrt{3}} f_{NN\eta} \epsilon_\eta m_\eta^{3/2} (\pi/\tau_\eta)^{1/2},\end{aligned}\tag{5-30}$$

where

$$\epsilon_A = \Re \alpha_A'(m_A^2).$$

Using the values

$$g^2/4\pi \approx 14.5,$$

$$\epsilon_\pi \approx 1/30 m_\pi^2 \quad (30),$$

$$m_\pi \approx 135 \text{ MeV},$$

$$\tau_\pi \approx 2 \times 10^{-16} \text{ sec},$$

(5-31)

we estimate that

$$\tilde{\eta}^{\gamma\gamma\pi}(m_\pi^2) \tilde{\eta}^{N\bar{N}\pi}(m_\pi^2) \approx -6.23 \times 10^{-5}.\tag{5-32}$$

An idea of the physical magnitude of this number may be obtained by computing the π^0 -contribution to the differential scattering cross section in the forward direction. From Eq. B-7, we have

$$\begin{aligned}\left(\frac{d\sigma}{d\Omega}\right)_{\pi^0} \xrightarrow[t \rightarrow 0^-]{s \rightarrow \infty} &= \frac{t}{128\pi^2 s} |A_3^R|^2 \\ &\approx \frac{1}{2s} \csc^2 \frac{\pi\alpha_\pi(0)}{2} \left(\frac{s}{s_0}\right)^{2\alpha_\pi(0)} |\tilde{\eta}^{\gamma\gamma\pi}(0) \tilde{\eta}^{N\bar{N}\pi}(0)|^2 \\ &\approx 0.014 \left(\frac{s}{s_0}\right)^{-0.67} \frac{m_\pi^2}{s} \mu\text{b/sr},\end{aligned}$$

with the approximations $\tilde{\eta}_i(0) \approx \tilde{\eta}_i(m_\pi^2)$ and $\alpha_\pi(t) \approx (t - m_\pi^2) \epsilon_\pi$.

If $s_0 \approx m_\pi^2$ and if we take $s = 2$ (GeV)², say, then

$$\left(\frac{d\sigma}{d\Omega}\right)_{\pi^0} \sim 6 \text{ } \mu\text{b/sr.}$$

We see that the π^0 Regge term will not contribute significantly to the asymptotic cross sections even at such low asymptotic energies as $W \sim \sqrt{2}$ GeV or $E_\gamma \approx 0.6$ GeV. The contribution of η and its interference with π^0 should be roughly of the same order; we hesitate to make a more accurate estimate since we have no information on the width of the 2γ -decay of the η .

From Eqs. B-12 and B-7, we have the following expressions for the asymptotic total and differential forward cross sections in channel I:

$$\sigma_T \xrightarrow{s \rightarrow \infty} \frac{m}{s} \text{ Abs } [A_2^R - A_1^R + \frac{s}{2m^2} (A_5^R - A_4^R)]_{t=0}, \quad (5-33)$$

$$\begin{aligned} \frac{d\sigma}{d\Omega} \xrightarrow[t \rightarrow 0]{s \rightarrow \infty} \frac{m^2}{32\pi^2 s} \left\{ |A_1^R + \frac{s}{2m^2} A_4^R|^2 + |A_2^R + \frac{s}{2m^2} A_5^R|^2 \right. \\ \left. - \frac{t}{4m^2} |A_3^R|^2 + \frac{1}{2} \left| \frac{s}{2m^2} A_6^R \right|^2 \right\}. \end{aligned} \quad (5-34)$$

Since the Pomeranchuk Regge terms are absent in A_3^R and A_6^R , we may as well omit these amplitudes. Equations 5-33 and 5-34 can be rewritten in a more compact form:

$$\sigma_T \sim \frac{1}{s} \text{ Abs } (A_+ + A_-) |_{t=0}, \quad (5-35)$$

$$\frac{d\sigma}{dt} \sim \frac{4\pi}{s} \frac{d\sigma}{d\Omega} \sim \frac{1}{8\pi s^2} (|A_+|^2 + |A_-|^2), \quad (5-36)$$

where

$$A_{\pm} = - \frac{8\pi s_0}{m^2} \frac{1 + e^{-i\pi\alpha_p}}{2\sin\pi\alpha_p} \gamma_{\pm}^{\chi\chi p} (\gamma_0^{N\bar{N}p} + \gamma_1^{N\bar{N}p})(s/s_0)^{\alpha_p}, \quad (5-37)$$

$$\begin{aligned}\eta_{\pm}^{\gamma\gamma P} &= (m^3/2qs_0)(\tilde{\eta}_2^{\gamma\gamma P} \pm \tilde{\eta}_0^{\gamma\gamma P}), \\ \eta_0^{N\bar{N}P} &= \tilde{\eta}_0^{N\bar{N}P}, \\ \eta_1^{N\bar{N}P} &= -(\omega/m)\tilde{\eta}_1^{N\bar{N}P}.\end{aligned}\tag{5-37}$$

Since, as shown in Appendix C, η 's and α 's are real for $t < 0$, and since

$$\begin{aligned}\text{Abs} [(1 + e^{-i\pi\alpha_P})/2\sin\pi\alpha_P]_{t=0} &= -1/2, \\ |(1 + e^{-i\pi\alpha_P})/2\sin\pi\alpha_P|_{t=0} &= 1/2,\end{aligned}$$

we find

$$\sigma_T \sim \frac{4\pi}{m^2} (\eta_+ + \eta_-) \eta_0, \tag{5-38}$$

$$\frac{d\sigma}{dt} \sim \frac{1}{16\pi} \sigma_T^2 F (s/s_0)^{2\alpha-2}, \tag{5-39}$$

$$F = (\eta_+^2 + \eta_-^2)/(\eta_+ + \eta_-)^2 = 1 + (\eta_0/\eta_2)^2. \tag{5-40}$$

We have dropped the superscripts $\gamma\gamma P$ and $N\bar{N}P$ and the subscript P . The term $\eta_1^{N\bar{N}P}$ has been neglected since it behaves like $t\eta_0^{N\bar{N}P}$ at $t = 0$ according to our estimates in Appendix C. One might expect that the factor F be equal to unity, as is the case, e.g., in $N\pi$ -scattering. The reason for the presence of the extra term in F is that the differential cross section has a photon helicity-flip amplitude $\phi_3 = \langle 1/2 -1 | \phi | 1/2 1 \rangle$ which does not vanish in the forward direction as one can see from Eqs. 2-21. This term does not appear in the formula for the total cross section since the latter involves only non-flip amplitudes ϕ_1 and ϕ_5 . A similar term, namely ϕ_4 , is present in the backward

scattering along with the "maximum helicity-flip" amplitudes ϕ_2 and ϕ_6 .

Setting

$$\alpha(t) \simeq 1 + \epsilon t,$$

$$\epsilon = \alpha'(0),$$

for small t in Eq. 5-39, we get a formula exhibiting the shrinking diffraction peak characteristic of Regge differential cross sections:

$$d\sigma/dt \sim (\sigma_1^2/16\pi) F \exp[-2\epsilon|t| \log(s/s_0)]. \quad (5-41)$$

We must emphasize that Eqs. 5-38 and 5-39 are valid for energies high enough so that contributions from other Regge trajectories, namely the second Pomeranchuk (P'), if it exists, and the ABC (σ) trajectories, are not important. Since, without doubt, $\alpha_{P'}(0) > \alpha_\sigma(0)$, we must make sure that $(s/s_0)^{\alpha_{P'}(0) - \alpha_P(0)}$ is much greater than one. Unfortunately, this criterion involves an unknown parameter s_0 about which we have at present very little to say, save that it should be so chosen that the t -dependent factor in front of $(s/s_0)^{\alpha_{P'}}$ should be as nearly constant as possible. This is not saying much since we have no idea about the behavior of this factor for any given choice of s_0 . One way of obtaining information about s_0 would be to do very high energy experiments and fit the data by Eq. 5-41 on the assumption that the first Pomeranchuk trajectory dominates the cross section for any reasonable value of s_0 . We note that we

should have written s_0^p instead of s_0 since, presumably, different unknown constants should be associated with each Regge trajectory.

The second point to note is our implicit assumption that no Regge cuts exist near the leading vacuum trajectory. Let us now drop this assumption and investigate the role of these cuts. We may remark that some work on Regge cuts has already appeared in the literature; e.g., Gatland and Moffat (31) examined the p - p and p - \bar{p} scattering data by taking into account a Regge cut with the quantum numbers of the vacuum in addition to the usual Regge poles. Our treatment of the vacuum cut will be similar to that presented by these authors.

Consider a cut having the quantum numbers of the vacuum. A generalization of Eqs. 5-37 leads to

$$A_{\pm}^c = - \frac{8\pi s_0}{m^2} \int_{\alpha_-(t)}^{\alpha_+(t)} d\alpha \frac{1 + e^{-i\pi\alpha}}{2\sin\pi\alpha} \eta_{\pm}^{\gamma c}(t, \alpha) \cdot [\eta_0^{N\bar{N}c}(t, \alpha) + \eta_i^{N\bar{N}c}(t, \alpha)] (s/s_0)^{\alpha}, \quad (5-42)$$

where $\alpha_+(0) = 1$ and $\text{Re } \alpha_+(t) \geq \text{Re } \alpha_-(t)$. We take $\alpha_+(0) = 1$ in order to insure that the total cross section does not increase beyond bound as $s \rightarrow \infty$. The case $\alpha_+(0) < 1$ is not as interesting since then the Pomeranchuk Regge pole dominates the cross sections for sufficiently high energies, and hence the cut may be neglected. For lower energies the cut may be important, especially if the difference $\alpha_- - \alpha_+$ is small. We note the asymptotic expansion

$$\begin{aligned}
 & \int_{\alpha_-(t)}^{\alpha_+(t)} d\alpha (s/s_0)^\alpha f(t, \alpha) \\
 & \xrightarrow{s \rightarrow \infty} \frac{(s/s_0)^{\alpha_+(t)}}{\log(s/s_0)} \left[f(t, \alpha_+(t)) - \frac{\partial f(t, \alpha_+(t)) / \partial \alpha_+(t)}{\log(s/s_0)} \right. \\
 & \quad \left. + \dots \right] \\
 & \sim \frac{(s/s_0)^{\alpha_+(t)}}{\log(s/s_0)} f(t, \alpha_+(t)), \tag{5-43}
 \end{aligned}$$

assuming that $\alpha_+(t) > \alpha_-(t)$. Using this result, we can write Eq. 5-42 as

$$\begin{aligned}
 A_{\pm}^c & \sim - \frac{8\pi s_0}{m^2} \frac{1 + e^{-i\pi\alpha_+(t)}}{2\sin\pi\alpha_+(t)} \eta_{\pm}^{\gamma\gamma^c}(t) \\
 & \cdot [\eta_0^{N\bar{N}^c}(t) + \eta_1^{N\bar{N}^c}(t)] (s/s_0)^{\alpha_+(t)} / \log(s/s_0), \tag{5-44}
 \end{aligned}$$

where we have abbreviated

$$\eta_i^{\gamma\gamma^c}(t, \alpha_+(t)) \eta_j^{N\bar{N}^c}(t, \alpha_+(t)) = \eta_i^{\gamma\gamma^c}(t) \eta_j^{N\bar{N}^c}(t).$$

We see that the Regge cut terms are characterized by the presence of logarithmic factors; we are justified in neglecting higher order logarithmic terms in Eq. 5-43 only if $\log(s/s_0) \gg 1$ (assuming $|f'| \sim |f|$, etc.). Keeping the vacuum pole and cut terms only, we find to first order in $1/\log(s/s_0)$

$$\begin{aligned}
 d\sigma/dt & \sim (d\sigma/dt)_p [1 + C(s, t)], \\
 C(s, t) & = C_0 (s/s_0)^{\alpha_+(t) - \alpha_p(t)} / \log(s/s_0), \tag{5-45} \\
 C_0 & = 2 \cdot \frac{\eta_+^{\gamma\gamma^p} \eta_+^{\gamma\gamma^c} + \eta_-^{\gamma\gamma^p} \eta_-^{\gamma\gamma^c}}{(\eta_+^{\gamma\gamma^p})^2 + (\eta_-^{\gamma\gamma^p})^2} \cdot \frac{\eta_0^{N\bar{N}^c}}{\eta_0^{N\bar{N}^p}},
 \end{aligned}$$

where $(d\sigma/dt)_p$ is the vacuum pole cross section given by Eq. 5-39. For small t ,

$$\alpha_+(t) - \alpha_p(t) \approx t[\alpha_+'(0) - \alpha_p'(0)] \equiv \epsilon' t$$

so that

$$\frac{d\sigma}{dt} \sim \left(\frac{d\sigma}{dt}\right)_p \left\{ 1 + C \cdot \frac{\exp[-\epsilon' |t| \log(s/s_0)]}{\log(s/s_0)} \right\}. \quad (5-46)$$

We see that the cut contribution decreases logarithmically with energy only in the extreme forward direction. At larger angles, the cut may or may not dominate the pole depending whether $\epsilon' < 0$ or $\epsilon' > 0$, respectively.

From Eq. 5-35, we obtain

$$\sigma_T \sim (\sigma_T)_p + \frac{4\pi}{m^2} (\eta_+^{\gamma\gamma c} + \eta_-^{\gamma\gamma c}) \eta_0^{N\bar{N}c} / \log(s/s_0). \quad (5-47)$$

Thus the $N\gamma$ total cross section approaches the constant value $(\sigma_T)_p$ logarithmically. Strictly speaking, $(\sigma_T)_p$ is also a function of s if we include Regge poles other than P . However, it differs from the constant asymptotic value by terms proportional to negative powers of (s/s_0) so that its s -dependence may be neglected in comparison to the logarithmic term in Eq. 5-47.

As we have seen, the total $N\gamma$ cross section does not contain the π^0 , η , and D Regge pole contributions. They occur in the differential cross section formulae but are dominated by the vacuum Regge terms. To study the behavior of the π^0 , η , and D Regge trajectories, one might consider polarization experiments. Since such experiments are rather difficult to perform, we shall not present asymptotic polarization formulae for the nucleon Compton scattering process. They could be rather easily obtained by substituting Eqs. 5-29 into polarization formulae

given by Frolov (32) provided one takes into account differences between his and our definitions of Mandelstam amplitudes. It appears that processes other than nucleon Compton scattering should be considered if one is interested in studying the π^0 , η , and D Regge trajectories.

VI. CONCLUSIONS

The high-energy limits of nucleon Compton scattering amplitudes and cross sections in the forward and backward directions have been examined on the basis of the Regge hypothesis.

We have presented a detailed reggeization procedure of the partial wave expansion in channel II; the backward asymptotic scattering in channel I was shown to be controlled by the nucleon and its isobar Regge poles in channel II under the assumption that there are no cuts in the complex angular momentum plane. Residues of the nucleon Regge pole were evaluated by requiring that they agree with those obtained by the renormalized perturbation theory to second order in the electromagnetic coupling constant. Both the charge and the magnetic moment couplings were included. Residues of the isobar Regge poles were evaluated by employing the unitarity condition and using the experimental data on pion photoproduction amplitudes in the vicinity of the N_3^* and N_1^* resonances. We have shown that the Regge formalism has a region of "maximum validity" at laboratory angles approaching 90° for large incident photon energies. Under certain reasonable assumptions about the behavior of Regge trajectories and residues, we have discussed the validity of our formulae for the differential cross section in the backward direction and have

obtained a rough estimate of its magnitude assuming that the N_3^* Regge trajectory dominates in the energy region under consideration. It was found that the presence of complex-conjugate (dual) fermion Regge poles leads to oscillations of cross sections. Approximate formulae for finding the amplitude and the "wavelength" of these oscillations have been derived. The possibility of experimentally detecting cross section oscillations depends critically on the value of the unknown parameter $m[d\alpha(\bar{W})/d\bar{W}]_{\bar{W}=0}$; it appears that detection might barely be possible with available photon energies provided that the value of this parameter lies between 1 and 2.

The asymptotic forward scattering was treated by reggeizing channel III. It was shown that the vacuum (P), ABC (σ), π^0 , η , and pseudovector D Regge trajectories could contribute to our amplitudes (the ρ^0 and ω trajectories were excluded by parity arguments). Of these, however, only P and σ contributed significantly to the total and forward differential cross sections at high energies. The π^0 and η Regge pole residues were evaluated by matching them with perturbation theory results. The π^0 -contribution to the forward scattering cross section was estimated to be $\sim 6 \mu\text{b/sr}$ at a photon lab energy of 0.6 GeV. The contributions of a possible vacuum Regge cut were computed under the assumption that the cut extends as far as the Pomeranchuk Regge pole at $t = 0$. The cross sections were found to be modified by terms proportional to powers of

$1/\log(s/s_0)$.

It is essentially trivial to apply our results to electron Compton scattering. The considerations of Part V for the forward scattering remain unmodified except for formal substitutions $\eta_i^{N\bar{N}P} \rightarrow \eta_i^{e^-e^+P}$, etc. Let us briefly consider the necessary changes for the backward scattering. In electron Compton scattering there is only the electron Regge pole in channel II to take into account. Its contributions are given by Eqs. 4-56, 4-57, etc. The differential cross section is given by Eq. 4-69 with

$$\rho = \frac{1 + e^{-i\pi\alpha(\bar{W})}}{2\sin\pi\alpha(\bar{W})} \left(\frac{s}{s_0}\right)^{\alpha(\bar{W})},$$

$$\rho' = \frac{1 + e^{+i\pi\alpha(\bar{W})}}{2\sin\pi\alpha(\bar{W})} \left(\frac{s}{s_0}\right)^{\alpha(\bar{W})}.$$

It is quite feasible to test the "elementarity" of the electron by comparing Eq. 4-69 with experimental results; the corresponding test of the nucleon is obscured by the fact that N_3^* dominates nucleon Regge terms or is at least comparable to them. The analog of Eq. 4-81 for the electron is

$$\frac{d\sigma}{d\Omega} \sim \frac{e^4}{128} [\alpha'(m_e)]^2 \sec^2 \frac{\pi\alpha(\bar{W})}{2} \exp[2\alpha(\bar{W})\log(s/s_0)],$$

with the approximation $\eta_{\pm}(0) \approx \eta_{\pm}(m_e)$ and for small $|\bar{W}|$.

Writing $\delta = m_e \alpha'(m_e)$, we find

$$\frac{d\sigma}{d\Omega} \sim 0.625 \delta^2 \sec^2 \frac{\pi\delta}{4} \exp\left\{-\left[1 + \frac{s(1 + \cos\theta)}{2m_e^2}\right]\right. \\ \left. \cdot \delta \log \frac{s}{s_0}\right\} \text{ mb/sr,}$$

where we have set

$$\alpha(W) \approx 0 + (\bar{W}^2 - m_e^2) \delta / 2m_e^2.$$

It would be very interesting to have an experimental test of this formula.

APPENDIX A

In this appendix we shall compute the d -, Δ -, and \mathcal{J} -functions used in the text and shall obtain their asymptotic behavior.

We shall need expressions for the $d_{\lambda\mu}^{\mathcal{J}}(\theta)$ with $\lambda, \mu = \pm \frac{1}{2}, \pm \frac{3}{2}$ and $(\lambda, \mu) = (0, 0), (1, 0), (0, 2), (1, 2),$ and $(1, -2)$. We dispose of the last five d -functions first.

From Appendix B of Jacob and Wick (9), we have

$$d_{m0}^{\mathcal{J}}(\theta) = [4\pi/(2J+1)]^{1/2} Y_{Jm}(\theta, 0), \quad (A-1)$$

$$d_{00}^{\mathcal{J}}(\theta) = P_J(\cos \theta), \quad (A-2)$$

$$d_{10}^{\mathcal{J}}(\theta) = -[J(J+1)]^{-1/2} \sin \theta P_J'(\cos \theta), \quad (A-3)$$

$$d_{20}^{\mathcal{J}}(\theta) = [(J-1)J(J+1)(J+2)]^{-1/2} \cdot [2P_{J-1}'(\cos \theta) - J(J-1)P_J(\cos \theta)], \quad (A-4)$$

$$d_{m1}^{\mathcal{J}}(\theta) = [J(J+1)]^{-1/2} \{-m[(1+\cos \theta)/\sin \theta] d_{m0}^{\mathcal{J}}(\theta) - [(J-m)(J+m+1)]^{1/2} d_{m+1,0}^{\mathcal{J}}(\theta)\}, \quad (A-5)$$

where $P_J'(\cos \theta) = dP_J(\cos \theta)/d(\cos \theta)$ and $Y_{Jm}(\theta, \varphi)$ are spherical harmonics as defined by Eqs. III.20 and III.21 of Rose (33):

$$Y_{Jm}(\theta, \varphi) = \left[\frac{2J+1}{4\pi} \frac{(J-m)!}{(J+m)!} \right]^{1/2} e^{im\varphi} (-\sin \theta)^m \cdot d^m P_J(\cos \theta)/d(\cos \theta)^m \quad (A-6)$$

We shall need the relations (9)

$$d_{\lambda\mu}^{\mathcal{J}}(\theta) = d_{-\mu, -\lambda}^{\mathcal{J}}(\theta), \quad (A-7)$$

$$d_{\lambda\mu}^J(\theta) = (-1)^{\lambda-\mu} d_{\mu\lambda}^J(\theta), \quad (\text{A-8})$$

$$d_{\lambda\mu}^J(\theta) = (-1)^{J+\lambda} d_{\lambda,-\mu}^J(\pi - \theta). \quad (\text{A-9})$$

By Eq. A-8 we have

$$d_{02}^J(\theta) = d_{20}^J(\theta).$$

Using Eq. A-5 with $m = -2$, we find

$$\begin{aligned} d_{-2,1}^J(\theta) &= [J(J+1)]^{-1/2} \left\{ 2 \frac{1 + \cos \theta}{\sin \theta} d_{-2,0}^J(\theta) \right. \\ &\quad \left. - [(J+2)(J-1)]^{1/2} d_{-1,0}^J(\theta) \right\}. \end{aligned}$$

From Eqs. A-3, A-4, A-7, and the relation (33)

$$d_{\lambda\mu}^J(\theta) = d_{\mu\lambda}^J(-\theta), \quad (\text{A-10})$$

we obtain

$$\begin{aligned} d_{1,-2}^J(\theta) &= [J(J+1)]^{-1} [(J-1)(J+2)]^{-1/2} (\sin \theta)^{-1} \\ &\quad \cdot \left\{ (J-1)[2J + (2J^2 + 5J + 2) \cos \theta] P_J(\cos \theta) \right. \\ &\quad \left. - 4(1 + \cos \theta) P'_{J-1}(\cos \theta) - (J^2 - 1)(J+2) P_{J+1}(\cos \theta) \right\}. \end{aligned} \quad (\text{A-11})$$

From this it follows by Eq. A-9 that

$$\begin{aligned} d_{12}^J(\theta) &= - [J(J+1)]^{-1} [(J-1)(J+2)]^{-1/2} (\sin \theta)^{-1} \\ &\quad \cdot \left\{ (J-1)[2J - (2J^2 + 5J + 2) \cos \theta] P_J(\cos \theta) \right. \\ &\quad \left. - 4(1 - \cos \theta) P'_{J-1}(\cos \theta) + (J^2 - 1)(J+2) P_{J+1}(\cos \theta) \right\}. \end{aligned} \quad (\text{A-12})$$

Turning now to d-functions of half-integral J , we find from Table II, Appendix B, of Jacob and Wick (9) and from our Eqs. A-7 and A-8 the following set of functions:

$$d_{-1/2, -1/2}^J(\theta) = (J + 1/2)^{-1} \cos \theta/2 [P_{J+1/2}'(\cos \theta) - P_{J-1/2}'(\cos \theta)], \quad (A-13)$$

$$d_{-1/2, 1/2}^J(\theta) = (J + 1/2)^{-1} \sin \theta/2 [P_{J+1/2}'(\cos \theta) + P_{J-1/2}'(\cos \theta)], \quad (A-14)$$

$$d_{-1/2, 3/2}^J(\theta) = - (J + 1/2)^{-1} \cos \theta/2 \cdot \left[\left(\frac{J - 1/2}{J + 3/2} \right)^{1/2} P_{J+1/2}'(\cos \theta) - \left(\frac{J + 3/2}{J - 1/2} \right)^{1/2} P_{J-1/2}'(\cos \theta) \right], \quad (A-15)$$

$$d_{-1/2, -3/2}^J(\theta) = - (J + 1/2)^{-1} \sin \theta/2 \cdot \left[\left(\frac{J - 1/2}{J + 3/2} \right)^{1/2} P_{J+1/2}'(\cos \theta) + \left(\frac{J + 3/2}{J - 1/2} \right)^{1/2} P_{J-1/2}'(\cos \theta) \right]. \quad (A-16)$$

To compute the remaining functions, we use Eq. A3 of Jacob and Wick with $\lambda = -3/2$ and $\mu = 3/2$:

$$d_{-3/2, 3/2}^J(\theta) = \left(\frac{J - 3/2}{J + 3/2} \right)^{1/2} d_{-2, 1}^{J-1/2}(\theta) \cos \theta/2 + d_{-1, 1}^{J-1/2}(\theta) \sin \theta/2. \quad (A-17)$$

Making the required substitutions, we find

$$d_{-3/2, 3/2}^J(\theta) = [(J + 1/2)(J + 3/2)]^{-1} (1 - \cos \theta)^{-2} \cdot \left\{ [(1 - \cos \theta)(J - 1/2)(2J \cos \theta - J - 9/2) - 4] P_{J-1/2}'(\cos \theta) + [4 - (J - 1/2)^2(1 - \cos \theta)] P_{J-3/2}'(\cos \theta) \right\} \sin \theta/2. \quad (A-18)$$

Using Eq. A-9 and the relation $P_\ell(-x) = (-1)^\ell P_\ell(x)$, we obtain

$$d_{-3/2, -3/2}^J(\theta) = -[(J + 1/2)(J + 3/2)]^{-1} (1 + \cos \theta)^{-2} \cdot \left\{ [(1 + \cos \theta)(J - 1/2)(2J \cos \theta + J + 9/2) + 4] P_{J-1/2}'(\cos \theta) + [4 - (J - 1/2)^2(1 + \cos \theta)] P_{J-3/2}'(\cos \theta) \right\} \cos \theta/2. \quad (A-19)$$

This completes the listing of the d-functions.

Now we turn to the asymptotic behavior of the d-functions. It is clear that we can read it off from the explicit expressions obtained above. However, it may be of interest to exhibit

formulae for the asymptotic behavior of an arbitrary d-function.

We start with a representation of the d-functions given by

Eq. 4.14 of Rose (33),

$$d_{m'm}^J(\theta) = \left[\frac{(J-m)!(J+m')!}{(J+m)!(J-m')!} \right]^{1/2} [(m'-m)!]^{-1} (\cos \theta/2)^{2J+m-m'} \\ \cdot (-\sin \theta/2)^{m'-m} F(m'-J, -m-J; m'-m+1; \\ -\tan^2 \theta/2), \quad (\text{A-20})$$

valid for $m' \geq m$. For large $\cos \theta$

$$-\tan^2 \theta/2 = -\frac{1 - \cos \theta}{1 + \cos \theta} \rightarrow 1.$$

Using an integral representation for the hypergeometric function (34) and setting its argument equal to unity, we have

$$F(a, b; c; 1) = \frac{\Gamma(c)}{\Gamma(b)\Gamma(c-b)} \int_0^1 t^{b-1} (1-t)^{c-a-b-1} dt \\ = \Gamma(c)\Gamma(c-a-b)/\Gamma(c-a)\Gamma(c-b).$$

Letting $a = m' - J$, $b = -m - J$, and $c = m' - m + 1$, we obtain

$$d_{m'm}^J(\theta) \xrightarrow{\cos \theta \rightarrow 1} \Gamma(2J+1) [\Gamma(J+m'+1)\Gamma(J-m'+1) \\ \Gamma(J+m+1)\Gamma(J-m+1)]^{-1/2} (\cos \theta/2)^{2J+m-m'} \\ \cdot (-\sin \theta/2)^{m'-m}.$$

Since (34)

$$\Gamma(2J+1) = \pi^{-1/2} 2^{2J} \Gamma(J+1/2) \Gamma(J+1)$$

and

$$P_{J-1/2}(\cos \theta) \xrightarrow{\cos \theta \rightarrow 1} \frac{2^{J-1/2} \Gamma(J)}{\sqrt{\pi} \Gamma(J+1/2)} (\cos \theta)^{J-1/2}, \quad (\text{A-21})$$

we find

$$d_{m'm}^J(\theta) \sim 2J \Gamma^2(J + \frac{1}{2}) [\Gamma(J + m' + 1) \Gamma(J - m' + 1) \Gamma(J + m + 1) \Gamma(J - m + 1)]^{-1/2} (-\tan \theta/2)^{m'-m} \cos \theta/2 \cdot P_{J-1/2}(\cos \theta) \quad (A-22)$$

for $m' \geq m$. For $m' < m$, we use the symmetry relations, Eqs. A-7 and A-8. Equation A-22 is useful for half-integral values of J . For integral J values, we obtain

$$d_{m'm}^J(\theta) \sim \Gamma^2(J + 1) [\Gamma(J + m' + 1) \Gamma(J - m' + 1) \Gamma(J + m + 1) \Gamma(J - m + 1)]^{-1/2} (-\tan \theta)^{m'-m} P_J(\cos \theta). \quad (A-23)$$

Using Eqs. A-22 and A-23, we find the following asymptotic forms of our d-functions:

$$\begin{aligned} d_{-1/2,-1/2}^J(\theta) &\sim \frac{2J}{J + \frac{1}{2}} P_{J-1/2}(\cos \theta) \cos \theta/2, \\ d_{-1/2,1/2}^J(\theta) &\sim \frac{2J}{J + \frac{1}{2}} P_{J-1/2}(\cos \theta) \sin \theta/2, \\ d_{-1/2,3/2}^J(\theta) &\sim - \left(\frac{J - \frac{1}{2}}{J + \frac{3}{2}} \right)^{1/2} d_{-1/2,-1/2}^J(\theta), \\ d_{-1/2,-3/2}^J(\theta) &\sim - \left(\frac{J - \frac{1}{2}}{J + \frac{3}{2}} \right)^{1/2} d_{-1/2,1/2}^J(\theta), \\ d_{-3/2,-3/2}^J(\theta) &\sim \frac{J - \frac{1}{2}}{J + \frac{1}{2}} d_{-1/2,-1/2}^J(\theta), \\ d_{-3/2,3/2}^J(\theta) &\sim - \frac{J - \frac{1}{2}}{J + \frac{3}{2}} d_{-1/2,1/2}^J(\theta), \\ d_{00}^J(\theta) &= P_J(\cos \theta), \\ d_{10}^J(\theta) &\sim - \sqrt{\frac{J}{J + 1}} \tan \theta P_J(\cos \theta), \\ d_{02}^J(\theta) &\sim - \sqrt{\frac{(J - 1)J}{(J + 1)(J + 2)}} P_J(\cos \theta), \end{aligned} \quad (A-24)$$

$$\begin{aligned} d_{12}^J(\theta) &\sim - \sqrt{\frac{(J-1)J}{(J+1)(J+2)}} d_{10}^J(\theta), \\ d_{1,-2}^J(\theta) &\sim d_{12}^J(\theta). \end{aligned} \quad (\text{A-24})$$

From Eq. 4-2 we have

$$x \sim -\bar{s}/2p^2, \quad \bar{s} \rightarrow \infty.$$

Noting the formula (34)

$$P_\alpha(-x \pm i\epsilon) = -\frac{2}{\pi} \sin \pi \alpha Q_\alpha(x) + e^{\pm i\pi \alpha} P_\alpha(x), \quad (\text{A-25})$$

giving \bar{s} a small positive imaginary part according to the definition of the physical sheet, and remembering that $p^2 < 0$ for $\bar{s} > 0$, we obtain

$$\begin{aligned} P_\alpha(-x) &\xrightarrow{x \rightarrow \infty} e^{-i\pi \alpha} P_\alpha(x) + O(x^{-\alpha-1}) \\ &\xrightarrow{x \rightarrow \infty} e^{-i\pi \alpha} \pi^{-1/2} \frac{\Gamma(\alpha + 1/2)}{\Gamma(\alpha + 1)} \left(\frac{\bar{s}}{\bar{s}_0}\right)^\alpha \left(\frac{\bar{s}_0}{-p^2}\right)^\alpha + O(x^{-\alpha-1}). \end{aligned}$$

Using this and setting $J = \alpha + 1/2$, we get from Eqs. 4-11

$$\begin{aligned} \Delta_{12}^{\alpha+1/2(\pm)}(x) &\sim \frac{1}{2} (1 \pm e^{-i\pi \alpha}) \left(\frac{\bar{s}}{\bar{s}_0}\right)^\alpha \left[\frac{2}{\sqrt{\pi}} \frac{\Gamma(\alpha + 3/2)}{\Gamma(\alpha + 2)} \left(\frac{\bar{s}_0}{-p^2}\right)^\alpha \right], \\ \Delta_{3,4}^{\alpha+1/2(\pm)}(x) &\sim - \sqrt{\frac{\alpha}{\alpha+2}} \Delta_1^{\alpha+1/2(\pm)}(x), \\ \Delta_5^{\alpha+1/2(\pm)}(x) &\sim - \Delta_6^{\alpha+1/2(\pm)}(x) \sim \frac{\alpha}{\alpha+2} \Delta_1^{\alpha+1/2(\pm)}(x). \end{aligned} \quad (\text{A-26})$$

The cosine of the scattering angle in channel III becomes, for large s ,

$$x_t = (s - \bar{s})[t(t - 4m^2)]^{-1/2} \xrightarrow{s \rightarrow \infty} s/2\omega q$$

with $s \rightarrow s + i\epsilon$, $\epsilon > 0$. We take the branch cut in the complex t -plane to run from 0 to $4m^2$ so that

$$\omega q = [t(t/4 - m^2)]^{1/2} \gtrless 0 \quad \text{for } t \begin{cases} > 4m^2 \\ < 0 \end{cases}$$

and

$$\Im \omega q \geq 0 \text{ for } t = t_0 \pm i\epsilon, \quad 0 < t_0 < 4m^2.$$

Thus

$$\Im x_t < 0 \text{ for } t < 0$$

and hence

$$P_\alpha(x_t) \xrightarrow{x_t \rightarrow \infty} e^{-i\pi\alpha} P_\alpha(-x_t) + O(x^{-\alpha-1}).$$

Eqs. 5-3, 5-4, and A-24 now yield

$$\begin{aligned} \mathcal{V}_1^{\alpha(\pm)}(x_t) &\sim -\sqrt{\frac{(\alpha-1)\alpha}{(\alpha+1)(\alpha+2)}} \mathcal{V}_2^{\alpha(\pm)}(x_t), \\ \mathcal{V}_{2,3}^{\alpha(\pm)}(x_t) &\sim \frac{1}{2} (e^{-i\pi\alpha} \pm 1) \left(\frac{s}{s_0}\right)^\alpha \left[\frac{1}{\sqrt{\pi}} \frac{\Gamma(\alpha+\frac{1}{2})}{\Gamma(\alpha+1)} \left(\frac{-s_0}{\omega q}\right)^\alpha \right], \\ \mathcal{V}_{4,5}^{\alpha(\pm)}(x_t) &\sim \sqrt{\frac{\alpha-1}{\alpha+2}} \frac{\alpha}{\alpha+1} \mathcal{V}_2^{\alpha(\pm)}(x_t)/x_t, \\ \mathcal{V}_6^{\alpha(\pm)}(x_t) &\sim -\sqrt{\frac{\alpha}{\alpha+1}} \mathcal{V}_2^{\alpha(\pm)}(x_t)/x_t. \end{aligned} \tag{A-27}$$

APPENDIX B

In this appendix we shall derive unitarity relations and formulae for scattering cross sections.

The elastic unitarity relation for channel I is not needed in our calculations since it gives contributions of order e^4 to the absorptive parts of various amplitudes. However, the result of the optical theorem is based on the elastic unitarity relation, and hence we may as well derive the latter in order to fix multiplicative factors. The $N\pi$ -intermediate state contributions to absorptive parts can then be immediately written down by inspection of elastic absorptive parts.

According to our normalization convention,

$$\begin{aligned} \text{Abs } \langle \lambda_2 \mu_2 | T | \lambda_1 \mu_1 \rangle &= \frac{1}{2i} \langle \lambda_2 \mu_2 | T - T^* | \lambda_1 \mu_1 \rangle \\ &= -\frac{1}{2} \int \frac{d^3 p}{(2\pi)^3} \int \frac{d^3 k}{(2\pi)^3} \cdot (2\pi)^4 \delta(p_1 + k, -p - k) \\ &\quad \cdot \sum_{\lambda, \mu} \langle \lambda_2 \mu_2 | T^* | \lambda \mu \rangle (4Ep)^{-1} \langle \lambda \mu | T | \lambda_1 \mu_1 \rangle. \end{aligned} \quad (\text{B-1})$$

Substituting the partial wave expansions of $\phi = - (8\pi W)^{-1} T$,

$$\langle \lambda \mu | \phi | \lambda_1 \mu_1 \rangle = p^{-1} \sum_J (2J+1) \mathcal{D}_{\nu_1 \nu}^{J*}(\varphi', \theta', -\varphi') \Phi_{\nu \nu_1}^J \quad (\text{B-2})$$

$$\begin{aligned} \langle \lambda \mu | \phi | \lambda_2 \mu_2 \rangle &= p^{-1} \sum_{J, M} (2J+1) \mathcal{D}_{M \nu}^{J*}(\varphi', \theta', -\varphi') \\ &\quad \cdot \Phi_{\nu \nu_2}^J \mathcal{D}_{M \nu}^J(\varphi, \theta, -\varphi), \end{aligned} \quad (\text{B-3})$$

where (θ', φ') are the angles of \underline{p} with respect to \underline{p}_1 , and (θ, φ) those of \underline{p}_2 with respect to \underline{p}_1 , into the unitarity relation, we find

$$\text{Abs } \langle \lambda_2 \mu_2 | \phi | \lambda_1 \mu_1 \rangle = p^{-1} \sum_{\nu} \sum_J (2J+1) \Phi_{\nu \nu_2}^{J*} \Phi_{\nu \nu_1}^J \cdot \mathcal{D}_{\nu, \nu_1}^{J*}(\varphi, \theta, -\varphi). \quad (\text{B-4})$$

We have used the orthogonality relation

$$\int_0^{2\pi} d\varphi \int_0^\pi \sin \theta d\theta \mathcal{D}_{\mu \nu}^{J*}(\varphi, \theta, -\varphi) \mathcal{D}_{\nu_1 \nu}^J(\varphi, \theta, -\varphi) = 4\pi (2J+1)^{-1} \delta_{J'J} \delta_{\mu \nu_1}. \quad (\text{B-5})$$

Substituting the analog of Eq. B-2 into Eq. B-4 and making use of Eq. B-5 to project out partial waves from $\text{Abs } \langle \phi \rangle$, we obtain

$$\text{Abs } \Phi_{\nu_2 \nu_1}^J = \sum_{\nu} \Phi_{\nu \nu_2}^{J*} \Phi_{\nu \nu_1}^J. \quad (\text{B-6})$$

The unitarity relation with an $N\pi$ -intermediate state,

$$\text{Abs } \Phi_{\nu_2 \nu_1}^J = \sum_{\lambda} Z_{\lambda \nu_2}^{J*} Z_{\lambda \nu_1}^J,$$

follows from Eq. B-6 and the observation that the normalizations of Φ^J and Z^J are equivalent.

The differential cross section for polarized scattering in channel I is given by

$$\begin{aligned} \left(\frac{d\sigma}{d\Omega} \right)_{\text{pol.}} &= \int \frac{d^3 p}{(2\pi)^3} \int \frac{k_2^2 dk_2}{(2\pi)^3} \frac{|\langle \lambda_2 \mu_2 | S - 1 | \lambda_1 \mu_1 \rangle|^2}{(2\pi)^4 \delta^{(4)}(0) (1 + p/E)} \\ &= |\langle \lambda_2 \mu_2 | \phi | \lambda_1 \mu_1 \rangle|^2. \end{aligned}$$

The unpolarized differential cross section is

$$\left(\frac{d\sigma}{d\Omega} \right)_{\text{unpol.}} = \frac{1}{4} \sum_{\nu_1 \nu_2} |\langle \lambda_2 \mu_2 | \phi | \lambda_1 \mu_1 \rangle|^2$$

Using relations such as

$$\langle \frac{1}{2} 1 | \phi | \frac{1}{2} 1 \rangle = \langle -\frac{1}{2} -1 | \phi | -\frac{1}{2} -1 \rangle = \phi_1,$$

etc., and substituting from Eqs. 2-21, we find

$$\begin{aligned} \left(\frac{d\sigma}{d\Omega} \right)_{\text{unpol.}} &= (8\pi W)^{-2} \left\{ [2m^2 + p^2(1 - \cos\theta)] (|A_1|^2 + |A_2|^2) \right. \\ &+ \frac{p^2}{2} (1 - \cos\theta) |A_3|^2 + \frac{2p^2 W}{m^2} [W - p(1 - \cos\theta)] \\ &\cdot (|A_4|^2 + |A_5|^2) + \frac{p^2 W^2}{2m^2} (1 + \cos\theta) |A_6|^2 \\ &\left. + 2p[2W - p(1 - \cos\theta)] \Re(A_1 A_4^* + A_2 A_5^*) \right\}. \end{aligned} \quad (\text{B-7})$$

The total elastic cross section is given by

$$\begin{aligned} \sigma_{\tau}^{(\text{el})}(s) &= \frac{1}{4} \sum_{\nu_1 \nu_2} \int d\Omega |\langle \lambda_1 \mu_1 | \phi | \lambda_2 \mu_2 \rangle|^2 \\ &= \frac{\pi}{2p^2} \sum_{J, J'} (2J+1)(2J'+1) \sum_{\nu_1 \nu_2} \int_{-1}^1 d(\cos\theta) \\ &\cdot \Phi_{\nu_1 \nu_1}^{J*} \Phi_{\nu_2 \nu_2}^{J'} d_{\nu_1 \nu_2}^J d_{\nu_1 \nu_2}^{J'}. \end{aligned} \quad (\text{B-8})$$

Using formulae (9)

$$\begin{aligned} d_{\lambda \mu}^J d_{\lambda' \mu'}^{J'} &= \sum_{\ell} C(J J' \ell; \lambda, -\lambda') C(J J' \ell; \mu, -\mu') \\ &\cdot (-1)^{\lambda' - \mu'} d_{\lambda - \lambda', \mu - \mu'}^{\ell}, \end{aligned} \quad (\text{B-9})$$

$$d_{00}^{\ell}(\theta) = P_{\ell}(\cos\theta),$$

and (33)

$$C(J J' 0; \nu, -\nu) = (-1)^{J-\nu} (2J+1)^{-1/2} \delta_{JJ'}, \quad (\text{B-10})$$

we find

$$\begin{aligned} \sigma_{\tau}^{(\text{el})}(s) &= \pi p^{-2} \sum_J (2J+1) \sum_{\nu_1 \nu_2} |\Phi_{\nu_1 \nu_1}^J|^2 \\ &= \pi p^{-1} \sum_{\nu} \text{Abs} \langle \lambda \mu | \phi(W, 1) | \lambda \mu \rangle = \sigma_{\tau}^{(\text{in})}(s), \end{aligned} \quad (\text{B-11})$$

since, schematically,

$$\text{Abs} \langle i | T | i \rangle \sim \sum_n |\langle i | T | n \rangle|^2$$

$$= |\langle i|T|i \rangle|^2 + \sum_{n \neq i} |\langle i|T|n \rangle|^2$$

$$\sim \sigma_T^{(el)} + \sigma_T^{(in)}$$

Summing over λ and μ in Eq. B-11, we find

$$\sigma_T(s) = \frac{2\pi}{p} \text{Abs} (\phi_1 + \phi_5)_{\Theta=0}$$

$$= \text{Abs} \left[\frac{m}{2pW} (A_2 - A_1) + \frac{1}{2m} (A_5 - A_4) \right]_{t=0}. \quad (\text{B-12})$$

APPENDIX C

In this appendix we shall investigate the analytic properties of various amplitudes occurring in the text.

We base our investigation on the Mandelstam representation of nucleon Compton scattering amplitudes as given, e.g., by Hearn and Leader (6):

$$A_i(s, \bar{s}, t) = P_i + \frac{1}{\pi^2} \int_{(m+m_\pi)^2}^{\infty} ds \int_{(m+m_\pi)^2}^{\infty} d\bar{s} \frac{\chi_i(s', \bar{s}')}{(s'-s)(s'-\bar{s})} + \frac{1}{\pi^2} \int_{(m+m_\pi)^2}^{\infty} ds' \int_{(2m_\pi)^2}^{\infty} dt' \frac{\rho_i(s', t')}{t'-t} \left(\frac{1}{s'-s} + \frac{\epsilon_i}{\bar{s}'-\bar{s}} \right), \quad (C-1)$$

where

$$P_i = R_i \left(\frac{1}{s-m^2} + \frac{\epsilon_i}{s-\bar{m}^2} \right) + \frac{r_i}{t-m_\pi^2}, \quad (C-2)$$

the ϵ_i are given by Eq. 2-10, R_i by Eq. 3-4, and r_i by Eq. 3-9. No pole term is given for the η -particle since its mass is above the 2π threshold. The double spectral functions satisfy the crossing relation

$$\chi_i(s, \bar{s}) = \epsilon_i \chi_i(\bar{s}, s). \quad (C-3)$$

The given representation holds to second order in the electromagnetic coupling constant. We have omitted possible subtractions.

The explicit appearance of fixed nucleon and pion pole terms is misleading from the Regge point of view. We can remedy the situation by the following artifice. Considering the pion pole for simplicity, we write

$$\frac{r_i}{t - m_\pi^2} = \frac{\beta_i(t, x_t)}{\sin \pi \alpha_\pi(t)} - \gamma_i(t, x_t),$$

where

$$\gamma_i(t, x_t) = \frac{\beta_i(t, x_t)}{\sin \pi \alpha_\pi(t)} - \frac{r_i}{t - m_\pi^2},$$

$$\beta_i(m_\pi^2, x_t) = \pi \alpha_\pi'(m_\pi^2) \quad \text{for all } x_t.$$

The x_t -dependence of β_i is given by an appropriate linear combination of Legendre polynomials obtained by reggeization. The term $\gamma_i(t, s)$ is nonsingular at $t = m_\pi^2$ and hence belongs to the double-integral terms in Eq. C-1. Thus the A_i are expressed in terms of a Regge pole and an integral contribution. The foregoing procedure can be applied to the nucleon pole terms bearing in mind slight complications caused by the fact that we have dual poles. Thus, formally at least, we obtain a Mandelstam representation containing no fixed poles.

We shall need single-variable dispersion relations for the A_i ; they can be obtained from Eq. C-1 in a well-known way. For fixed s , we have

$$\begin{aligned} A_i(s, \bar{s}, t) &= \frac{1}{\pi} \int_{(m+m_\pi)^2}^{\infty} dv \frac{A_{i,2}(s, v, t)}{v - \bar{s}} \\ &+ \frac{1}{\pi} \int_{(2m_\pi)^2}^{\infty} dv \frac{A_{i,3}(s, 2m^2 - s - v, v)}{v - t}. \end{aligned} \quad (C-4)$$

The fixed- t dispersion relations read

$$\begin{aligned} A_i(s, \bar{s}, t) &= \frac{1}{\pi} \int_{(m+m_\pi)^2}^{\infty} dv \left[\frac{A_{i,1}(v, 2m^2 - v - t, t)}{v - s} \right. \\ &+ \left. \frac{A_{i,1}(2m^2 - v - t, v, t)}{v - \bar{s}} \right]. \end{aligned} \quad (C-5)$$

Here $A_{i,k}$, $k = 1, 2, 3$, are the absorptive parts of the A_i in

the three channels given by

$$\begin{aligned}
 A_{i,1}(s, \bar{s}, t) &= \epsilon_i A_{i,2}(\bar{s}, s, t) \\
 &= \frac{1}{\pi} \int_{(m+m_\pi)^2}^{\infty} dv \frac{\chi_i(s, v)}{v - \bar{s}} + \frac{1}{\pi} \int_{(2m_\pi)^2}^{\infty} dv \frac{\rho_i(s, v)}{v - t}, \\
 A_{i,3}(s, \bar{s}, t) &= \frac{1}{\pi} \int_{(m+m_\pi)^2}^{\infty} dv \rho_i(v, t) \left(\frac{1}{v - s} + \frac{\epsilon_i}{v - \bar{s}} \right). \quad (C-6)
 \end{aligned}$$

We have ignored pole terms in Eqs. C-4 and C-5. Integrals in these equations exist only if $A_{i,k} \sim v^a$, $a < 0$, as $v \rightarrow \infty$.

If $a > 0$, then we must perform a number of subtractions. We assume that, for $i = 1, \dots, 6$, $k = 1, 2, 3$,

$$|A_{i,k}(s, v)| \leq C v^{a(s)} \quad \text{as } v \rightarrow \infty, \quad (C-7)$$

where $a(s)$ is real and

$$\max_{-\infty < s < \infty} a(s) < \infty. \quad (C-8)$$

This assumption is necessary if the theory is to admit only a finite number of subtractions. Whether or not a finite number of subtractions suffice in a complete theory is another matter.

Let us consider the analyticity properties of amplitudes in channel I. The asymptotic behavior of a typical Mandelstam amplitude in the backward scattering direction is given by

$$A(s, \bar{s}) \xrightarrow{s \rightarrow \infty} A^R(s, \bar{s}) = a(s, \bar{W}) + a(s, -\bar{W}), \quad (C-9)$$

$$a(s, \bar{W}) = \frac{1}{2} [P_{\alpha(\bar{W})}(-s/2\bar{p}^2) + \sigma P_{\alpha(\bar{W})}(s/2\bar{p}^2)] \frac{R(\bar{W})}{\sin \pi \alpha(\bar{W})}, \quad (C-10)$$

where we keep only the dominant Regge pole. From the Mandelstam representation, $A(s, \bar{s})$ has a cut in \bar{s} from $(m + m_\pi)^2$ to ∞ and from $-\infty$ to $2m^2 - 4m_\pi^2 - s$. As $s \rightarrow \infty$, the left-hand cut

recedes to $-\infty$, so that $A^R(s, \bar{s})$ has only the right-hand cut in \bar{s} . In terms of \bar{W} , $A^R(s, \bar{s})$ has two cuts: $(-\infty, -\bar{W}_0)$ and (\bar{W}_0, ∞) , where $\bar{W}_0 = m + m_\pi$. This means that $a(s, \bar{W})$ also has these two cuts. However, it is possible to choose $a(s, \bar{W})$ so that it contains only one, say the right-hand, cut. Then $a(s, -\bar{W})$ would have a left-hand cut in \bar{W} , and the sum of the two functions would have the required two cuts. That this is indeed possible we can show by an actual construction. Write a dispersion relation for A^R :

$$A^R(s, \bar{s}) = \frac{1}{\pi} \int_{\bar{W}_0^2}^{\infty} d\xi \frac{\rho(s, \xi)}{\xi - \bar{s}}.$$

We assume that no subtractions are necessary — an inessential simplification. Then we have

$$A^R(s, \bar{s}) = \frac{1}{2\pi} \int_{\bar{W}_0^2}^{\infty} d\xi \frac{\rho(s, \xi)}{\sqrt{\xi}(\sqrt{\xi} - \bar{W})} + \frac{1}{2\pi} \int_{\bar{W}_0^2}^{\infty} d\xi \frac{\rho(s, \xi)}{\sqrt{\xi}(\sqrt{\xi} + \bar{W})}. \quad (C-11)$$

Define the first integral to be $a(s, \bar{W})$. It is fairly easy to convince oneself that this decomposition is unique in the sense that any other function $a'(s, \bar{W})$ having only the right-hand cut is equal to $a(s, \bar{W})$. Obviously, infinitely many decompositions of A^R are possible in which $a(s, \bar{W})$ has both cuts. For simplicity, we shall assume that $a(s, \bar{W})$ is defined by the first integral in Eq. C-11. This seems the most natural definition. From Eq. C-10 it now follows that $\alpha(\bar{W})$ and $R(\bar{W})$ also have only the right-hand cut. Since γ_{\pm}^2 are essentially the same as R (except for factors which are analytic functions in α), we see

that they have no discontinuity below \bar{W}_0 .

From its definition, Eq. C-11, it is obvious that $a(s, \bar{W})$ is a real analytic function:

$$a(s, \bar{W}) = a^*(s^*, \bar{W}^*). \quad (C-12)$$

Since $P_\alpha(x)$ is also a real analytic function of α and x , it follows from Eqs. C-10 and C-12 that

$$\begin{aligned} & [P_{\alpha(\bar{W})}(-s/2\bar{p}^2) + \sigma P_{\alpha(\bar{W})}(s/2\bar{p}^2)] R(\bar{W}) / \sin \pi \alpha(\bar{W}) \\ &= [P_{\alpha^*(\bar{W}^*)}(-s/2\bar{p}^2) + \sigma P_{\alpha^*(\bar{W}^*)}(s/2\bar{p}^2)] R^*(\bar{W}^*) / \sin \pi \alpha^*(\bar{W}^*). \end{aligned} \quad (C-13)$$

Taking $s = s' + i\epsilon$, s' real, $\epsilon > 0$, we have asymptotically

$$\begin{aligned} P_\alpha(\pm s/2\bar{p}^2) & \xrightarrow{s' \rightarrow \infty} \pi^{-1/2} \frac{\Gamma(\alpha + 1/2)}{\Gamma(\alpha + 1)} \left| \frac{s}{s_0} \right|^\alpha \\ & \cdot [(\pm s_0/\bar{p}^2)^\alpha \theta(\pm \bar{p}^2) + e^{-i\pi\tau\alpha} (\mp s_0/\bar{p}^2)^\alpha \theta(\mp \bar{p}^2)], \end{aligned} \quad (C-14)$$

$$s_0 > 0,$$

$$\tau = \text{sgn } \text{Im } s \equiv \text{Im } s / |\text{Im } s|,$$

$$\theta(x) = 1 \text{ if } x > 0, = 0 \text{ if } x < 0.$$

We have used Eq. A-25. Equations C-13 and C-14 give, as $s \rightarrow \infty$,

$$|s/s_0|^{\alpha(\bar{W}) - \alpha^*(\bar{W}^*)} = \mathcal{R}^*(\bar{W}^*) / \mathcal{R}(\bar{W}), \quad (C-15)$$

$$\begin{aligned} \mathcal{R}(\bar{W}) &= \pi^{-1/2} \frac{\Gamma[\alpha(\bar{W}) + 1/2]}{\Gamma[\alpha(\bar{W}) + 1]} \frac{R(\bar{W})}{2 \sin \pi \alpha(\bar{W})} \\ &\cdot [(s_0/\bar{p}^2)^{\alpha(\bar{W})} \theta(\bar{p}^2) + \sigma (-s_0/\bar{p}^2)^{\alpha(\bar{W})} \theta(-\bar{p}^2)]. \end{aligned} \quad (C-16)$$

Since the right-hand side of Eq. C-15 is independent of s , we must have

$$\alpha(\bar{W}) = \alpha^*(\bar{W}^*), \quad (C-17)$$

i.e., α is a real analytic function. But then so is \mathcal{R} and hence R and, ultimately, η_+ and η_- . We can write the asymptotic form of Eq. C-10 as

$$a(s, \bar{W}) \sim [\sigma + e^{-i\pi\tau\alpha(\bar{W})}] \mathcal{R}(\bar{W}) |s/s_0|^{\alpha(\bar{W})}; \quad (C-18)$$

the discontinuity in s of $a(s, \bar{W})$ comes entirely from the term $e^{-i\pi\tau\alpha}$ and is given by

$$\begin{aligned} [a(s, \bar{W})]_s &= \frac{1}{2i} [a(s + i\epsilon, \bar{W}) - a(s - i\epsilon, \bar{W})] \\ &\sim -\sin\pi\alpha(\bar{W}) \mathcal{R}(\bar{W}) |s/s_0|^{\alpha(\bar{W})}. \end{aligned} \quad (C-19)$$

As shown before, R and α are real for $\bar{W} < \bar{W}_0$; this means that $[a]_s$ is also real as long as \bar{W} remains real and less than \bar{W}_0 . In general, it acquires an imaginary part if \bar{W} becomes complex. However, the discontinuity in s of the total asymptotic Mandelstam amplitude, $[A^R]_s$, has no imaginary part for a purely imaginary $\bar{W} = -\bar{W}^*$:

$$\begin{aligned} \Im [A^R(s, \bar{s})]_s &= \Im \{ [a(s, \bar{W})]_s + [a(s, -\bar{W})]_s \} \\ &= \Im \{ 2 \Re [a(s, \bar{W})]_s \} = 0 \end{aligned}$$

since

$$\begin{aligned} [a(s, -\bar{W})]_s &= \frac{1}{2i} [a(s + i\epsilon, -\bar{W}) - a(s - i\epsilon, -\bar{W})] \\ &= \frac{1}{2i} [a(s - i\epsilon, \bar{W}) - a(s + i\epsilon, \bar{W})]^* \\ &= [a(s, \bar{W})]_s^*. \end{aligned}$$

This is to be expected since the absorptive part in s of $A^R(s, \bar{s})$ should be real in the physical region of channel I.

We now wish to investigate the behavior of Regge amplitudes at the critical points $W = m$ and $W = 0$. Using Eqs. 2-14 and B-5, we find

$$\Phi_{\nu_1, \nu_2}^J(W) = \frac{1}{2} p \int_{-1}^1 dx d_{\nu_1, \nu_2}^J(\theta) \phi_{\nu_1, \nu_2}(W, x). \quad (C-20)$$

With the help of Eqs B-9, we obtain

$$\begin{aligned} d_{-1/2, -1/2}^J(\theta) \cos \theta/2 &= \frac{1}{2} [P_{J-1/2}(x) + P_{J+1/2}(x)], \\ d_{-1/2, 1/2}^J(\theta) \sin \theta/2 &= \frac{1}{2} [P_{J-1/2}(x) - P_{J+1/2}(x)]. \end{aligned} \quad (C-21)$$

From Eqs. 4-18, C-20, 4-4, and C-21, it follows that

$$f_{11}^{J\pm}(W) = \frac{1}{2} p \{ \varphi_1^\ell(W) + \varphi_1^{\ell+1}(W) \pm [\varphi_2^\ell(W) - \varphi_2^{\ell+1}(W)] \}, \quad (C-22)$$

where $J = \ell + 1/2$ and

$$\varphi_i^\ell(W) = \frac{1}{2} \int_{-1}^1 dx P_\ell(x) \varphi_i(W, x). \quad (C-23)$$

Using Eqs 2-21 and C-4, we find

$$\begin{aligned} f_{11}^{J\pm\sigma}(W) &= - (p/16\pi W) \{ m(A_{1,1}^{\ell,\sigma} - A_{2,2}^{\ell,\sigma}) + (pW/m)(A_{4,4}^{\ell,\sigma} - A_{5,5}^{\ell,\sigma} \\ &\quad + A_{6,6}^{\ell,\sigma}) + (\ell \rightarrow \ell + 1) \pm [E(A_{1,1}^{\ell,\sigma} + A_{2,2}^{\ell,\sigma}) + p(-A_{3,3}^{\ell,\sigma} \\ &\quad + A_{4,4}^{\ell,\sigma} + A_{5,5}^{\ell,\sigma})] \mp (\ell \rightarrow \ell + 1) \}, \end{aligned} \quad (C-24)$$

where $\sigma = \pm$ denotes the signature and

$$\begin{aligned} A_{i,1}^{\ell,\sigma} &= \frac{1}{2p^2} \left\{ \frac{1}{\pi} \int_{(2m_\pi)^2}^{\infty} dv Q_\ell(1 + v/2p^2) A_{i,3}(s, v) \right. \\ &\quad \left. + \frac{\sigma}{\pi} \int_{(m+m_\pi)^2}^{\infty} dv Q_\ell \left(1 + \frac{v - m^4/s}{2p^2} \right) A_{i,2}(s, v) \right\}. \end{aligned} \quad (C-25)$$

Using the formula (35)

$$Q_\nu(x) \xrightarrow{x \rightarrow \infty} \pi^{-1/2} 2^{-\nu-1} \Gamma(\nu+1) x^{-\nu-1/2} \Gamma(\nu+3/2), \quad (C-26)$$

we can easily see that amplitudes $f^{\alpha+1/2, P, \sigma}$ have the expected threshold behavior

$$f \sim p^{2\alpha+1}$$

at $p \approx 0$. This is the behavior of the N_1^* and N_3^* Regge amplitudes obtained by taking into account parts of Mandelstam amplitudes receiving contributions from the spectral functions. The nucleon Regge terms have been treated separately in Part IV.

We have implicitly been assuming, and we will continue to do so for the sake of simplicity, that no subtractions are necessary in Eq. C-4. A finite number of subtractions would not alter our arguments about the threshold behavior of the amplitudes. One consequence of our assumption is that integrals in Eq. C-25 exist for $\ell \geq 0$.

In order to examine the behavior of our amplitudes at $W \approx 0$, let us for a moment consider the first integral in Eq. C-25:

$$I_{i,3}^{\ell}(s) = \int_{(2m_{\pi})^2}^{\infty} dv Q_{\ell}(1 + v/2p^2) A_{i,3}(s, v). \quad (C-27)$$

We are interested in the approach $|W| \rightarrow 0$ with W purely imaginary. This is the situation encountered in computing cross sections. Since

$$p = (W^2 - m^2)/2W \xrightarrow{W \rightarrow 0} -m^2/2W,$$

we have $p^2 = m^4/4W^2 < 0$ and

$$I_{i,3}^{\ell}(s) \xrightarrow{s \rightarrow 0} 4m_{\pi}^2 \int_1^{\infty} du Q_{\ell}(1 - ux) a_i(u), \quad (C-28)$$

where we have set

$$u = v/4m_\pi^2,$$

$$x = -8m_\pi^2 s/m^4 > 0,$$

$$a_i(u) = A_{i,3}(0, 4m_\pi^2 u).$$

Let us split the range of integration in Eq. C-28:

$$\begin{aligned} & \int_1^\infty du Q_\rho(1 - ux) a_i(u) \\ &= \int_1^{1/x} du Q_\rho(1 - ux) a_i(u) + \int_{1/x}^\infty du Q_\rho(1 - ux) a_i(u) \quad (C-29) \end{aligned}$$

for fixed $x > 0$. Consider the first integral. The argument of the Legendre function Q_ρ varies between 0 and $1 - x < 1$. Q_ρ is a continuous function of its argument, and it is not hard to show that it is of bounded variation on the interval $[0, 1 - x]$. Its total variation is given by

$$V_\rho(\eta) = \int_0^\eta d\xi |Q'_\rho(\xi)|, \quad \eta < 1,$$

and is an increasing function of η . Thus we can write

$$Q_\rho(\eta) = V_\rho(\eta) - W_\rho(\eta)$$

as a difference of two increasing functions with

$$W_\rho(\eta) = \int_0^\eta d\xi |Q'_\rho(\xi)| - Q_\rho(\eta).$$

Now $a_i(u)$ is an analytic function of u and hence continuous on $[1, 1/x]$. Thus we can apply the mean value theorem for integrals (36) with the result

$$\int_1^{1/x} du Q_\rho(1 - ux) a_i(u)$$

$$\begin{aligned}
 &= \int_1^{1/x} du V_e(1 - ux) a_i(u) - \int_1^{1/x} du W_e(1 - ux) a_i(u) \\
 &= a_i(u_1) \int_1^{1/x} du V_e(1 - ux) - a_i(u_2) \int_1^{1/x} du W_e(1 - ux),
 \end{aligned}$$

where

$$u_1, u_2 \in [1, 1/x].$$

Now

$$\begin{aligned}
 \int_1^{1/x} du Q_e(1 - ux) &\equiv \int_1^{1/x} du Q_e(1 - ux) P_0(1 - ux) \\
 &\sim -x^{-1} [\ell(\ell + 1)]^{-1} [(1 - x/2)^{1/2} + \sqrt{\pi} \sin \frac{\pi(\ell + 1)}{2}] \\
 &\quad \cdot \Gamma(1 + \ell/2) / \Gamma(1/2 + \ell/2) \\
 &= O(x^{-1}),
 \end{aligned}$$

as $x \rightarrow 0^+$, by Eqs. 3.12(3) and 3.4(21) of Erdélyi et al. (35).

Also, by integration by parts,

$$\int_1^{1/x} du V_e(1 - ux) = x^{-1} \int_0^{1-x} d\xi [(1 - x) - \xi] |Q'_e(\xi)|.$$

Fix $\delta > 0$ such that $x < \delta$ and $Q'_e(\xi) > 0$ for $\xi > 1 - \delta$. It is always possible to find such number for small enough x since $Q_e(\xi)$ and $Q'_e(\xi) \rightarrow +\infty$ as $\xi \rightarrow 1^-$. We have

$$\begin{aligned}
 0 &\leq \int_1^{1/x} du V_e(1 - ux) \\
 &= x^{-1} \int_0^{1-\delta} d\xi [(1 - x) - \xi] |Q'_e(\xi)| + x^{-1} \int_{1-\delta}^{1-x} d\xi [(1 - x) \\
 &\quad - \xi] |Q'_e(\xi)| \\
 &= O(x^{-1}) + x^{-1} \{ (x - \delta) Q_e(1 - \delta) + [\ell(\ell + 1)]^{-1} \\
 &\quad \cdot [(2x - x^2)^{1/2} Q'_e(1 - x) - (2\delta - \delta^2)^{1/2} Q'_e(1 - \delta)] \} \\
 &= O(x^{-1})
 \end{aligned}$$

since the first integral has a limit as $x \rightarrow 0^+$. Thus

$$\begin{aligned} \int_1^{1/x} du Q_e(1-ux) a_i(u) \\ = [a_i(u_1) - a_i(u_2)] O(x^{-1}) \end{aligned}$$

and

$$\left| \int_1^{1/x} du Q_e(1-ux) a_i(u) \right| \leq (|a_i(u_1)| + |a_i(u_2)|) O(x^{-1}).$$

As $x \rightarrow 0^+$, $u_1, u_2 \in [1, 1/x] \rightarrow [1, +\infty)$ so that

$$|a_i(u_{1,2})| \leq C x^{-\alpha},$$

according to Eq. C-7. But a is just the highest-lying Regge α in channel I evaluated at $W = 0$:

$$a = \alpha(0).$$

Thus

$$\left| \int_1^{1/x} du Q_e(1-ux) a_i(u) \right| \leq C' x^{-1-\alpha(0)}.$$

The second integral in Eq. C-29 is easily estimated.

We have

$$\int_{1/x}^{\infty} du Q_e(1-ux) a_i(u) = x^{-1} \int_{-\infty}^0 d\xi Q_e(\xi) a_i\left(\frac{1-\xi}{x}\right).$$

Choose $x > 0$ small enough so that $(1-\xi)/x$ is large enough for the asymptotic estimate

$$\left| a\left(\frac{1-\xi}{x}\right) \right| \leq C \left(\frac{1-\xi}{x}\right)^{\alpha(0)}$$

to apply. Then

$$\int_{1/x}^{\infty} du Q_e(1-ux) a_i(u) \sim C x^{-1-\alpha(0)} \int_{-\infty}^0 d\xi (1-\xi)^{\alpha(0)} Q_e(\xi),$$

where the integral exists for $\Re \ell > \alpha(0)$, and the expression

is defined for $\Re \ell < \alpha(0)$ by an analytic continuation of the result valid for $\Re \ell > \alpha(0)$. Combining our estimates, we find that

$$I_{1,3}^{\ell}(s) \sim (-s)^{-1-\alpha(0)}$$

as $s \rightarrow 0^-$. The second integral in Eq. C-25 has the same behavior. Thus

$$A_{\ell}^{\ell,\sigma} \sim W^{-2\alpha(0)}$$

and

$$f_{11} \sim R_{11} \sim W^{-2\alpha(0)-3},$$

$$\tilde{\eta}_1^2 \sim \text{constant},$$

from Eqs. C-24, 4-34, and 4-57.

Finally, let us make a quick estimate of the behavior of the partial wave amplitudes in channel III at $t = 0$ and $J = 1$ (corresponding to the Pomeranchuk trajectory). From Eqs. 2-16 and B-5, we find

$$\Psi_k^J(W_t) = \frac{1}{2} (q\omega)^{1/2} \int_{-1}^1 dx_t d_{\sigma_1(k)\sigma_2(k)}^J(\theta_t) \psi_k(W_t, x_t).$$

Using Eqs. 2-24 to express ψ_k in terms of the Mandelstam amplitudes and then using the fixed- t representation, Eq. C-5, we find

$$\begin{aligned} \Psi_1^J = & (q\omega)^{1/2} (32\pi^2\omega)^{-1} \int_{-1}^1 dx d_{\sigma_2}^J \int ds' \left\{ q(A_{2,1} - A_{1,1}) \left(\frac{1}{s'-s} \right. \right. \\ & \left. \left. + \frac{1}{s'-\bar{s}} \right) + \omega x(A_{4,1} - A_{5,1}) \left(\frac{1}{s'-s} - \frac{1}{s'-\bar{s}} \right) \right\} \end{aligned}$$

and similar expressions for the other Ψ_k^J which we shall not

write down. We note from Appendix A that the d-functions are just linear combinations of Legendre polynomials P and their first derivatives times possibly powers of $\cos \theta$ and $\sin \theta$; at $J = 1$ they roughly behave as follows:

$$d_{00}^J \sim P_J,$$

$$d_{10}^J \sim \sin \theta P_J',$$

$$d_{02}^J \sim P_{J-1}' / \sqrt{J-1},$$

$$d_{12}^J \sim (1 - \cos \theta) P_{J-1}' / \sin \theta \sqrt{J-1}.$$

Interchanging the orders of integration in Eq. C-30 and performing the x -integrations, we obtain Froissart's definition (37) of the partial wave amplitude Ψ_J^J which can be continued to complex J :

$$\Psi_J^J \sim \omega^{-1/2} \int ds' (A_{2,1} - A_{1,1}) (2q\omega) Q_J(\xi),$$

$$\xi = (s' + \omega^2 + q^2 - i\epsilon) / 2q\omega.$$

We have neglected terms of higher order in ω . Now

$$Q_J(\xi) = Q_J(\xi') + \frac{i\pi}{2} \operatorname{sgn}(q\omega) P_J(\xi'),$$

where ξ' is ξ without the $-i\epsilon/2q\omega$ term. Here Q_J and P_J are the Legendre functions on the cut $[-1, 1]$ discussed by Erdélyi et al. (35) on p. 143. Using formulae of this reference, we find

$$Q_J(\xi'), Q_J'(\xi') \xrightarrow{\xi' \rightarrow 0} \text{const.},$$

$$P_J(\xi'), P_J'(\xi') \xrightarrow{\xi' \rightarrow 0} \text{const.},$$

(C-31)

$$Q_J(\xi) \xrightarrow[\xi \rightarrow \infty]{} \xi^{-n-1}. \quad (C-31)$$

The contributions of the Born terms correspond to $\xi' \simeq 0$:

$$\xi'(s' = m^2) = (m^2 + \omega^2 + q^2)/2\omega q = \omega/q \xrightarrow[\omega \rightarrow 0]{} 0.$$

The terms in which $\xi' \rightarrow \infty$ come from the double spectral functions:

$$\xi'(s' > m^2) = [(s' - m^2) + 2\omega^2]/2\omega q \xrightarrow[\omega \rightarrow 0]{} \infty.$$

From Eqs. C-31 we see that Born terms are dominant at $\omega \simeq 0$.

Thus we find

$$\Psi_1^J \sim \omega^{-1/2} \cdot \omega^{-1} (J-1)^{-1/2} \sim \omega^{-5/2}$$

since

$$J \rightarrow \alpha_p(t) \simeq 1 + t \alpha_p'(0) = 1 + 4\omega^2 \alpha_p'(0).$$

Using Eqs. 5-20 and 5-26, we obtain

$$g_{20}^{J+} = 2\Psi_1^J \sim R_{20}/\omega^2 \sim \omega^{-5/2}$$

or, from Eq. 5-28,

$$\tilde{\eta}_2^{YYP} \tilde{\eta}_0^{N\bar{N}P} \sim \text{const.}$$

Similarly, we find

$$\tilde{\eta}_0^{YYP} \tilde{\eta}_0^{N\bar{N}P} \sim \text{const.},$$

$$\tilde{\eta}_0^{YYP} \tilde{\eta}_1^{N\bar{N}P} \sim \omega,$$

so that

$$\tilde{\eta}_2^{YYP} \sim \tilde{\eta}_0^{YYP},$$

$$\tilde{\eta}_1^{N\bar{N}P} \sim \tilde{\eta}_0^{N\bar{N}P} \cdot \omega.$$

REFERENCES

1. T. Regge, Nuovo Cimento 14, 951 (1959).
2. T. Regge, Nuovo Cimento 18, 947 (1960).
3. G. F. Chew, S. C. Frautschi, S. Mandelstam, Phys. Rev. 126, 1202 (1962).
4. S. C. Frautschi, M. Gell-Mann, F. Zachariasen, Phys. Rev. 126, 2204 (1962).
5. Hung Cheng and D. H. Sharp, Ann. Phys. (to be published).
6. A. C. Hearn and E. Leader, Phys. Rev. 126, 789 (1962).
7. J. W. DeWire, M. Feldman, V. L. Highland, R. Littauer, Phys. Rev. 124, 909 (1961).
8. R. E. Prange, Phys. Rev. 110, 240 (1958).
9. M. Jacob and G. C. Wick, Ann. Phys. 7, 404 (1959).
10. A. H. Rosenfeld (private communication to Prof. F. Zachariasen)
11. A. Abashian, N. E. Booth, K. M. Crowe, Phys. Rev. Letters 5, 258 (1960).
12. A. Abashian, N. E. Booth, K. M. Crowe, Phys. Rev. Letters 7, 35 (1961).
13. J. Hamilton, P. Menotti, G. C. Oades, L. L. Vick, Phys. Rev. 128, 1881 (1962).
14. P. Dennery and H. Primakoff, Phys. Rev. Letters 8, 350 (1962).

15. R. Blankenbecler, L. F. Cook, Jr., M. L. Goldberger,
Phys. Rev. 128, 2440 (1962).
16. K. Igi, Phys. Rev. Letters 9, 76 (1962).
17. M. Gell-Mann, California Institute of Technology
Synchrotron Laboratory Report CTSL-20 (March 15, 1961).
18. M. Gell-Mann, "Applications of Regge Poles," CERN preprint
4199/TH.281 (June 28, 1962).
19. V. N. Gribov, Proceedings of the 1962 Annual International
Conference on High Energy Physics at CERN (CERN, Geneva,
1963), p. 547.
20. G. F. Chew, M. L. Goldberger, F. E. Low, Y. Nambu,
Phys. Rev. 106, 1345 (1957).
21. K. M. Watson, Phys. Rev. 95, 228 (1954).
22. Ph. Salin, "Analysis of Positive Pion Photoproduction,"
Université de Bordeaux preprint PTB-13 (May, 1962).
23. M. Gourdin and Ph. Salin, Nuovo Cimento 27, 193 (1963).
24. Ph. Salin, "Positive and Neutral Pion Photoproduction
Analysis," Université de Bordeaux preprint PTB-16
(November, 1962).
25. M. Sands, J. G. Teasdale, R. L. Walker, Phys. Rev. 95,
592L (1954).
26. J. M. Charap and E. J. Squires, Phys. Rev. 127, 1387 (1962).
27. T. Kinoshita, "Fermion Regge Poles and the Asymptotic
Behaviour of Backward Meson-Nucleon Scattering," CERN
report CERN 62-33 (November 7, 1962).

28. F. Chilton, Phys. Rev. 123, 656 (1961).
29. J. J. Sakurai, Lectures in Theoretical Physics, Vol. II, Interscience (1960), p. 91.
30. A. P. Contogouris, S. C. Frautschi, How-sen Wong, Phys. Rev. 129, 974 (1963).
31. I. R. Gatland and J. W. Moffat, Phys. Rev. 129, 2812 (1963).
32. G. V. Frolov, Soviet Physics JETP 12, 1277 (1961).
33. M. E. Rose, Elementary Theory of Angular Momentum, John Wiley (1957).
34. W. Magnus and F. Oberhettinger, Formulas and Theorems for the Functions of Mathematical Physics, Chelsea (1954).
35. A. Erdélyi, W. Magnus, F. Oberhettinger, F. G. Tricomi, Higher Transcendental Functions, Vol. I, McGraw-Hill (1953).
36. T. M. Apostol, Mathematical Analysis, Addison-Wesley (1957).
37. M. Froissart, Phys. Rev. 123, 1053 (1961).